**NTNU**
Det skapende universitet

# Metabolsk Tilpasning til Hypoksi i Prostatakreftcellelinjen DU-145 og i Glioblastoma-Astrocytoma Kreftcellelinjen U-87 MG

**Elise Midtbust**

# Preface

This master thesis is submitted for the degree of M.Sc. in Biotechnology at the Norwegian University of Science and Technology (NTNU). The experimental work presented in this master thesis was conducted at the Department of Biotechnology (IBT) spring and fall 2016.

I would like to thank my supervisor Professor Per Bruheim for the opportunity to work on this project, and for help throughout the project, both experimentally and thesis writing. I would also like to thank co-supervisor ph.D candidate Lisa Marie Røst for guidance, enthusiasm and useful discussions regarding experimental results. Finally, I would like to thank my fellow student Ulrikke Dahl Brinch for collaboration with laboratory work and data analysis.

Trondheim, January 2017
Elise Midtbust

# Abstract

Regions with low oxygen tension (hypoxic regions) are frequently found in solid tumors. The hypoxic conditions arise as the rapid cellular proliferation exhaust the oxygen supply. The hub protein proliferationg cell nuclear antigen (PCNA) bind proteins involved in a genotoxic stress response through a AlkB homologue 2 PCNA-interacting motif (APIM)-sequence. By blocking PCNA-interactions and prevent cellular repair, ATX-101 to improve cellular sensitivity to the DNA damaging agent cisplatin under atmospheric oxygen conditions. The hypoxic tumor cells respond poorly to commonly used cancer treatments, such as chemotherapy. Thus, the efficacy of ATX-101 and ATX-101+cisplatin was assessed under hypoxic (1% $O_2$) conditions on the prostate cancer cell line DU-145. The efficacy was evaluated 24, 48, 72 and 96 hours after treatment addition in a hypoxic environment by performing cell viability assays. The ATX-101 and ATX-101+cisplatin on DU-145 cells was not altered under hypoxic conditions. This is a finding of clinical importance.

The reduced cellular oxygen tension induces metabolic changes that permit further cancer cell survival and growth. In this thesis, metabolic adaptions to hypoxia in DU-145 and glioblastoma astrocytoma U-87 MG cells were investigated. Metabolic consequences were evaluated 48 and 72 hours after hypoxic treatment. Alternations is in the exometabolome were analysed by measuring glucose, glutamine and lactate in culture medium samples utilizing nuclear magnetic resonance (NMR). Both hypoxic and normoxic incubated U-87 MG cells and DU-145 cells consumed high amounts of major carbon and energy sources, and about half of the glucose consumed was converted to lactate. The endometabolome were analysed using two target mass spectrometric (MS) metabolic profiling methods: capIC-MS/MS and RP LC-MS/MS. Analysis revealed that no entire metabolic pathways were clearly affected by the hypoxic treatment. However, some metabolites within the glycolysis, tricarboxylic (TCA) cycle and the pentose phosphate pathway (PPP) were found prominently and/or statistically significantly changed by hypoxic treatment. Altogether, these findings suggest that metabolic adaptions to hypoxia is not yet fully understood, and motivates for further research on this topic.

# Sammendrag

Regioner med lav oksygentensjon (hypoksiske regioner) er karakteristisk for solide tumorer. Hypoksiske forhold fremkommer når den raske cellulære prolifereringen begrenser oksygentilførselen. Proteinkomplekset "proliferating cell nuclear antigen" (PCNA) binder proteiner involvert i en gentoksisk stressrespons gjennom en AlkB homolog 2 PCNA-interacting motif (APIM)-sekvens. Ved å blokkere PCNA-interaksjoner og hindre cellulær reparasjon, øker ATX-101 cellulær sensitivitet mot DNA-skadelige stoffer ved atmosfæriske oksygenforhold. Hypoksiske kreftceller responderer dårlig på standard brukte kreftbehandlinger, som cellegift. Derfor ble effekten av ATX-101 og ATX-101+cisplatin, vurdert under hypoksiske (1% $O_2$) forhold på prostatakreftcellelinjen DU-145. Effekten ble evaluert 24, 48, 72 og 96 timer etter tilsats av behandling i et hypoksisk miljø ved å gjennomføre celleoverlevelse assay. Effekten av ATX-101 og ATX-101+cisplatin på DU-145 var ikke forandret under hypoksiske forhold. Dette er et funn av klinisk betydning.

Den reduserte cellulære oksygentensjonen induserer metabolske forandringer som fremmer videre overlevelse og vekst av kreftceller. I denne oppgaven ble metabolske tilpasninger til hypoksi i DU-145 og glioblastoma astrocytoma U-87 MG-celler undersøkt. Metabolske konsekvenser ble evaluert 48 og 72 timer etter hypoksisk behandling. Endringer i eksometabolome ble analysert ved måling av glukose-, laktat-, og glutaminkonsentrasjoner i vekstprøver ved bruk av kjernemagnetisk resonans (NMR). Både hypoksiske og normoksiske inkuberte celler konsumerte store mengder av hoved karbon-, og energikilder, og omtrent halvparten av den konsumerte glukosen ble konvertert til laktat. Endometabolomet ble analysert ved hjelp av to target massespektrometriske (MS) metabolomanalyser: capIC-MS/MS og RP LC-MS/MS. Analysene viste at ingen hele metabolske sporveier åpenbart ble påvirket av hypoksisk behandling. Likevel ble noen metabolitter i glykolysen, sitronsyresyklusen og pentose fosfat sporveien markant og/eller statistisk signifikant forandret av den hypoksiske behandlingen. I sin helhet indikerer funnene at metabolske forandringer indusert av hypoksi ikke er fullstendig forstått, og motiverer til videre forskning på dette emnet.

# Contents

x

# Abbrevations

| | |
|---|---|
| 1,3BPG | 1,3-Bisphophoglycerate |
| 2HG | OH-glutarate |
| 3PG/2PG | 3-phosphoglycerate/ 2-phosphoglycerate |
| 6PG | 6-phosphoglycerate |
| a-KG | a-ketoglutarate |
| ACN | Acetonitrile |
| ADP | Adenosine diphosphate |
| AMP | Adenosine monophosphate |
| AMPK | AMP-activated protein kinase |
| Anova | Analysis of variance |
| APIM | AlkB homologue 2 PCNA-interacting motif |
| ATP | Adenosine triphosphate |
| CaplC | Capillary ion chromatography |
| CDP | Cytidine diphosphate |
| CE | Capillary electrophoresis |
| Cisplatin | Cis-diamminedichloroplatinum (11) |
| Cit | Citrate |
| CMP | Cytidine monophosphate |
| $CO_2$ | Carbon dioxide |
| CPP | Cell penetrating peptide |
| CTP | Cytidine triphosphate |
| DHAP | Dihydroxyacetone phosphate |
| dTDP | Deoxythymidine diphosphate |
| dTMP | Deoxythymidine monophosphate |
| DNA | Deoxyribonucleic acid |
| dTTP | Deoxythymidine triphosphate |
| E4P | Erythrose 4-phosphate |
| EC | Energy charge |
| EDAC | N-(3-Dimethylaminopropyl)-N'-ethylcarbodimide hydrochloride |
| EI | Electron impact ionization |
| ESI | Electrospray ionization |
| F1,6BP | Fructose 1,6-biphosphate |

| | |
|---|---|
| F1P | Fructose 1-phosphate |
| F6P | Fructose 6-phosphate |
| FBS | Fetal bovine serum |
| Fum | Fumarate |
| G1P/M1P | Glucose 1-phosphate/Mannose 1-phosphate |
| G6P | Glucose 6-phosphate |
| GA3P | Glyceraldehyde 3-phosphate |
| GC | Gas chromatography |
| GDP | Guanosine diphosphate |
| Glc | Glucose |
| Gln | Glutamine |
| GLUT | Glucose transporter |
| GL3P | Glycerol 3-phosphate |
| GBM | Glioblastoma multiforme |
| GMP | Guanosine monophosphate |
| GTP | Guanosine triphosphate |
| HIF | Hypoxia-inducible factor |
| HILIC | Hydrophilic interaction liquid chromatography |
| IBT | Department of Biotechnology |
| IA | Itatonic acid |
| IC | Ion-exchange chromatography |
| Icit | Isocitrate |
| IKM | Depatment of Cancer Research and Molecular Medicine |
| IMP | Inosine monophospate |
| ISTD | Internal standard |
| ITP | Inosine triphosphate |
| KOH | Potassium hydroxide |
| L | Liter |
| LC | Liquid chromatography |
| LDH | Lactate dehydrogenase |
| LMW | Low molecular weight |
| $LN_2$ | Liquid nitrogen |
| M | Molar ( mol/L) |
| M6P | Mannose 6-phosphate |

| | |
|---|---|
| Mal | Malate |
| MeOH | Methanol |
| MRM | Multiple reaction monitoring |
| MS | Mass spectrometry |
| MQ-water | Milli-Q water |
| m/z | Mass-to-charge ratio |
| $N_2$ | Nitrogen gas |
| NaCl | Sodium chloride/saline |
| $NAD^+$ | Nicotinamide adenine dinucleotide |
| NADH | Reduced nicotinamide adenine dinucleotide |
| $NADP^+$ | Nicotinamide adenine dinucleotide phosphate |
| NADPH | Reduced nicotinamide adenine dinucleotide phosphate |
| $NaHCO_3$ | Sodium bicarbonate |
| NaOH | Sodium hyroxide |
| $NH^+_4$ | Ammonia |
| NLS | Nuclear localization signal |
| NMR | Nuclear magnetic resonance |
| NTNU | Norwegian University of Science and Technology |
| $O_2$ | Oxygen |
| OAA | Oxaloacetate |
| OXPHOS | Oxidative phosphorylation |
| o-BHA | ortho-benzylhydroxylamine  hydrochcloride |
| OHpro | OH-proline |
| PBS | Phosphate buffered saline |
| PC | Principal component |
| PCA | Principal component analysis |
| PCF | Propyl chloroformate |
| PCNA | Proliferating cell nuclear antigen |
| PDH | Pyruvate dehydrogenase |
| PDK | Pyruvate dehydrogenase kinase |
| PEP | Phosphoenolpyruvate |
| PIP-box | PCNA-interacting peptide-box |
| PK | Pyruvate kinase |
| PPP | Pentose phosphate pathway |

| | |
|---|---|
| PTM | Post-translational modification |
| Pyr | Pyruvate |
| QqQ | Triple quadrupole |
| R5P | Ribose 5-phosphate |
| RCF | Relative centrifugal force |
| RL5P | Ribulose 5-phosphate |
| RNA | Ribonucleic acid |
| RP | Reversed phase |
| S7P | Sedoheptulose 7-phosphate |
| Succ | Succinate |
| TCA | Tricarboxylic acid |
| UDP | Uridine diphosphate |
| UMP | Uridine monophosphate |
| UPLC | Ultra performance liquid chromatography |
| UTP | Uridine  triphosphate |
| v/v | Volume by volume |
| X5P | Xylulose 5-phosphate |
| w/v | Weight by volume |

# 1. Introduction

Cancer is a collective term on a group of diseases [1], and a leading cause of death worldwide. In 2015 alone, more than 32000 incidents of cancer were registered in Norway, and over 5000 of these incidents were prostate cancer [2] .

Cancer is caused by a step-wise accumulation of gene mutations. One of the major hallmarks of cancer is sustained proliferative signalling. Whereas normal cells require growth-promoting signals to progress through the cell cycle, cancer cells overcome this growth factor dependency due to certain gene mutations [1]. Cancer cells can thus proliferate at a rapid rate. This rapid proliferation leads to an imbalance of cell replication and cell death, a feature that favours growth of a tumor [3]. The tumor cells frequently exhaust the oxygen supply, resulting in formation of tumor regions with low oxygen tension. The phenomenon of low oxygen tension is termed hypoxia [4]. In response to hypoxia, cancer cells elicit metabolic changes which enables further cell survival and growth under hypoxia [5]. Knowledge about these metabolic adaptions is important for understanding how hypoxic cancer cells survive, and may open new doors for targeting these cells in cancer therapy.

Tumor hypoxia has traditionally been viewed as a therapeutic concern. Several clinical and experimental studies have demonstrated that hypoxic cancer cells acquire resistance to commonly used cancer treatments, such as radiotherapy and chemotherapy [6]. Glioblastoma multiforme (GBM, grade IV astrocytoma) are among the most malignant brain tumors. The commonly found hypoxic regions in GBM promotes resistance to cancer therapy and worsen the clinical outcome [7]. An understanding of how hypoxia affects existing cancer treatments, allows improvement of anticancer therapy and thus patient survival.

## 1.1 Characteristics of Cancer Cell Metabolism

Cellular proliferation requires energy in form of adenosine triphosphate (ATP), macromolecules (nucleotides, amino acids, lipids etc.) and reducing power. Cancer cells are characterized by an excessive cellular proliferation which impose a large requirement for macromolecules. Normal healthy cells on the other hand, are generally not actively proliferating, and require only ATP to maintain normal cellular processes. To meet the requirements of cellular proliferation, cancer cells alter their metabolic pathways. The metabolism is altered as a result of multiple dysregulated intracellular signalling pathways, often caused by mutations in proto-oncogenes (i.e. gene that is converted to oncogene upon mutation) [8, 9].

The fact that cancer cells exhibit a distinct metabolism compared to normal cells was first observed by Otto Warburg in 1924. Under aerobic conditions, normal cells oxidize glucose to carbon dioxide ($CO_2$) and water ($H_2O$) through glycolysis and the citric acid cycle. The metabolism of glucose is coupled to production of a large amount of ATP by oxidative phosphorylation [10]. Under anaerobic conditions, normal cells rely on glycolysis for energy production, as oxidative phosphorylation requires oxygen. In anaerobic conditions, pyruvate produced by glycolysis is converted to lactate by lactate dehydrogenase (LDH) enzyme. Warburg discovered that some types of cancer cells exclusively use glycolysis for energy production, secreting large amount of lactate, even though enough oxygen is available to support oxidative phosphorylation (Figure 1) [11]. This phenomenon is termed "the Warburg effect", and the metabolism is termed aerobic glycolysis. Aerobic glycolysis is a less efficient way of generating ATP compared to oxidative phosphorylation, as degradation of one molecule glucose to lactate result in a net gain of 2 molecules of ATP, while oxidation of one molecule glucose in the citric acid cycle ultimately lead to the production of 36 molecules of ATP [12]. The origin of the aerobic glycolytic phenotype is not yet fully discovered. One explanation to the Warburg effect, is that glycolytic intermediates produced in glycolysis rapidly enter biosynthetic pathways, satisfying the increased requirement of macromolecules [13].
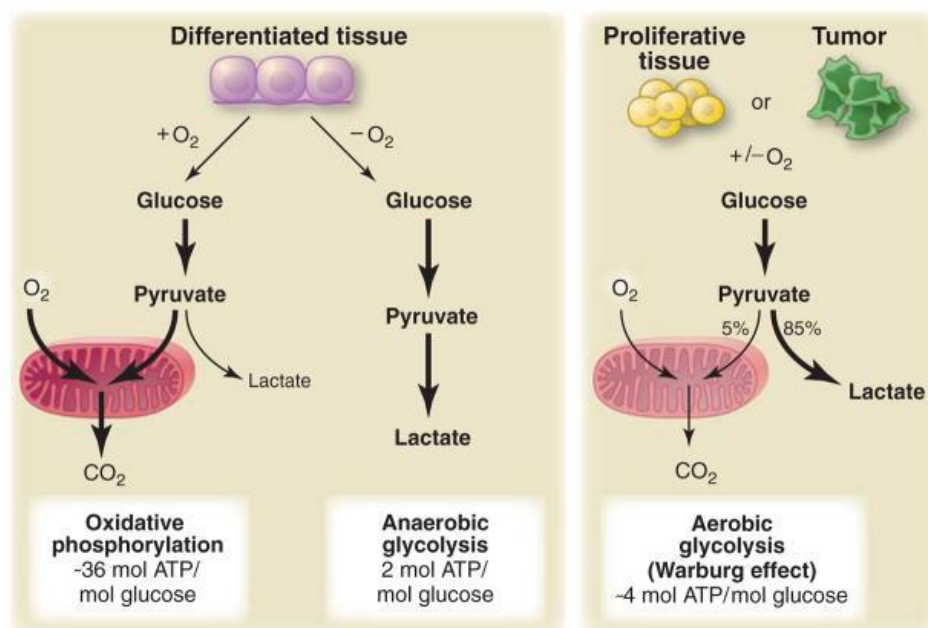
**Figure 1.1:** Illustration of differences in energy production between nonproliferating (differentiated) cells and proliferative cell/cancer cells. When oxygen is present, nonproliferating cells metabolize pyruvate completely by oxidative phosphorylation, while when oxygen is limited, nonproliferating cells generate lactate from pyruvate by anaerobic glycolysis. Generation of lactate cycles NADH back to NAD+, allowing continued glycolysis, but is less efficient than oxidative phosphorylation for ATP production. Proliferative cells and cancer cells convert to mainly glucose to lactate, although oxygen is present. Figure obtained from [12].

Furthermore, a large portion of glucose-derived carbons are diverted into the serine synthesis pathway and the pentose phosphate pathway [14]. Cancer cells frequently have up-regulated pyruvate kinase muscle enzyme 2 (PKM2), which exist as a dimer or tetramer. In its dimer form, PKM2 have low affinity for its substrate phosphoenolpyruvate. Activation of PKM2 block the glycolytic flux towards pyruvate production, and cause accumulation of glycolytic intermediates which are shuttled into biosynthetic pathways [15].

As most of the glucose-derived carbons are directed towards biosynthetic intermediates and lactate production, less is directed towards the triacylcarboxylic (TCA) cycle. In non-proliferating cells, the TCA cycle serves mainly to support bioenergetics. In comparison, carbons that enters the TCA cycle in proliferating cells are used as precursors for fatty acid and amino acid (and thereby nucleotides) synthesis. To support cellular proliferation, cancer cells can utilize glutamine as an alternative carbon source. Glutamine-derived carbon can be oxidized in the TCA cycle to support bioenergetics and replenish TCA intermediates, which can be used as anabolic building blocks [9]. Glutamine is also a nitrogen donor required for the *de novo* synthesis of nucleotides (purines and pyrimidines), and serves as the major nitrogen source for amino acid and lipid synthesis [16, 17].

## 1.2 Cancer Cell Metabolism under Hypoxic Conditions

Metabolic adaptions to hypoxia are elicited directly by the reduced oxygen availability and through indirect mechanisms such as activation of hypoxia-inducible factor 1 and 2 (HIF-1 and HIF-2) [5].

### 1.2.1 Hypoxia Inducible Factors

The metabolic adaption to hypoxia involves stabilization of hypoxia-inducible factor 1 and 2 (HIF-1 and HIF-2). HIF is a heterodimeric master transcription factor composed of one HIF-1β subunit and one of two α subunits (HIF-1α or HIF-2α). Whereas the HIF-1β subunit is constitutively transcribed and translated, the stabilization of the HIF-α subunit is post-translationally regulated by cellular $O_2$ levels [18-20]. Under normal oxygen (normoxic) conditions, HIF-α is hydroxylated on certain proline residues by HIF prolyl hydroxylases (PDH) and degraded by proteasome. When oxygen availability is reduced, proline residues become less hydroxylated and HIF-α accumulates and associate with HIF-1β. It is thought that HIF-α is maximally stabilized around 1% $O_2$. The HIF transcription factors bind to a consensus sequence 5'-(A/G) CGTG-3' named hypoxia-responsive elements (HREs) and activate transcription of several hypoxia-responsive genes. HIF-1α or HIF-2α have different expression profiles and different gene targets, causing the HIF-response to vary between cancer cell types [5, 21].

### 1.2.2 Mitochondrial Redox Status

Hypoxia directly alter the mitochondrial redox status. Reduced electron transfer to oxygen slows the electron transport chain, resulting in decreased reduced adenine dinucleotide (NADH) oxidation, and increased NADH/NAD+ ratio in the mitochondria. When NAD+ is limited, NAD+ consuming reactions in the TCA cycle are inhibited, and less NADH is transported via the malate-aspartate shuttle to the mitochondrial matrix. Under these conditions, cells become dependent upon glycolysis for energy production. To maintain an appropriate NADH/NAD+ ratio that favour glycolysis, pyruvate is reduced to lactate while NADH is oxidized. To prevent intracellular acidification and hence inhibition of glycolysis, lactate is excreted out of the cell through monocarboxylate transporters. HIF-1 support lactate production through up-regulating expression of lactate dehydrogenase A enzyme (LDH-A), which  reduce pyruvate to lactate [5].

Reactive oxygen species (ROS) are produced from metabolic reactions in the mitochondria. Under hypoxic conditions, the production of mitochondrial ROS increases. This is due to an imbalance between the input of electrons carried by NADH and reduced flavin adenine dinucleotide ($FADH_2$) and transfer of electrons to oxygen. The excessive production of ROS may oxidize and damage macromolecules. Nevertheless, HIF-1 counter the formation of ROS under hypoxia by decreasing the level of NADH and $FADH_2$ and by enhancing Complex IV (COX) effectivity. COX is a multimerix enzyme in the respiratory chain that catalyse the transfer of electrons to molecular oxygen. HIF-1 mediates replacement of subunit COX4-1 with subunit COX4-2, which increases the efficacy of COX under hypoxic conditions. By activating the gene encoding pyruvate dehydrogenase kinase 1 (PDK1), HIF-1 reduces the entry of pyruvate into the TCA cycle. PDK1 phosphorylates and inhibit the mitochondrial pyruvate dehydrogenase (PDH) enzyme that convert pyruvate to acetyl-CoA. In addition to shunt glucose towards lactate production, induction of PDK1 reduce the electron flow from NADH and $FADH_2$ to the mitochondrial respiratory chain [22, 23].

### 1.2.3 Glucose Fate

To sustain cellular proliferation under hypoxia, the glycolytic flux must increase significantly to compensate for the incomplete oxidation of pyruvate to $CO_2$ in the mitochondria. Generation of high glycolytic flux depends on an increased cellular uptake of glucose. Nevertheless, hypoxia through HIF-1, induces glucose transporters (GLUT1, GLUT2) [22]. Hypoxia through HIF-1, also induce glycolytic enzymes, among others hexokinase 1, phosphofructokinase-1 (PFK-1) and glyceraldehyde 3-phosphate dehydrogenase (GAPDH) [5]. Some cancer cells up-regulate glucose 6-phosphate dehydrogenase (G6PDH) under hypoxic conditions. G6PDH catalyse the conversion of glucose 6-phosphate (G6P) to 6-phosphogluconate (6PG), the entry step to the pentose phosphate pathway (PPP). Through a series of reactions, the PPP generates ribose 5-phosphate (R5P), used for synthesis of nucleotides and reduced nicotinamide adenine dinucleotide phosphate (NADPH) [24]. Production of NADPH through the PPP is thought to be important for regeneration of reduced glutathione (GSH) under hypoxic conditions. GSH cycle between oxidised and reduced forms, and the reduced form is a natural antioxidant that scavenge ROS in mitochondria [5, 25, 26].

### 1.2.4 Glutamine Fate

As a consequence of limited entrance of pyruvate into the mitochondria under hypoxic conditions, the reductive pathway of glutamine catabolism may be favoured to replenish the citrate pool. In this pathway, α-ketoglutarat (α-KG) is converted to isocitrate by isocitrate dehydrogenase 1 or 2 (IDH1, IDH2), and isocitrate is isomerized to citrate. Citrate is futher converted to acetyl CoA which act as a carbon source to fuel anabolic processes, such as fatty acid synthesis. The regulation of glutamine metabolism is not well understood, but it has been suggested that a high α-KG/citrate ratio favour the reductive pathway. The switch from oxidative to reductive glutamine metabolism involves HIF activation, but exactly how HIF induces a switch remains unclear [27]. Additionally, cancer cells with IDH mutations get the ability to convert α-KG to 2-hydroxyglutarate (2-HG), a potential oncometabolite. Interestingly, the level of 2HG was been shown increased in hypoxic glioblastoma cells [28].

## 1.3 Cisplatin in Cancer Therapy

Cis-diamminedichloroplatinum (cisplatin) is today a widely used DNA-damaging chemotherapautic agent for treatment of many types of cancer [29, 30]. The chemotherapeutic agent is administered intravenously, enters cells and is spontaneously activated to a form that binds more readily to its cellular targets. The activated cisplatin form is allowed to interact with nucleophilic sites of macromolecules, forming protein, RNA and DNA lesions [31]. Formation of DNA lesions interferes with replication and transcription. DNA lesions can be recognised by DNA repair pathways, or activate the apoptotic pathway, resulting in cell death [32]. The goal with cisplatin treatment is generation of DNA lesions, followed by induction of apoptosis in cancer cells, [33]. As cancer cells are characterized by mutations in DNA repair pathways and in cell regulatory systems causing rapid growth, these cells are more susceptible to DNA damages compared to normal cells. However, a major disadvantage of cisplatin, are toxic side effects on non-targeted tissues because of lack of cancer cell specificity. Undesirable and adverse side effects include nephrotoxicity (kidney damage), neurotoxicity (nerve damage) and ototoxicity (hearing loss) [34]. These side effects, especially nephrotoxicity, limits the allowed dose of cisplatin. Another major limitation of cisplatin is development of cisplatin resistance, which reduces its clinical efficacy [35].

## 1.4 Proliferating Cell Nuclear Antigen

Proliferating cell nuclear antigen (PCNA) is a protein belonging to the DNA sliding clamp protein family. PCNA forms a ring-shaped complex which encircles DNA and slide freely in both directions. PCNA serves as a binding platform for protein-protein and protein-DNA interactions that occur during the replication process [36]. PCNA has also several interaction partners involved in cytosolic cellular processes, and has been linked to regulation of apoptosis, metabolism and antitumor immunity [37-39]. Proteins bind to PCNA via two sequence motifs, a PCNA-interacting peptide sequence (PIP box) and AlkB homologue 2 PCNA-interacting motif (APIM). These sequence motifs interact with the same pocket of PCNA, and PCNA-interacting proteins hence compete for binding. Proteins involved in DNA replication bind mainly to PCNA via PIP box, whereas proteins involved in the genotoxic stress response, like DNA repair proteins, bind to PCNA via APIM. Posttranslational modifications (PTMs) on PCNA can increase binding affinity of APIM-containing proteins. Cancer cells are stressed as a consequence of genomic mutations, a state which can induce PTMs that increases PCNAs binding affinity for APIM-containing proteins [40]. Targeting PCNA could be a strategy for cancer therapy, as it interacts with numerous proteins and has a vital role in regulation of cellular homeostasis [41].

ATX-101 is a synthetic produced APIM-containing peptide. The peptide has a cell penetrating tail that enables it to enter cells and bind to PCNA. ATX-101 hence prevents APIM-containing proteins that normally interact with PCNA from binding. It has been shown that ATX-101 induces apoptosis and sensitize cancer cells to DNA damaging agents. The effects of ATX-101 are mediated by its ability to inhibit PCNA interactions (Figure 1.2) with APIM containing DNA repair proteins and thus blocking the normal cellular defence mechanism to DNA damage. The DNA damages introduced by chemotherapeutics are hence not repaired, leading to apoptosis. [41].
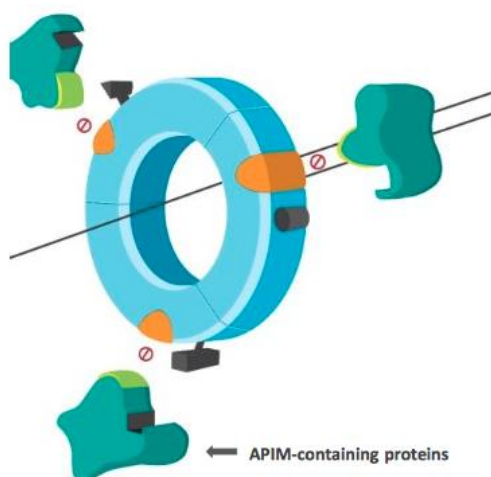
**Figure 1.2:** ATX-101 contain an APIM sequence (orange), which allows it to bind to PCNA (blue) and prevent APIM-containing proteins (green) from binding. Figure is obtained from APIM Therapautics.

ATX-101 is also capable of inducing cellular apoptosis as a single agent, depending on the type of cell line. For instance, haematological cancer cell lines, such as JJN-3, are highly sensitive to ATX-101 as a single agent. As a general tendency, cancer cells are more sensitive to ATX-101 than normal cells. Cancer cells are characterized by genomic instability, a feature that may cause PTM of PCNA to bind APIM-containing proteins with high affinity. As normal cells are not stressed to the same extent and do not posses this specific PTM, ATX-101 preferably targets cancer cells. The exact nature of this PTMs is not yet known [41, 42].

## 1.5 Metabolome and Metabolomics

Metabolism is a collective term on all chemical reactions that occur in a biological system, and include both anabolism and catabolism. The former represent energy-requiring synthetic reactions whereas the latter represent energy-yielding degradative reactions. The term metabolome is defined as the complete set of all low-molecular weight (<1500 Da) metabolites in a biological system. The metabolome comprises both the endometabolome and the exometabolome. The former represents metabolites excreted from a biological system, and the latter represent intracellular metabolites in a biological system [22, 43]. Exometabolome analysis is used for characterization of consumption of extracellular substrates and production and excretion of metabolic products [44]. The endometabolome is considered to be the "true" metabolome, and may reflect cellular physiological state.

The term metabolomics refers to analytical techniques used for identification and quantification of metabolites in a biological sample [45]. Whereas genomics, transcriptomics and proteomics involves analysis of single genes, mRNA and proteins respectively, metabolomics is the study of biochemical activity [44]. Metabolites are final products of gene transcription and therefore defines the cellular phenotype [44]. Studying metabolites is hence useful for understanding disease phenotypes [43].

Several approaches for investigating the metabolome exist. These approaches include metabolic profiling, metabolic fingerprinting and metabolic footprinting. Metabolic profiling involves analytical methods for identification of a class of compounds or metabolites in a particular pathway. Metabolic fingerprinting is the unspecific analysis of patterns of intracellular metabolites, while metabolic footprinting is the unspecific analysis of extracellular metabolites [46]. Metabolomic strategies includes both targeted and non-targeted analysis of metabolites. Targeted metabolomics involves measure of a defined group of metabolites, while non-targeted metabolomics involves analysis of all measurable metabolites in a sample [45].

Metabolic profiling is challenging as metabolites are diverse in their physical and chemical properties. A single technique that can be used to identify all metabolite classes (i.e. amino acids, sugars, lipids, nucleotides, organic acids and phosphorylated metabolites) does not currently exist. Therefore, a combination of analytical approaches is applied to increase the coverage of identified metabolites [43]. Furthermore, rapid turnover of metabolites requires fast quenching (i.e. cool down of metabolism) of metabolism and extraction of metabolites [46]. Metabolic quenching leads to a "snapshot" of the metabolome at a certain cellular time point.

### 1.5.1 Analytical Methods

Detection and analysis of the metabolome relies on methods like nuclear magnetic resonance (NMR) and mass spectrometry (MS). To date, these are two main techniques used to investigate the metabolome [47]. In this master project, established MS profiling and NMR methods were utilized, and these technologies will be described briefly.

MS involves 1) ionization of atoms or molecules from a biological sample, 2) separation of ions based on their mass-to-charge ratio (m/z) as they pass through a mass filter, and 3) detection of separated ions [47]. Several different ion sources, mass filters and detectors exist. The choice of analytical setup depends on which metabolite class is being analysed, whether the analysis is qualitative or quantitative and on the separation step used.

A separation step is generally accomplished before MS to improve sensitivity (detection of low abundance metabolites) and selectivity (separation of metabolites). The most commonly used separation techniques are liquid and gas chromatography columns (LC and GC respectively). Chromatography separation involves interaction of different metabolites with a stationary phase inside the chromatography column, causing retention of metabolites to different extents based on their chemical properties. The retention time (the time that metabolite requires to pass through the column) is used together with the m/z values to generate the two axis of the spectral data [47]. Whether GC-MS or LC-MS is chosen depends on the chemical nature of the metabolites in the sample.

GC-MS utilize a gas that carries metabolite through a column, and is used for separation of small, volatile compounds. GC-MS can also be applied to non-volatile compounds by including chemical derivatization step prior to analysis to provide volatility [46]. When GC is used for separation, the ionization technique applied is typically electron impact ionization (EI).

LC-MS utilize a solvent that carries metabolites through a column and allows separation of non-volatile and complex extracts (i.e. polar and ionic compounds) [48]. Amino acids can be analysed when a derivatization step involving propyl chloroformate is included. Normal phase (NP) and reverse phase (RP) are two types of LC. NP utilize a polar stationary phase and a hydrophobic mobile phase, whereas the RP utilize a hydrophobic stationary phase and a polar mobile phase [48]. Hydrophilic interaction LC (HILIC) is a sub NP technique used to separate small polar compounds [49]. A typical LC-MS system consist of metabolite separation by LC, followed by detection of metabolites by electrospray ionisation (ESI) mass spectrometer [50].

Ion-exchange chromatograpy (IC) and capillary electrophoresis (CE) are less common separation techniques. CapIC consist of a capillary version of IC coupled to MS. CapIC is applied to separate low molecular phosphometabolites and nucleotides. CapIC-MS/MS has been demonstrated to give a high resolving power of phosphorylated metabolites compared to RP LC and HILIC [51]. As a result of several combination of ionization techniques, mass filters, detectors and separation methods, numerous analytical setups are available.

NMR is based on energy absorption and re-emission of the atom nuclei because of variations in a magnetic field. The metabolomics data obtained depend on the atom nuclei being targeted. Hydrogen is the most commonly targeted nucleus ($^1$H-NMR) in biological samples because of its natural abundance. The NMR spectral data allows allows for quantification of metabolites, and provides information about molecular structure. The peak generated by a molecule can be used as an indirect measure of the quantity of the metabolite in the sample, whereas the pattern of the spectral peak gives information about the molecular structure of the metabolite [47]. All metabolites in a sample can theoretically be detected using NMR. In addition, NMR can be performed without using separation steps (as in MS). Compared to MS, NMR is a less sensitive detection technique, and the use of NMR is restricted by the minimum concentration of individual metabolites [52].

## 1.6 Aim of Study

The first aim of this MSc project was to investigate whether the efficacy of ATX-101, both as a single agent and in combination with cisplatin, was altered in a hypoxic environment. This aim was achieved by performing cell viability assays on hypoxic treated human prostate DU-145 and rat glioloblastoma F98 cells.

The main aim of this MSc project was to expand the current understanding of hypoxia induced metabolic adaptions in DU-145 and human glioblastoma astrocytoma (grade IV) U-87 MG cells, using established MS and NMR methods.

# 2. Materials and Methods

## 2.1 Cell Cultivation

The cell lines DU-145 and F98 were received in February 2016 from IKM, DMF at NTNU, whereas the U-87 MG cell line was received in August 2016 from European Collection of Cell Cultures (ECACC, UK) via Sigma-Aldrich. All cell lines are adherently, and were maintained in ventilated and sterile cell culture flasks (VWR), treated to allow attachment of cells. Cells were cultivated in small culture flasks (75 cm$^2$) during the first part of the project, and in large culture flasks (182,5 cm$^2$) during the second part. The culture medium Minimum Essential Medium Eagle (Sigma-Aldrich) was used for U-87 MG cell line, the culture medium RPMI-1640 Medium (Sigma-Aldrich) for the DU-145 cell line, whereas Dulbecco's Modified Eagle's Medium (Sigma-Aldrich) was used for the F98 cell line. Culture media were supplemented with 50 mL fetal bovine serum (FBS, Sigma-Aldrich), 5 mL Amphotericin B (250 µg/mL, Sigma-Aldrich), Gentamicin (10 mg/mL, Sigma-Aldrich) and L-glutamine (200 mM, Biochrom). Cells were cultured at 37°C in a humidified atmosphere of 5% $CO_2$.

To keep cells at an optimal density for continued growth, cells were subcultured three times a week before they reached 100% confluence (surface area completely covered by cells). The old cell culture medium was removed and the cell monolayer washed with preheated phosphate buffered saline (PBS). A preheated (37°C) trypsin solution (Biochrom AG, 0,25%, without $Ca^{2+}$ and $Mg^{2+}$) was added, and the flask incubated for three minutes to allow cell detachment. Culture medium was added, cells were resuspended, and a certain amount of the cell suspension was removed to obtain split ratios ranging from 1:4 to 1:10 for DU-145 cells, 1:6 to 1:10 for F98 cells and 1:2 to 1:5 for U87-MG cells. Volumes of PBS, trypsin and culture media applied to the different culture flasks used in this study are presented in Table 2.1.

**Table 2.1:** Overview of the different volumes of PBS, trypsin and culture media added to the different culture flask types (small, large). Surface areas of the flask types are given.

| Culture flask | Area (cm$^2$) | PBS (mL) | Trypsin (mL) | Culture media (mL) |
|---|---|---|---|---|
| Small | 75 | 10 | 1 | 15 |
| Large | 182,5 | 25 | 3 | 46,5 |

**2.1.2 Cell Freezing and Thawing**

Master cell banks were established from early passages of each cell line by applying a general technique of cryopreservation for adherent cells in liquid nitrogen (-196°C). The freezing procedure was initiated when the cell culture was dense (80-90% confluent). Cells were harvested, and counted by the use of an automated Cell Count (Moxi Z, Orflo). Freezing medium was made by diluting sterile-filtered dimethylsulfoxide (DMSO, Sigma-Aldrich, 10%) in FBS to obtain 20% (v/v) DMSO. The cell culture volume needed to obtain $1*10^6$ cells/mL per vial was transferred to a sterile centrifuge tube (VWR, 15 mL) and centrifuged (130 RCP, 5 min, 8°C). The supernatant was removed from the tube, and freezing medium was applied to obtain a dilution of 1:2 cell suspension to freezing medium. Cells were resuspended in the freezing medium, and cell suspension was aliquoted into sterile plastic vials (VWR, 1.5 mL) with 1 mL per vial. Vials were cooled in a controlled rate freezing apparatus (Mr. Frosty) at a rate of 1°C/min until the temperature reached -80°C. The frozen vials were then transferred to permanent storage in the vapour phase of a liquid nitrogen tank (-196°C).

Vials were thawed through the progress of the study to create a new working culture stock. The frozen vial was removed from the liquid nitrogen tank, the exterior washed with 70% (v/v) ethanol in MQ-water and the cap carefully removed to release any nitrogen gas which might be present. The vial was then capped and quickly placed in a preheated water bath (37°C). Only the vial up to the cap was immersed to prevent contamination or leakage. When about 80% of the ice had thawed (after 1-2 min), the cell suspension was transferred to a culture flask (VWR, 75 cm$^2$). Appropriate culture medium was applied drop-wise to the culture flask to obtain a concentration of 0,5% DMSO, avoiding potential DMSO toxicity. The culture flask was then incubated (37°C, 5% $CO_2$), and further examined microscopically for adherent cells after 4 hours. When a large majority of the cells were attached to the flask surface the culture medium was changed to remove traces of DMSO.

## 2.2 Experimental Designs – Part 1

### 2.2.1 Cell Growth under Hypoxic Conditions

A study was performed to determine DU-145 and F98 cell growth during hypoxic (1% $O_2$) versus normoxic incubation (~21% $O_2$) conditions. Cells ($3x10^4$ cells/mL) were seeded on eight 96-well microtiter plates (Sigma-Aldrich) and pre-incubated in an atmospheric incubator at 37°C and 5% $CO_2$ for 24 hours. Four plates were then placed in a hypoxic SubChamber System (1% $O_2$), and four plates were placed in an atmospheric incubator (~21% $O_2$) at 37°C and 5% $CO_2$. A potential hypoxic effect on cell growth was investigated 24, 48, 72 and 96 hours after treatment exposure by MTT assay. The SubChamber System is described more detailed in Appendix A.1.

### 2.2.2 Exposure to ATX-101 and Cisplatin

A series of stress response studies were conducted to optimize treatment concentrations of ATX-101 and cisplatin on DU-145 and F98 cells. The experimental setup included four different treatments: control, ATX-101 (provided by IKM), cisplatin (provided by IKM) and ATX-101+cisplatin. Cells ($3x10^4$ cells per mL) were seeded on four 96-well microtiter plates (Sigma-Aldrich) and incubated at 37°C and 5% $CO_2$ for four hours to allow cell attachment. Treatment was then added to 6/8 replicate wells on each microtiter plate, and cells incubated at 37°C and 5% $CO_2$. The treatment effect on cell growth was investigated 24, 48, 72 and 96 hours after treatment exposure by MTT assay. Treatment concentrations applied to DU-145 and F98 cells are presented in Table 2.2.

**Table 2.2** Overview of treatments (ATX-101, cisplatin and ATX-101+cisplatin) applied to DU-145 and F98 cells. Treatments are listed with final concentration in cell culture dish. Each treatment was added to 6/8 replicate wells on each microtiter plate. The control represents untreated cells.

| Cell line | Sample treatment | Concentration in dish [µM] |
|---|---|---|
| DU-145 | Control | - |
| | ATX-101 | 6, 8 |
| | Cisplatin | 0.125, 0.25, 0.5 |
| | ATX-101 + cisplatin | 6+0.125, 6+0.25, 8+0.125, 8+0.25, 6+0.5, 8+0.5 |
| F98 | Control | - |
| | ATX-101 | 6, 8.5, 11, 13, 14, 15, 16 |
| | Cisplatin | 0.15, 0.2, 0.25, 0.3, 0.4, 0.5 |
| | ATX-101 + cisplatin | 6+0.25, 6+0.5, 16+0.25, 16+0.5, 8,5+0.15, 8,5+0.3 |
| | | 15+0.15, 15+0.3, 11+0.2, 11+0.4, 13+0.2, 13+0.4 |
| | | 14+0.2, 15+0.2, 15+0.3 |

### 2.2.2 Exposure to ATX-101 and Cisplatin under Hypoxic Conditions

A study was performed to investigate the efficacy of ATX-101, as a single agent and in combination with cisplatin, on DU-145 and F98 cells under hypoxic incubating conditions. The experimental setup included four different treatments: control, ATX-101, cisplatin and ATX-101+cisplatin, incubated in parallels under hypoxic and normoxic conditions. Cells ($3x10^4$ cells per mL) were seeded on eight 96-well microtiter plates (Sigma-Aldrich) and incubated for four hours to allow cell attachment. Hereafter, each treatment was added to 6/8 replicate wells on each microtiter plate, and cells were immediately incubated at 37°C and 5% $CO_2$ under either hypoxic (1% $O_2$) or normoxic (∼21% $O_2$) conditions. The treatment effect on cell growth under hypoxic conditions was investigated 24, 48, 72 and 96 hours after treatment exposure by MTT assay. The concentrations of ATX-101 and cisplatin applied to DU-145 and F98 cells are presented in Table 2.3.

**Table 2.3:** Overview of treatments (ATX-101, cisplatin and ATX-101+cisplatin) appied to DU-145 and F98 cells. Treatments are listed with final concentration in cell culture dish. Each treatment was added to 6/8 replicate wells on each microtiter plate. The The control represents untreated cells.

| Cell line | Sample treatment | Concentration in dish [μM] |
|---|---|---|
| DU-145 | Control | - |
| | ATX-101 | 8, 10 |
| | Cisplatin | 0.25, 0,5 |
| | ATX-101 + Cisplatin | 8+0.25, 8+0.5, 10+0.25, 10+0.5 |
| F98 | Control | - |
| | ATX-101 | 12, 13, 14, |
| | Cisplatin | 0.2 |
| | ATX-101 + Cisplatin | 12+0.2, 13+0.2, 14+0.2 |

## 2.3 MTT Assay

For monitoring effects of hypoxic incubation and/or ATX-101 and ATX-101 treatment, on DU-145 and F98 cells, 3-(4,5-dimethylthiazol-2-yl)-2,5-diphenyltetrazolium bromide (MTT) reduction assays were performed. The MTT assay is based on the conversion of yellow water-soluble MTT into a purple colored formazan product by viable cells with active metabolism. The quantity of formazan is directly proportional to the number of viable cells. Thus, by measuring absorbance at 570 nm (maximum absorbance of formazan), the number of viable cells can be found.

After 24, 48, 72 and 96 hours of hypoxic incubation and/or ATX-101 and ATX-101+cisplatin exposure, 100 µL medium was removed from each well and 100 µL MTT-solution (5 mg/mL, Sigma-Aldrich) was applied. Plate(s) were further incubated for four hours in the atmospheric incubator (37°C, 5% $CO_2$). MTT-containing medium (130 µL) was then removed from each well while taking care not to remove any crystals at the bottom of the wells. Isopropanol-HCl (100 µL) was applied to each well, and the plate covered with aluminium foil and vigorously mixed for 1 hour. Complete solubilisation of formazan crystals was then confirmed microscopically. Optical density in each well at 565 nm was measured using a microplate reader (Tecan Inifinite M200 Pro).

The MTT-solution applied was prepared by dissolving 500 mg MTT in sterile PBS. The solution was sterilised by filtration, wrapped with aluminium foil and stored in the refrigerator (4 °C). The reader is referred to Appendix A.2 for theory behind the MTT assay.

## 2.4 Experimental Designs – Part 2

A study was performed to investigate whether incubation in a hypoxic environment cause metabolic alternations in DU-145 and U-87 MG cells. Hypoxic and normoxic incubating conditions are hereafter referred to as treatments. The experimental setup consisted of hypoxic and normoxic treatment, and a time series of 48, 72 and 96 hours (in total 6 sample groups). The time series applied was inspired by other scientific performed studies on hypoxia induced metabolic alternations. One biological replica with four technical replicas was included in this study.

At day -1, cells were plated on 36 cell culture dishes (VWR, 63,6 cm$^2$) in densities of $2*10^5$ cells per plate for DU-145 and $4,5*10^5$ cells per plate for U-87 MG. Culture dishes were placed in an atmospheric incubator at 37°C and 5% $CO_2$ for 24 hours to allow cell division without stress. Old medium was then removed, and fresh medium applied. Fresh culture medium was collected and stored in the freezer, for use as 0 hour sample in exometabolome analysis. Hereafter, 18 culture dishes were placed in a hypoxic chamber (1% $O_2$), and 18 placed in an atmospheric incubator (~21% $O_2$). After incubating cells for 48 hours, sampling and sample preparation was performed on four hypoxic and four normoxic treated cell culture dishes.

In parallel, cell counts were performed on two hypoxic and two normoxic treated cell culture dishes. The remaining dishes were incubated for another 24 and 48 hours before repeating the procedure of sampling and cell counting. The steps from cell seeding until sampling is illustrated in Figure 2.1.
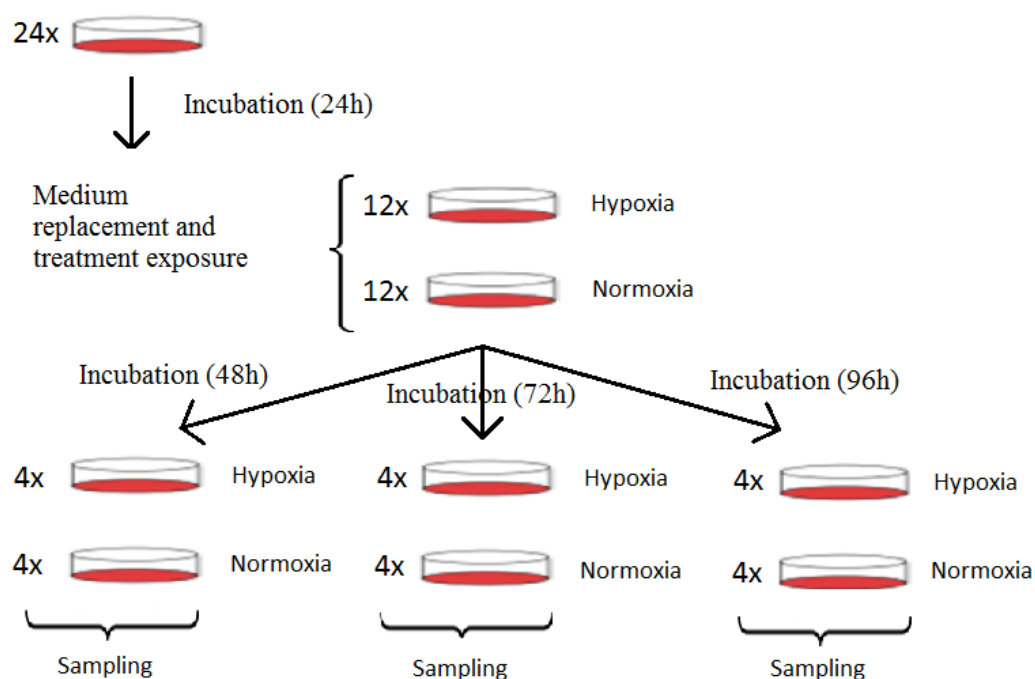
**Figure 2.1.** Overview of the steps from cell seeding until sampling. Dishes used for cell counting are not included in this illustration.

## 2.5 Sampling – Quenching and Metabolite Extraction

The sampling procedure consist of several consecutive steps including; quenching, washing and removal of medium and extraction of metabolites.

**Quenching**

One culture plate was sampled at a time, and the procedure was quickly performed to avoid alternations in metabolite pools, such as degradation of metabolites. First, quenching was initiated by placing the cell culture on a frozen metal block (-80°C). To achieve analysis of both intra- and extracellular metabolites, cells were separated from the culture medium (exometabolome) by pouring the culture media into a falcon tube and temporarily storing it on ice. The cell culture plate remained placed on the metal block in the next experimental steps. To remove extracellular metabolites, which may otherwise contaminate the endometabolome, cells were washed in three successive steps: first by NaCl (5 mL, 0,9%), then by NaCl (5 mL, 0,025%) and finally by Milli-Q-water (5 mL), all stored on ice. Cells were detached from the culture plate by adding cold ACN/MQ-water (10 mL, 50 vol%) and applying a cell scraper (VWR). Through careful and thorough scraping it was made sure that

17

as few as possible cells remained attached to the plate. Cells were collected in a falcon tube, and another cold ACN/MQ-water solution (5 mL, 50 vol%) was applied to wash the plate. This solution was collected in the same tube, and the tube was immediately placed in $LN_2$ and stored in the freezer (-80°C). Figure 2.2 illustrates the sampling procedure.
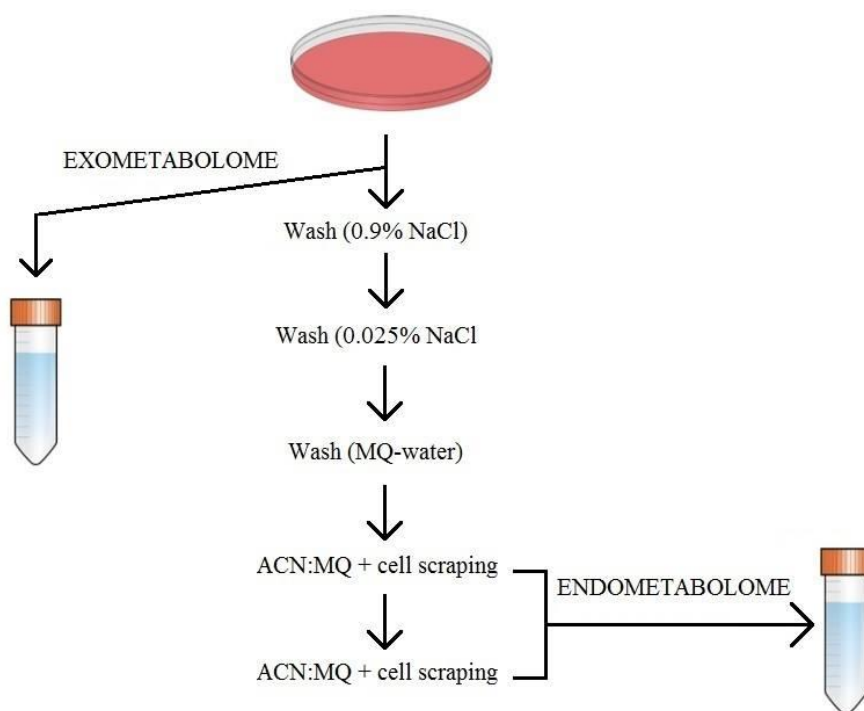


**Figure 2.2:** Overview of the sampling procedure performed on treated cell culture dishes. Culture medium (exometabolome) was collected, plates washed, and cells detached and collected (endometabolome) by scraping plates and adding ACN:MQ.

The tubes for exometabolome analysis were centrifuged (130 rcf, 5 min, 0°C), and the supernatant distributed into two separate tubes (VWR, 15 mL) with 2,5 mL in each tube. The exometabolite tubes were stored in the freezer (-20°C) until freeze-drying. Tubes were freeze-dried to obtain concentrated metabolites. A condenser of temperature -102/-105 °C and a system vacuum (SP scientific, BenchTop Pro) was applied. Prior to freeze-drying, tubes were collected from the freezer, capped with lids with holes and temporarily placed in $LN_2$. Zero hour medium samples also went through the same freeze-drying procedure. Freeze-dried samples were further stored at -20°C until additional preparation prior to NMR analysis.

**Metabolite Extraction**

Extraction of intracellular metabolites were aided by 3 freeze-thaw cycles. Frozen endometabolome tubes were collected and freeze-thawed by cycling tubes between an ethanol bath (0°C) and a $LN_2$ bath (-196°C), repeating each cycle three times. Tubes were vortexed between each freezing and thawing step to disrupt the cell membrane and facilitate metabolic leakage. The samples were pelleted by centrifugation (4500 rcf, 5 min, 0°C) of tubes, and the supernatant distributed into three separate tubes (VWR, 15 mL) with 4 mL in each tube. The endometabolite tubes were stored in the freezer (-20°C) until freeze-drying using the same instrumentation as on exometabolome tubes. Freeze-dried samples were further stored at -20°C until additional preparation prior to MS analysis.

## 2.6 Cell Counting

Two hypoxic and two normoxic treated cell culture dishes were removed from incubation and used for cell counting. Cell counting was performed to detect hypoxic treatment effect on cell growth, and to use for normalization of metabolome data. Cell cultures were washed with pre heated (37°C) PBS (7 mL, Oxoid), detached by trypsinization (1 mL, trypsin solution, Biochrom) and resuspended in appropriate culture medium (10 mL). Cell suspension (1 mL) was then collected to determine the cell number by the use of an automated cell counter (Moxi Z, ORFLO).

## 2.7 Nuclear Magnetic Resonance Analysis

The freeze-dried exometabolome samples were used for quantification of D-glucose, L-lactate and L-glutamine in by NMR analysis. All technical replicas within each sample group were analysed.

**Preparation for NMR**

Deuterium oxide ($d_2O$, Sigma Aldrich) was used as a solvent for freeze-dried samples. Freeze-dried samples were dissolved in 600 µL deuterium oxide ($d_2O$, Sigma Aldrich), and the solution vortexed. 500 µL of the dissolved exometabolites were transferred to a labelled NMR tube (Sigma Aldrich), and the tube capped. Creatine (Sigma Aldrich) was used as an external standard in the NMR procedure to allow for quantification. A solution of 70 mM creatine was prepared by dissolving 48,5 mg creatine in 5 mL $d_2O$ in a centrifuge tube (15 mL). The tube was vortexed and 500 µL solution transferred to a labelled NMR tube. Medium

collected at day 0 also went through NMR preparation and analysis. Samples were stored cold (4°C) until analysis.

**NMR Analysis of Glucose, Lactate and Glutamine**

NMR spectra of samples and external standard was recorded using a 400 MHz Avance III HD instrument equipped with a 5mm-SmartProbe z-gradient probe and Sample case. The 400 MHz Avance III HD instrument has an automatic sample changer with 24 positions. NMR tubes were wiped with paper wipes and placed in available slots in the autosampler. Samples were run in a randomized order, using a method which detect 1H nuclei. After NMR spectra recording, samples were stored cold (4°C) in case of re-analysis.

**2.7.1 Data Processing and Analysis**

Raw data obtained from exometabolite NMR analysis was processed using the NMR software package Topspin from Bruker. This software was used for quantification of glucose, lactate, glutamine and creatine from NMR data. Results were displayed as spectra, showing relative abundance of detected $H^1$ ions as a function of magnetic field strength (parts per million, ppm). Parameter settings were processed for all spectra: spectras were transformed with line broadening 0,3 Hz, phased and the baseline corrected. The creatine peak was integrated and set as eretic reference. Glucose, lactate and glutamine peaks were further processed: manual baseline correction close to peak of interest was performed, and peak was integrated manually. Raw datas were further exported to excel and normalized to the cell number in respective samples.

## 2.8 Target Mass Spectrometric Analysis

Freeze-dried metabolic extracts went through additional preparation prior to MS analysis. For quantification of amino acids, samples were derivatized by PCR. For quantification of phosphorylated metabolites and low-molecular weight organic acid, samples were spin filtered.

### 2.8.1 RP LC-MS/MS Analysis

**Derivatization**

Amino acids were quantified in freeze-dried metabolite extracts utilizing RP LC-MS/MS. Because of the polar nature of amino acids, a propyl chloroformate (PCF) derivatization step was preformed prior to chromatographic separation to improve their interaction with the hydrophobic column. All technical replicas within each sample group were analysed.

A dilution series (100, 25, 6.25, 1.56 and 0.39 µM) of a standard mixture (STD-mix, 1mM) in MQ-water (18.2 MΩcm) was prepared. The STD-mix contain 18 amino acids, which are given in Table H.1 in Appendix H.1.2. Each diluted STD-mix (200 µL) was transferred to a HPLC vial (Sigma Aldrich), NaOH (200 µL, 2 M, Sigma-Aldrich) added and the vial vortexed to mix. A blank sample of NaOH (400 µL, 1 M) was also prepared. The dilution series of STD-mix and the blank sample of NaOH were included in the MS analysis to enable absolute quantification of amino acids in metabolite extracts. Freeze-dried metabolite extracts were dissolved in NaOH (2 mL, 1 M, Sigma-Aldrich) and centrifuged (2 min, 180 rcf) in room temperature. Dissolved metabolite extracts (400 µL) were transferred to HPLC vials and the remaining extracts were stored in the freezer (-20°C).

The following derivatization procedure was preformed on all metabolite extracts, the dilution series of STD-mix and the blank sample of NaOH. Firstly, n-propanol (333 µL, Sigma-Adrich) and pyridine (67 µL, Sigma-Aldrich) was added. For one glass vial at a time, the derivatization reaction was initiated by adding PCF (40 µL, Sigma-Aldrich) and vortexing (30 sec). This step was performed twice. Hereafter, heptan (400 µL, Sigma-Aldrich) and $NaHCO_3$ (400 µL, 50 mM) was added and the the solution vortexed to obtain phase separation. Upper heptan phase (50 µL) containing derivatized metabolites was transferred to a new HPLC vial. Solvent was evaporated by flushing gently with $N_2$. Dry samples were reconstitured in 1:2 MQ-water:methanol (meOH) ammonium formate (400 µL, 10 mM), and reconstituted sample was transferred to a HPLC vial with insert. Samples were analysed using caps with holes. Remaining samples were stored in the freezer (-20°C) with cap without holes.

**RP LC-MS/MS analysis**

The RP LC-MS/MS instrumentation consisted of a Waters Acuity I-Class ultra performance liquid chromatography (UPLC) system coupled to a Waters TQ-S triple quadrupole (QqQ) mass spectrometer operated in positive electrospray ionization (ESI+) multiple reaction

monitoring (MRM) mode (UPLC-QqQ(ESI+)-MS). Sample aliquots (1 µL) were injected onto a Phenomenex EZ faast AAA-MS column (250x0,2 mm) with column particle size of 4 µm and temperature of 25°C. MQ-water and MeOH, both with 10 mM ammonium formate (Sigma-Aldrich) was applied as eluting solvents with a constant flow rate of 250 µL/min. The elution gradient as a function of time is given in Appendix H.1.1. Details about the MS settings can be obtained from supervisor P. Bruheim.

### 2.8.2 CapIC-MS/MS Analysis

**Spin filtration**

Phosphorylated metabolites and low molecular weight organic acids in freeze-dried metabolite extracts were quantified utilizing capIC-MS/MS. A spin filtration step was performed prior to MS analysis to remove compounds of molecular weight larger than 3 kD. Two technical replicas (parallel 1 and 2) of each sample group were analysed.

A dilution series (10000, 7500, 5000, 2500, 800, 200, 50, 10 nM) of a standard mixture (STD-mix) was prepared. The STD-mix contain various phosphorylated metabolites and a few organic acids given in table I.1 in Appendix I.1.2. 150 µL of each diluted standard-mix was transferred to a HPLC vial with insert, 10 µL internal standard (ISTD) containing $^{13}$C, $^{15}$N-AMP, $^{13}$C, $^{15}$N-ATP, d4-Succinate and d4-Citrate was added and the vials vortexed. In addition, a blank sample of 160 µL MQ-water (18.2 MΩcm) was prepared in a HPLC vial with insert. The dilution series of STD-mix with ISTD and the blank sample of MQ-water were included in the MS analysis to enable absolute quantification of phosphorylated metabolites and organic acids in metabolite extracts.

Freeze-dried metabolite extracts were collected from the freezer and kept on ice to prevent enzyme activation. Freeze-dried metabolite extracts were dissolved in 400 µL cold MQ-water (18.2 MΩcm) and centrifuged (10 min, 4500 rcf, 0°C) to wash tube-walls. Dissolved metabolite extract (370 µL) was transferred to a 3-kD-MW-spin cut-off-filter (VWR) and the tube centrifuged (10 min, 10000 rcf, 0°C). Filtrate (150 µL) was transferred to a HPLC vial with insert (VWR). Tubes were once more centrifuged (10 min, 10000 rcf, 0°C) and another 150 µL filtrate was transferred to HPLC vials without inserts. Vials without inserts were stored at -20°C. ISTD was added to vials containing filtered metabolite extracts, and the vials vortexed.

**CapIC-MS/MS analysis**

The capIC-MS/MS instrumentation consists of a capillary ion chromatography (Thermo Dionex ICS-4000 Capillary High Pressure Ion Chromatography) coupled to a Waters TQ-S triple quadrupole mass spectrometer operated in negative ESI mode. Sample aliquots (5 µL) were injected onto an AG-11-HC column with column particle size of 4 µm and temperature of 15°C. Potassium hydroxide (KOH) was applied as the eluting solvent with a constant flow rate of 18 µL/min. The elution gradient is given as a function of time in Appendix I.1.1. After every analytical run, a wash run with an injection of 50% ACN/MQ-water with 0.01% ammonium hydroxide was applied with a constant flow of 30 µL/min. The total run time was 50 min. Details about the MS settings can be obtained from supervisor P. Bruheim.

**2.8.3 Data Processing and Analysis**

Raw data obtained from targeted RP LC-MS/MS analysis of amino acids and from capIC-MS/MS analysis of phosphorylated metabolites and low molecular weight organic acids were processed using TargetLynx Application Manager of MassLynx 4.1 Mass Spectrometry software from Waters. Results were displayed as spectra, showing relative abundance of detected ions as a function of their m/z. The measured mass spectrometric responses of standard series with known concentrations of specific metabolites and blank samples were used to generate linear calibration curve. Calibration curves were used for quantification of respective metabolites in samples. A metabolite with similar structure was used as reference for metabolites without respective standards included. Peaks were automatically integrated by the software package, but manually examined to ensure correct integration. Entire metabolites were excluded from the analysis if their concentrations were outside the standard curve, or if they were considered unstable with respect to the method. Raw datas were further exported to Microsoft Office Excel, and normalized to the cell number in respective samples.

Data obtained from RP LC-MS/MS and from capIC-MS/MS analysis were analysed in separate. Normalized data was imported to UnscramblerX, a multivariate data analysis software, for principal component analysis (PCA). The normalized data was automatically scaled to adjust for differences in orders of magnitude between measured metabolite concentrations and for high and low abundant metabolites. One technical replica was excluded from the analysis if it clearly deviated (outlayer) from the other technical replicas in means of concentration. In cases of two high and two low concentrations of a metabolite, all technical replicas were included. As only two technical replicas were analysed by capIC-

MS/MS, none of these technical replicas were excluded from PCA. Normalized data was also imported to Statplus and analysed using the statistical test ANOVA (described in Appendix D) and to Excel for performing log2-comparisions.

## 2.9 Preparation of Cell Extracts for ELISA Assay

The remaining cell suspension (10 mL) from the cell counting procedure was transferred to a tube and pelleted by centrifugation (130 rcf, 5 min, 0°C). The supernatant was discarded, and the cell pellet snap-frozen in $LN_2$. Cell pellet was further stored in the freezer (-80°C). Further on, cell extraction was performed on cell pellet samples.

Cell extraction buffer (Thermo Fischer) and cell pellet was collected from the freezer and thawed on ice. A complete cell extraction buffer was made by adding 1 mM PMSF (Sigma Aldrich) dissolved in isopropanol and protease inhibitor cocktail (Sigma Aldrich). PMSF and protease was added to inhibit proteolysis in cell extract. The cell pellet was resuspended in ice cold PBS, and cells were collected by centrifugation (300 rcf, 7 min, 4°C). PBS was removed, and 0,5 mL cell extraction buffer was added to each tube to lyse cells. Cell lysates were transferred to microcentrifuge tubes, tubes vortexed and incubated on ice for 30 min with occasional vortexing. Lysates were clarified by centrifugation (13000 rcf, 10 min, 4°C), and supernatant was transferred to new microcentrifuge tubes. Tubes were stored at -80°C until performing the ELISA assay.

## 2.10 ELISA Assay

Cells extracts tubes were collected from the freezer and thawed on ice. HIF-1α in DU-145 and U-87 MG cell extracts were measured using a HIF-1α ELISA kit, EHIF1A, from Thermo Fischer. The ELISA assay was performed as described by Thermo Fischer protocol of HIF-1α ELISA kit. Absorbance was measured using a microplate reader (Tecan Spark 10M) set at 450 and 550nm. The reader is referred to Appendix A.2 for theory behind the ELISA assay.

# 3. Results

## Part 1

This MSc project compromises two parts. In the first part, a stress response study was performed to determine if the efficacy of ATX-101, as a single agent and in combination with cisplatin, is altered under hypoxic incubating conditions. Two preliminarily studies were performed. First, cell growth and survival of DU-145 and F98 cells during hypoxic versus normoxic incubation conditions were determined. Second, suitable concentrations of ATX-101 and cisplatin to be used in the hypoxic experiment were determined.

## 3.1 Efficacy of ATX-101 under Hypoxic Conditions

### 3.1.1 Hypoxic Effects on DU-145 Cell Growth

An MTT assay was conducted to determine DU-145 cell growth under hypoxic versus normoxic incubating conditions. Figure 3.1 show the average DU-145 cell growth after incubation for 24, 48, 72 and 96 hours under hypoxic and normoxic conditions.
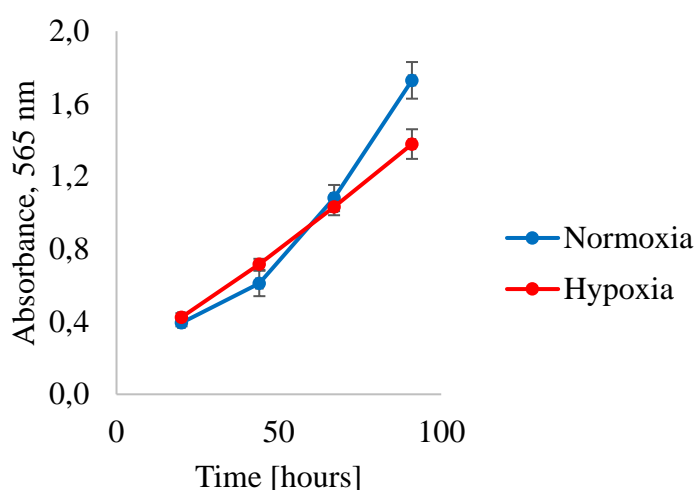


**Figure 3.1.** Average growth of DU-145 cells under normoxic and hypoxic incubating conditions. Cell growth is measured in a time series of 24, 48, 72 and 96 hours after incubation by MTT assay at 565 nm. Averages are based on 6 replicas within each treatment regime, and is given with standard deviations between replicas. Curves are colored with respect to treatment: blue curve represents normoxic incubation, and red curve represent hypoxic incubation.

As seen from Figure 3.1, both hypoxic and normoxic treated cells have experienced a close to exponential growth until 72 hour of incubation. Hereafter, a significantly reduced DU-145

cell growth is observed under hypoxic incubating conditions, indicating growth arrest at this time point.

### 3.1.2 Tuning of ATX-101 and Cisplatin Concentrations on DU-145

A series of MTT assays were performed to determine single drug concentrations of ATX-101 and cisplatin that reduce DU-145 cell growth by 30% ($IC_{30}$). These optimized concentrations of ATX-101 and cisplatin would later be applied in a hypoxic experiment.

DU-145 cells were treated with a series of cisplatin (0.125, 0.25 and 0.5 μM) and ATX-101 (6 and 8 μM) incubations. From these incubations, a cisplatin concentration of 0,5 μM and a ATX-101 concentration of 8 μM were found to be $IC_{30}$. Figure 3.2 show a potential increased efficacy of ATX-101 in cisplatin treated DU-145 cells.
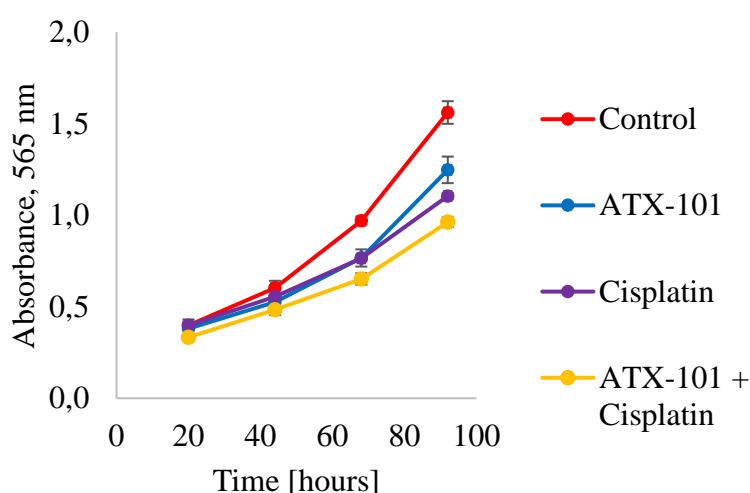


**Figure 3.2:** Average DU-145 cell growth within each treatment regime (control, ATX-101, cisplatin, ATX-101+cisplatin) measured by MTT assay at 565 nm. Optimized ATX+101 and cisplatin concentrations were applied. Averages are based on 6 replicas within each treatment regime, and is given with error bars indicating standard deviations. Curves are colored with respect to treatment: red curves represent control, blue curve ATX-101, purple curve cisplatin, and yellow curve ATX-101+cisplatin.

The treatment (ATX-101, cisplatin, ATX-101+cisplatin) effect on cell growth is clearest at 96 hours of incubation. At this time point, the control has the highest cell number, followed by treatment with ATX-101 and cisplatin. The combinatorial treatment has the lowest cell number. A clear reduction in cell growth is seen after cisplatin treatment, and an enhanced efficacy of cisplatin is seen when ATX-101 is given as an adjuvant. Furthermore, ATX-101 causes cell growth reduction when given as a single agent. It is evident that both ATX-101

and cisplatin affects the cell population over the whole time period. Nevertheless, cisplatin has the strongest effect after 72 hours of exposure.

### 3.1.3 Efficacy of ATX-101 under Hypoxic versus Normoxic Conditions on DU-145

An MTT assay was conducted to evaluate whether the efficacy of ATX-101, as a single agent and in combination with cisplatin, is altered when applied to DU-145 cells incubated under hypoxic conditions. DU-145 cell growth under normoxic and hypoxic incubating conditions was evaluated 24, 48, 72 and 96 hours after applying optimized concentrations of ATX-101 and cisplatin. Growth curves obtained from the MTT assays are presented in Figure 3.3.
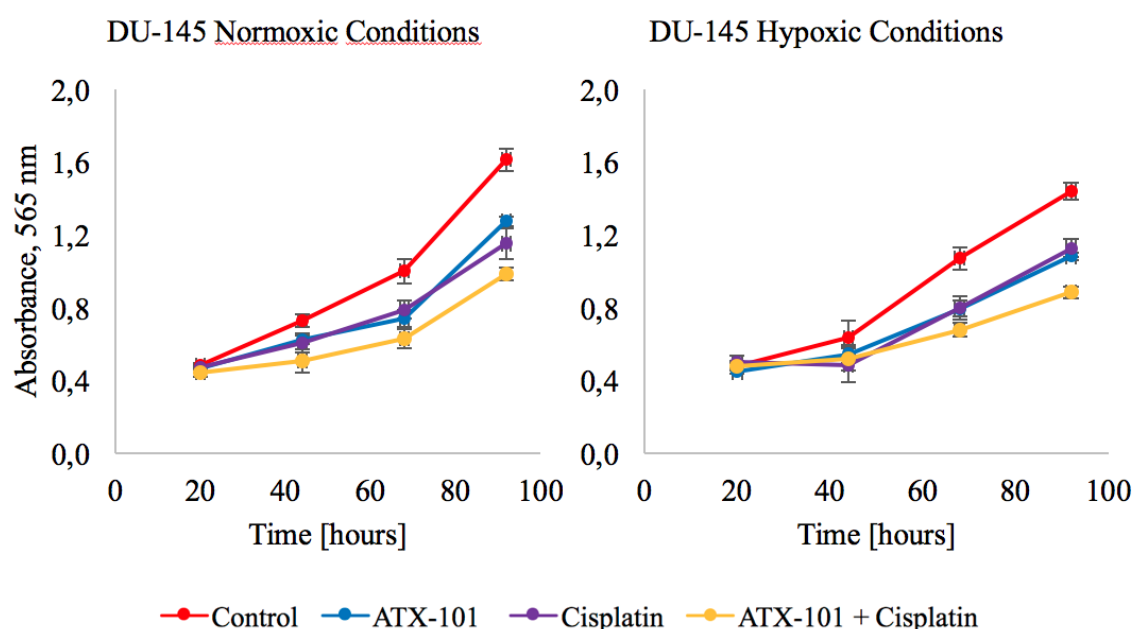


**Figure 3.3:** Average growth of DU-145 cells exposed to treatment (control, ATX-101, cisplatin, ATX-101+cisplatin) under normoxic and hypoxic incubating conditions. Cell growth is measured in a time series of 24, 48, 72 and 96 hours after incubation by MTT assay at 565 nm. Averages are based on 6 replicas within each treatment regime, and is given with error bars indicating standard deviations. Curves are colored with respect to treatment: red curves represent control, blue curve ATX-101, purple curve cisplatin, and yellow curve ATX-101+cisplatin.

The hypoxic incubated cells follow the same growth trend as the normoxic incubated cells, where the untreated control experience the highest cell growth, followed by ATX-101 and cisplatin, and the combinatorial treatment. As expected, ATX-101 cause growth reduction when applied as a single agent and in combination with cisplatin, to normoxic treated cells. It is evident that the efficacy of ATX-101 is not altered under hypoxic conditions, either when

given as a single agent or when given as an adjuvant. Hypoxic incubated cells grow slightly slower than normoxic incubated cells between 24 and 48 hours of incubation, indicating some growth arrest. This was evident for all treatment groups incubated under hypoxic conditions. However, the growth continues rapidly after 48 hours of hypoxic incubation. The slightly reduced growth of hypoxic control in the 24-48 time period, was not observed in the previously conducted growth measurement (Figure 3.1).

### 3.1.4 Hypoxic Effects on F98 Cell Growth

As for DU-145 cells, an MTT assay was conducted to determine F98 cell growth under hypoxic versus normoxic incubating conditions. Figure 3.4 show the average F98 cell growth after incubation for 24, 48, 72 and 96 hours under hypoxic and normoxic conditions.
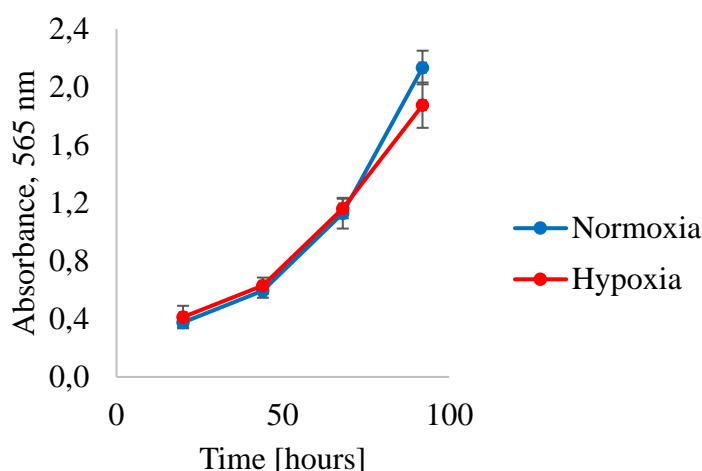


**Figure 3.4.** Average growth of F98 cells under normoxic and hypoxic incubating conditions. Cell growth is measured in a time series of 24, 48, 72 and 96 hours after incubation by MTT assay at 565 nm. Averages are based on 6 replicas within each treatment regime, and is given with standard deviations between replicas. Curves are colored with respect to treatment: blue curve represents normoxic incubation, and red curve represent hypoxic incubation.

As observed for DU-145 cells, hypoxic and normoxic incubated F98 cells follow an exponential growth. The cell growth is slightly reduced between 72 and 92 hours of hypoxic incubation, suggesting a minor growth arrest. Compared to DU-145 cells, a smaller hypoxic effect on F98 cell growth is observed after 72 hours of incubation.

### 3.1.5 Tuning of ATX-101 and Cisplatin Concentrations on F98

A series of MTT assays were performed to determine $IC_{30}$ concentrations of ATX-101 and cisplatin, and these optimal concentrations would later be applied in a hypoxic experiment.

F98 cells were treated with a series of cisplatin (0.15, 0.2, 0.25, 0.3, 0.4 and 0.5 µM), and ATX-101 (6, 8.5, 11, 13, 14, 15 and 16 µM) incubations, and it was found that exposure to 0,2 µM cisplatin caused 30% cell growth reduction. An $IC_{30}$ concentration of ATX-101 was not found. However, it is reasonable to assume that a $IC_{30}$ concentration of ATX-101 lies within the 12-14 µM range, as concentrations above cause large cell growth reduction and concentrations below have little effect on cell growth. Several attempts were made to find a $IC_{30}$ concentration of ATX-101 within the 12-14 µM range, but unfortunately the results were somewhat inconsistent. The average cell growth after exposing F98 cells to a combinatorial treatment of 13 µM ATX-101 and 0,2 µM cisplatin is presented in Figure 3.5.
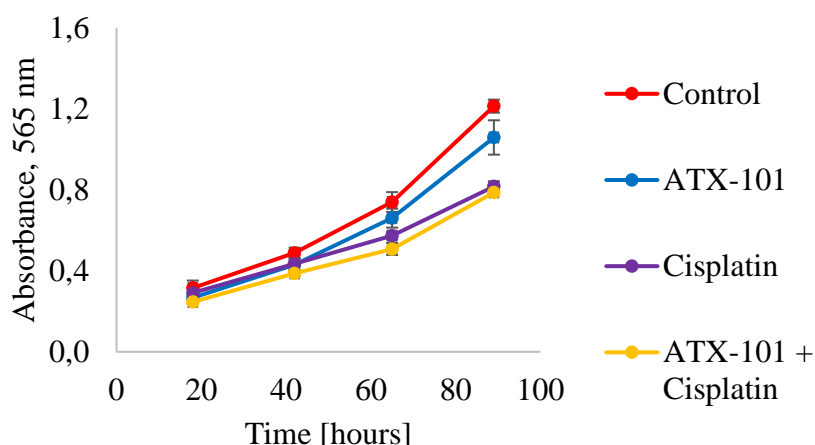


**Figure 3.5:** Average F98 cell growth within each treatment regime (control, ATX-101, cisplatin, ATX-101+cisplatin) measured by MTT assay at 565 nm. Optimized ATX+101 and cisplatin concentrations were applied. Averages are based on 6 replicas within each treatment regime, and is given with error bars indicating standard deviations. Curves are colored with respect to treatment: red curves represent control, blue curve ATX-101, purple curve cisplatin, and yellow curve ATX-101+cisplatin.

The untreated control has experienced highest cell growth, followed by treatment with ATX-101, then cisplatin and combinatorial treatment. It is clear that cisplatin cause cell growth reduction, and that ATX-101 cause a minor growth reduction (much less than 30%) when given as a single agent. The effect observed by the combinatorial treatment after 48 hours of incubation is mostly due to cisplatin. It is evident that cisplatin affects the cell population over

the whole time period. Compared to DU-145 cells, F98 cells show less sensitivity towards ATX-101, but higher sensitivity towards cisplatin.

### 3.1.6 Efficacy of ATX-101 under Hypoxic versus Normoxic Conditions on F98

An MTT assay was conducted to evaluate whether the efficacy of ATX-101, as a single agent and in combination with cisplatin, is altered when applied to F98 cells incubated under hypoxic conditions. ATX-101 (13 µM) and cisplatin (0,2 µM) was applied to F98 cells incubated under normoxic and hypoxic incubating conditions, and the cell growth evaluated after 24, 48, 72 and 96 hours of treatment exposure is presented in Figure 3.6.
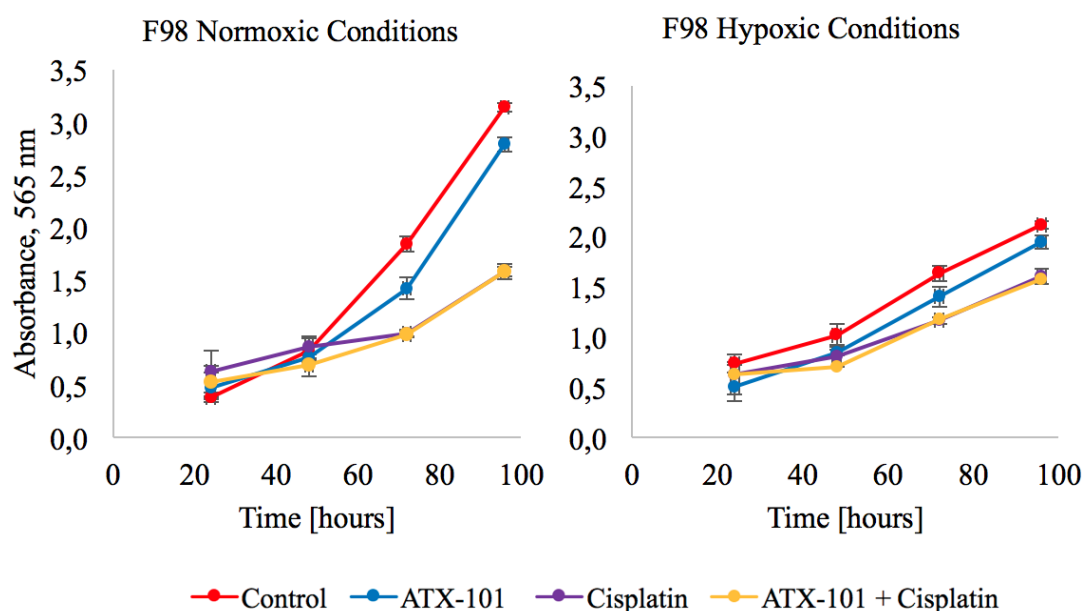


**Figure 3.6:** Average growth of F98 cells exposed to treatment (control, ATX-101, cisplatin, ATX-101+cisplatin) under normoxic and hypoxic incubating conditions. Cell growth is measured in a time series of 24, 48, 72 and 96 hours after incubation by MTT assay at 565 nm. Averages are based on 6 replicas within each treatment regime, and is given with error bars indicating standard deviations. Curves are colored with respect to treatment: red curves represent control, blue curve ATX-101, purple curve cisplatin, and yellow curve ATX-101+cisplatin.

At 24 hours of normoxic incubation, fewer cells are present in the untreated control compared to the other treatments. However, the growth increases prominently after 48 hours of incubation. Compared to previously conducted measurements of F98 cell growth under normoxic conditions (Figures 3.4 and 3.5), the control reach a much higher cell population at the final measurement (96 hours) in this experiment. In addition, cell growth of hypoxic control cells follows a less exponential pattern than observed earlier (Figure 3.4).

30

It is difficult to conclude about the effect of ATX-101 and cisplatin during the first 48 hours of incubation due to the fewer cells being present in the normoxic incubated control. Nevertheless, the hypoxic incubated cells follow more or less the same growth trend as the normoxic incubated cells after 48 hours of incubation, where the untreated control, followed by ATX-101, experience the highest cell growth. The cell growth is similar and lower after cisplatin and combinatorial treatment exposure. However, the cytotoxic effect observed by the combinatorial treatment is due to cisplatin, indicating that ATX-101 does not enhance the efficacy of cisplatin.

## Part 2

As the efficacy of ATX-101 on DU-145 was not altered under hypoxic incubating conditions, further metabolic profiling of an ATX-101 induced cytotoxic response was not performed in part 2 of the project. The main reason for this decision was that a metabolic profiling of DU-145 after ATX-101 treatment under normoxic incubating conditions had already been conducted in a different MSc project [53]. A study was instead performed to investigate metabolic adaptions in DU-145 cells after hypoxic incubating conditions. Because of lack of consistency in growth profiles obtained from F98 cells treated likewise, this cell line was excluded from the project. As it was of great interest to study hypoxic-induced metabolic adaptions in a glioblastoma cell line, the U-87 MG cell line was included in part 2 of the project.

Initially in part 2 of the project, an overall hypoxic treatment (i.e. incubating condition of 1% $O_2$) effect on DU-145 and U-87 MG cell growth was investigated by performing cell counts (section 3.2 and section 3.5). Potential hypoxic effects on the exometabolome (section 3.3 and 3.6) were assessed by NMR analysis, and on the exometabolome (section 3.4 and 3.7), applying targeted MS profiling methods. Metabolome data was analysed by PCA for detection of possible groupings of metabolites undergoing the same treatment regime. Additionally, a ELISA assay was performed to analyse the HIF-1 transcription factor in hypoxic treated samples (section 3.8).

## 3.2 Overall Hypoxic Effects on DU-145 Cell Growth

A cell count study was conducted to evaluate hypoxic treatment effect on DU-145 cell growth, and to use as a method for normalizing metabolome data. Cell counts were performed at three time points (48, 72 and 96 hours) after treatment exposure. Six identical plates were seeded, and two harvested and used for cell counting at each time point. The counted numbers of DU-145 cells in the differently treated sample groups are presented in Table 3.1. Growth curves for hypoxic and normoxic treated cells used for normalization of metabolome data are given in Figure G.1 in Appendix G.

**Table 3.1.** The number of DU-145 cells in culture plates after hypoxic and normoxic treatment for 48, 72 and 96 hours. Each sample group include two technical replicas (numbered 1-2). Average number of cell counts and standard deviation (std) are given. Reduced cell growth for each hypoxic treatment relative to normoxic treatment is calculated as percentage.

| Sample group | | Number of cells/mL [$x10^5$] | | | | |
|---|---|---|---|---|---|---|
| Treatment | Treatment length [h] | 1 | 2 | Average | Std | % reduction |
| Normoxia | 48 | 1,25 | 1,08 | 1,17 | 0,12 | - |
| | 72 | 2,45 | 2,65 | 2,55 | 0,14 | - |
| | 96 | 5,44 | 4,98 | 5,21 | 0,32 | - |
| Hypoxia | 48 | 1,19 | 1,22 | 1,21 | 0,021 | -3,4 |
| | 72 | 2,51 | 2,50 | 2,51 | 0,0070 | 1,8 |
| | 96 | 3,42 | 3,46 | 3,44 | 0,033 | 34,0 |

As seen in Table 3.1, a reduction in DU-145 cell growth is observed after 96 hours of incubation in hypoxic conditions, indicating growth arrest. Reduced cell growth after 96 hours of hypoxic incubation was observed in an earlier conducted DU-145 cell growth study (Section 3.1.1). Overall, normoxic treated cells have experienced an exponential growth throughout the whole incubation period, whereas the hypoxic treated cells followed an exponential growth until 72 hours of treatment (as observed in Figure G.1).

## 3.3 Quantification of Extracellular Metabolites in DU-145

NMR analyses were performed on DU-145 exometabolome samples to study whether the hypoxic treatment have a pronounced effect on the utilization of major energy and carbon sources (glucose and glutamine) and on production of lactate (metabolic product). Concentrations of glucose, glutamine and lactate obtained from processing of NMR datas are found in Appendix E.1. Glucose/glutamine consumption and lactate production were calculated (as described in Appendix F), and normalized to an average cell count in mid treatment (as described in Appendix G), to correct for cell reductions observed by treatment effects.  Unfortunately, glutamine could not be quantified in 96 hour treated samples, suggesting culture media deprivation of glutamine at this experimental time point. As complete exo-metabolome profiles were not obtained for 96 hour treated samples, downstream metabolic analysis of these samples was not performed.

### 3.3.1 Glucose/Glutamine Consumption and Lactate Production

Average normalized glucose/glutamine consumption and lactate production in the time periods 0-48 hours and 48-72 hours is presented in Figures 3.7 and 3.8, respectively. To account for exposure to treatment for different lengths, consumption and production per hour is presented.
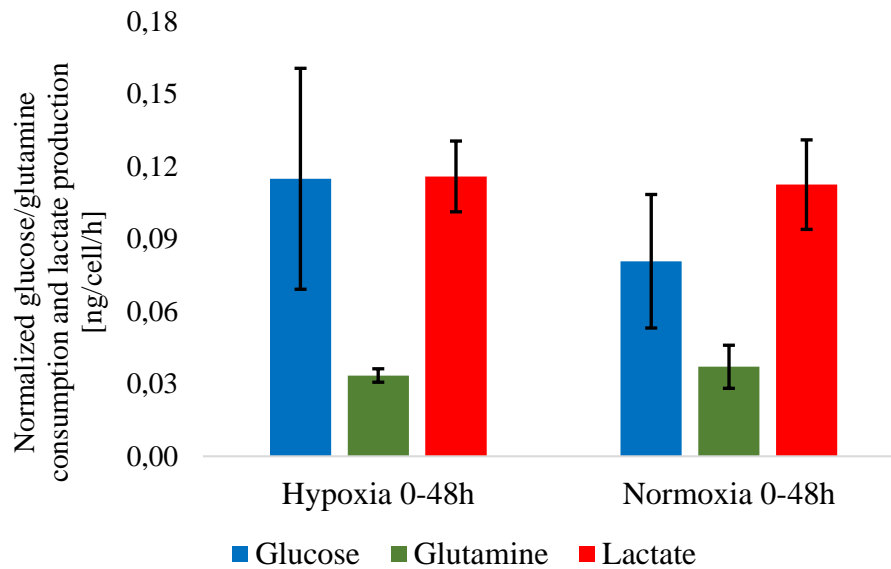
**Figure 3.7:** Average normalized glucose/glutamine consumption and lactate production in the time interval 0-48 hours in hypoxic and normoxic treated DU-145 samples. Consumption/production are based on the average of four technical replicas within each sample group. Averages are given with error bars, which represent standard deviations. Glucose consumption in given in blue, glutamine consumption in green and lactate production in red.
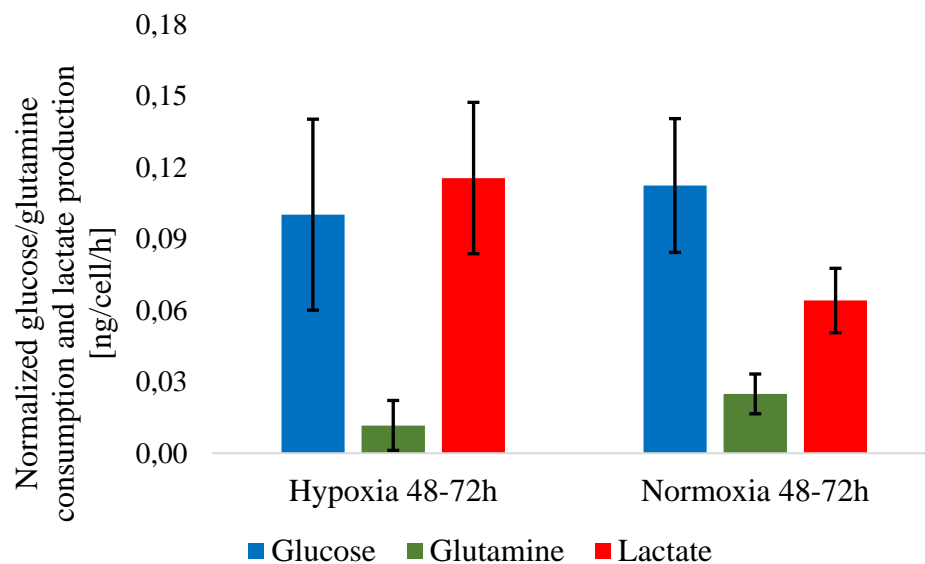


**Figure 3.8:** Average normalized glucose/glutamine consumption and lactate production in the time interval 48-72 hours in hypoxic and normoxic treated DU-145 samples. Consumption/production are based on the average of four technical replicas within each sample group. Averages are given with error bars, which represent standard deviations. Glucose consumption in given in blue, glutamine consumption in green and lactate production in red.

As illustrated in Figures 3.7 and 3.8, normalized glucose consumption is higher in hypoxic treated samples compared to normoxic treated samples during the first 48 hours of incubation, but approximately the same for hypoxic and normoxic treated samples during the 48-72 hour period. The normalized lactate production is much higher in the hypoxic treated samples in the 48-72 hour time period, and a significant difference was confirmed by ANOVA test results. However, the lactate production is approximately the same in hypoxic and normoxic treated samples during the first 48 hours of incubation. The glutamine consumption appears to be much higher during the first 48 hours of incubation than in the 48-72 hour time period, suggesting limited glutamine supply in the media. The glutamine consumption is higher in normoxic treated samples during the 47-72 hour time period, but approximately the same during the 0-48 hour period for both hypoxic and normoxic samples.

Overall, a trend in glucose consumption and lactate production is seen between hypoxic treated samples, and a greater variation in glucose consumption and lactate production is observed between the normoxic treated samples. Standard deviations are quire large, especially regarding glucose (in both time periods) and glutamine in the 48-72 hour time period. The ratios between lactate production and glucose consumption for the different sample groups were studied in Section 3.3.2.

### 3.3.2 Yield of Lactate from Glucose

The average consumption of glucose (ng/cell/h) and production of lactate (ng/cell/h) was used to calculate the yield of lactate (as described in Appendix B.2). The average lactate yield for each sample group, and the percentage reduced yield in hypoxic treated sample groups compared to the corresponding normoxic groups is presented in Table 3.2.

**Table 3.2:** The average yield of lactate from glucose in the time intervals 0-48 hours and 48-72 hours in hypoxic and normoxic treated DU-145 sample groups. Averages are based on the four technical replicas within each sample group. The percentage reduced lactate yield for each hypoxic treated sample group relative to corresponding normoxic treated sample group is calculated.

| Sample group | | Average yield $_{lactate/glucose}$ | % reduction |
|---|---|---|---|
| Treatment | Treatment interval [h] | | |
| Normoxia | 0-48 | 1,39 | - |
| | 48-72 | 0,57 | - |
| Hypoxia | 0-48 | 1,01 | 28 |
| | 48-72 | 1,15 | -102 |

As seen from Table 3.2, a slightly reduced lactate yield is observed during the first 48 hours of hypoxic incubation. This is caused by a decreased glucose consumption in normoxic treated samples during the first 48 hours of incubation, illustrated in Figure 3.7. A highly increased lactate yield (102%) is observed during 48-72 hours of hypoxic incubation. This increased lactate yield is mainly the result of a significantly reduced lactate production in the normoxic treated samples, illustrated in Figure 3.10. Overall, it is evident that a greater variation in lactate yield is observed between normoxic treated sample groups than between hypoxic treated sample groups. Whereas about 50% of the glucose consumed contributes to lactate production in hypoxic treated samples, about 70% and 30% of the glucose consumed contributes to lactate production in the periods 0-48 hour and 48-72 hour in normoxic treated sample.

## 3.4 Quantification of Intracellular Metabolites in DU-145

In addition to exometabolome analyses, complementary analyses of intracellular metabolites under hypoxic conditions relative to normoxic conditions were performed. This was achieved by investigating endometabolome samples by two target MS profiling methods: RP LC-MS/MS for investigation of amino acids, and capIC-MS/MS for investigation of phosphorylated metabolites and low molecular weight organic acids. All metabolome data presented in the following sections were normalized to the average cell count at the time of sampling (as described in Appendix D) to correct for cell reductions observed by treatment effects. Metabolome data was further automatically scaled and analysed by PCA to identify metabolite trends regarding treatment regime.

### 3.4.1 Metabolic Profiling of Amino Acid Pool

MS metabolic profiling by RP LC-MS/MS was performed on all technical replicates within each sample group to study the amino acid pool under hypoxic conditions. The concentrations of amino acids included in the RP LC-MS/MS analysis are listed in Table H.2 in Appendix H. The 48 hour normoxic replica 3 and the 72 hour normoxic replica 2 clearly deviated from the other technical replicas within respective sample groups in means of concentration, and were hence excluded from downstream metabolic analysis. Preliminarily PCA testing showed that glutamate dominated the separation of replicas and it was hence excluded from downstream PCA analysis in order to study the impact of other amino acids on the sample separation.

Glutamate was found to be highly elevated in 48 hour normoxic replicas 1 and 4, and in 72 hour hypoxic replicas 2 and 3, compared to the other replicas.

The resulting scores plot obtained from PCA including 17 out of 18 quantified amino acids is presented in Figure 3.9. In the scores plots, normoxic 72 hour replicas are colored in red, hypoxic 72 hour replicas colored in yellow, normoxic 48 hours replicas in blue and hypoxic 48 hour replicas in green. This applies for all presented scores plots.
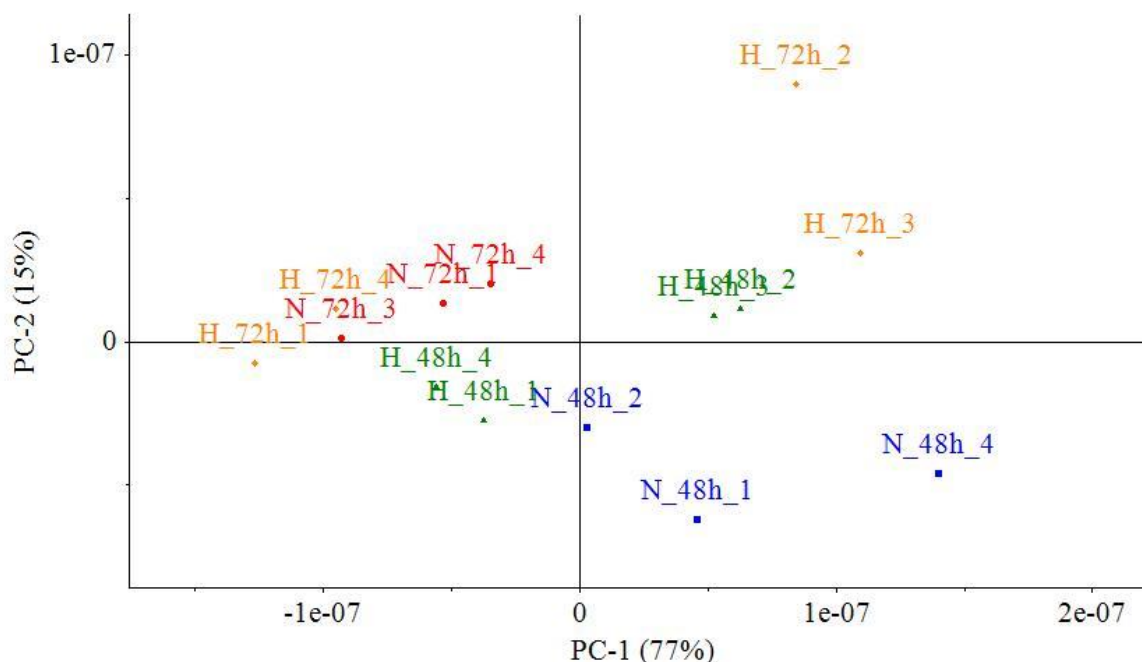


**Figure 3.9:** The PCA scores plot of data obtained from RP LC-MS/MS analysis of amino acids in DU-145 sample groups. The metabolome data was averaged based on the techinal reaplicas, normalized to the average cell count at the time of sampling, and automatically scaled. Technical replicas (numbered 1-4) are colored with respect to sample groups: 48 hour normoxic replicas in blue, 48 hour hypoxic replicas in green, 72 hour normoxic replicas in red and 72 hour hypoxic replicas in yellow. Abbreviations: N represent normoxi, H represent hypoxi.

In total, the two first principal components in Figure 3.9 explain 92% of the observed variance in the dataset, indicating that relations between sample groups can be interpreted with high certainty. A time dependent clustering of sample is observed, as the 72 hour treated sample groups (except H_72h_2 and H_72h_3) cluster in the upper, left panel of the plot, whilst the 48 hour treated sample groups are located lower and more to the right. A separation of 48 hour hypoxic and normoxic treated sample groups along PC-2 is evident (the hypoxic treated replicas are located slightly above the normoxic treated replicas). This indicate a

hypoxic effect on the amino acid pool at this time point. The variation between the 72 hour hypoxic replicas is large and is confirmed by an average RSD of 93%. Considering the large variations between 72 hour hypoxic treated replicas, it is difficult to to interpret any clustering trend.

The 48 hour and 72 hour treated sample groups were further analysed in separate by PCA. Resulting scores and loadings plots are found in Appendix K.1.1. A clear separation of hypoxic and normoxic treated technical replicas was observed within the scores plot of the 48 hour treated sample groups (Figure K.1). It is in general difficult to reason about metabolite trends from PCA plots. However, aspartate and alanine appears to have a large impact on the observed separation of replicates, and it appears that the aspartate concentration is higher in normoxic replicas compared to hypoxic replicas (Figure K.2). Within the scores plot of the 72 hour treated sample groups, a clustering of the hypoxic replicas 1 and 4 and the normoxic replicas was observed, whereas the hypoxic replicas 2 and 3 were found spread out in the plot (Figure K.3). This clustering pattern does not reveal an obvious hypoxic effect on amino acid contents. Several metabolites affected the sample separation, among others alanine and aspartate (Figure K.4).

It appears that some metabolites, such as glutamate, alanine and aspartate, have a large impact on the separation of replicas within the scores plot. However, for investigating metabolic alternations caused by a hypoxic effect in more details, single metabolites were studied by log2-comparisons and ANOVA significance tests. ANOVA was performed on technical replicas to test whether time-matched hypoxic and normoxic treated sample groups were significantly different in specific amino acids, applying a confidence level of 95%. Corresponding log2-comparisons were performed on average normalized values of technical replicas within each sample group. The resulting log2-comparisons ( $\frac{\text{hypoxia 48h}}{\text{normoxia 48h}}$ and $\frac{\text{hypoxia 72h}}{\text{normoxia 72h}}$ ) are presented in Table 3.3 as a heat map, where green represent an increase and red represent a decrease in amino acid concentrations. Significant differences are marked bold and colored black (**X**), whereas non-significant differences are colored grey (X).

**Table 3.3:** Results of log2 comparisons and ANOVA test results of amino acids detected by RP LC-MS/MS analysis, including $\frac{\text{hypoxia 48h}}{\text{normoxia 48h}}$ and $\frac{\text{hypoxia 72h}}{\text{normoxia 72h}}$. Log2 comparisons are marked as a cross, and visualized as a heat-map. Log2 values of $X \geq 1$ or $X \leq -1$ are colored dark green and red (X and X), values of $0{,}5 \leq X < 1$ or $-1 < X \leq -0{,}5$ are colored green and red and values between $0 \leq X < 0{,}5$ and $-0{,}5 < X \leq 0$ are colored bright green and red. Significant differences are marked bold and colored black (**X**), whereas non-significant differences are colored grey (X). Log2 values greater than 1 correspond to a at least a doubling relative to control, whereas log2 values less than -1 correspond to at least a halving relative to control.

| Metabolite | Hypoxia 48h/ Normoxia 48h | Hypoxia 72h/ Control 72h |
|---|---|---|
| Gly | X | X |
| Ala | X | X |
| Ser | X | X |
| Pro | X | X |
| Val | X | X |
| Thr | X | X |
| OHpro | X | X |
| Leu | X | X |
| Ile | X | X |
| Met | X | X |
| Phe | X | X |
| Asp | X | X |
| Tyr | X | X |
| Glu | X | X |
| Trp | X | X |
| Orn | X | X |
| Lys | X | X |

As seen from Table 3.3, the majority of the amino acids are slightly reduced by the 48 hour hypoxic treatment, but the aspartate level experience a great reduction. All amino acids are elevated by the 72 hour hypoxic treatment, and the majority are more than doubled. No similar decreases and increases in amino acid pools are observed after hypoxic treatment, except for the proline and threonine pools. However, no differences in amino acid concentrations in time-matched hypoxic and normoxic treated sample groups were found to be statistically significant.

### 3.4.2 Metabolic Profiling of Phosphometabololome Pool and Organic Acid Pool

MS metabolic profiling by capIC-MS/MS was performed on two technical replicates (1,2) within each sample group to study the organic acid pool and phosphometabolite pool under hypoxic conditions. The concentrations of metabolites included in the capIC-MS/MS analysis are listed in Table I.2-I.4 in Appendix I.I.3. The resulting PCA scores plot including all detected metabolites is presented in Figure 3.10.
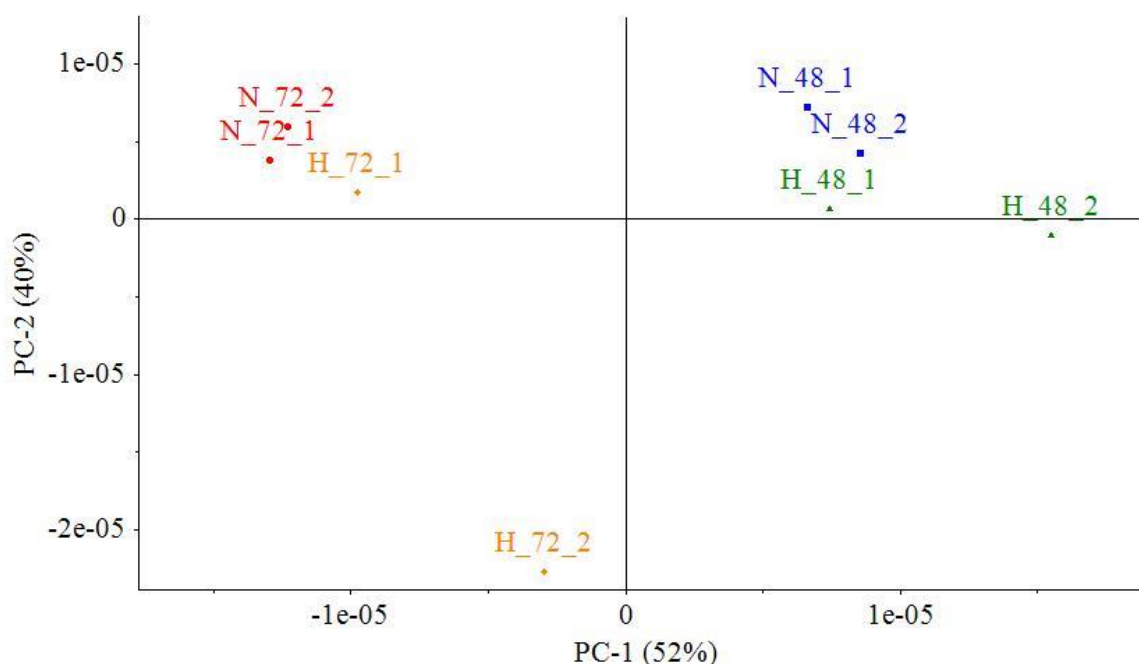


**Figure 3.10:** The PCA scores plot of data obtained from capIC-MS/MS analysis of organic acids and phosphometabolites in DU-145 sample groups. The metabolome data was averaged based on the techinal reaplicas, normalized to the average cell count at the time of sampling, and automatically scaled. Technical replicas (numbered 1-2) are colored with respect to sample groups: 48 hour normoxic replicas in blue, 48 hour hypoxic replicas in green, 72 hour normoxic replicas in red and 72 hour hypoxic replicas in yellow. Abbreviations: N represent normoxi, H represent hypoxi.

The most prominent trend in Figure 3.10 is a time-dependent clustering where the 72 hour technical replicas are separated from the 48 hour replicas along PC-1. This clustering pattern uggest that the time of sampling exerts the main effect on organic acid and phosphometabolome pool. Still, a discrimination of hypoxic and normoxic replicates sampled at the same time is evident, considering the separation of hypoxic and normoxic replicas along PC-2 where the hypoxic replicas are located slightly below the normoxic replicas.

The 48 hour and 72 hour sample groups were analysed by PCA in separate, and the scores plot and loadings plot obtained are found in Appendix K.2.1. Within the scores plot of 48 hour treated sample groups, the hypoxic and normoxic replicas were somewhat separated from each other along PC-1 (Figure K.9), suggesting a treatment effect. Several metabolites were found to contribute to the observed separation, among others ATP, succinate, malate and citrate (Figure K.10). It seems that the concentration of ATP is higher in the hypoxic replicas compared to the normoxic replicas, whereas the concentration of succinate and citrate concentrations is higher in normoxic replicas than in hypoxic replicas. Within the scores plot of the 72 hour treated sample groups, the normoxic and hypoxic replicas was somewhat separated along PC-1 (Figure K.11). ATP, succinate, malate, citrate and UTP affected largely the separation of replicas, and it seems that the hypoxic replicas have a higher ATP concentration, and a lower malate concentration than the normoxic replicas (Figure K.12). Interestingly, a higher ATP concentration was also observed within the hypoxic treated 48 hour replicas.

As for the amino acids, differences in intracellular concentrations of organic acids and phosphometabolites due to hypoxic treatment were studied in more details by performing log2-comparisons and ANOVA significance test. ANOVA was performed on technical replicas to test whether time-matched hypoxic and normoxic treated sample groups were significantly different in specific organic acids and phosphometabolites, applying a confidence level of 95%. Results of log2-comparisons ( $\frac{\text{hypoxia 48h}}{\text{normoxia 48h}}$ and $\frac{\text{hypoxia 72h}}{\text{normoxia 72h}}$ ) are presented as a heat map in Table 3.4, applying the same rules as earlier.

**Table 3.4:** Results of log2 comparisons and ANOVA test results of amino acids detected by capIC analysis, including $\frac{hypoxia\ 48h}{normoxia\ 48h}$ and $\frac{hypoxia\ 72h}{normoxia\ 72h}$. Log2 comparisons are marked as a cross, and visualized as a heat-map. Log2 values of $X \geq 1$ or $X \leq -1$ are colored dark green and red ($X$ and $X$), values of $0,5 \leq X < 1$ or $-1 < X \leq -0,5$ are colored green and red and values between $0 \leq X < 0,5$ and $-0,5 < X \leq 0$ are colored bright green and red. Significant differences are marked bold and colored black (**X**), whereas non-significant differences are colored grey (X). Log2 values greater than 1 correspond to a at least a doubling relative to control, whereas log2 values less than -1 correspond to at least a halving relative to control.

| Metabolite | Hypoxia 48h/ normoxia 8h | Hypoxia 72h/ normoxia 72h |
|---|---|---|
| **AMP** | **X** | X |
| ADP | X | X |
| ATP | X | X |
| GMP | X | X |
| GDP | X | X |
| GTP | X | X |
| dTMP | X | X |
| **dTDP** | **X** | X |
| dTTP | X | X |
| **CMP** | **X** | X |
| CDP | X | X |
| CTP | X | X |
| UMP | X | X |
| **UDP** | **X** | X |
| UTP | X | X |
| IMP | X | X |
| Pyruvate | X | X |
| Fumarate | X | X |
| Succinate | X | X |
| IA | X | X |
| Malate | X | X |
| α-ketoglutarate | X | X |
| 2HG | X | X |
| Citrate | X | X |
| Isocitrate | X | X |
| PEP | X | X |
| GL3P | X | X |
| **3PG/2PG** | **X** | X |
| **6PG** | **X** | X |
| GlcN-1P | X | X |
| Gal-1P | X | X |
| G1P | X | X |

| | | | |
|---|---|---|---|
| M1P | | X | X |
| **F1P** | | **X** | X |
| G6P | | X | X |
| F6P | | X | X |
| M6P | | X | X |
| S7P | | X | X |
| R5P/X5P/RL5P | | X | X |
| F16BP | | X | X |

Some similar reductions and elevations of metabolite pools are observed between samples exposed to 48 hour and 72 hour hypoxic treatment. The hypoxic treated samples show several common elevated glycolytic intermediates: glucose 6-phosphate (G6P), fructose 6-phosphate (F6P), 3-phosphoglycerate/2-phosphoglycerate (3PG/2PG) and phosphoenpolpyruvate (PEP). The change is more prominent in 72 hour treated samples, where several of these metabolites are at least doubled. The TCA intermediates are generally slightly reduced by the hypoxic treatment. The nucleoside mono-di- and triphosphates also appear to be moderately affected by the hypoxic treatment, except for the significantly reduced AMP, dTDP, CMP and UDP pools in the 48 hour hypoxic sample compared to the time-matched normoxic sample.

Interestingly, a slightly elevated ATP pool and a reduced AMP pool is observed in samples exposed to 48 and 72 hour hypoxic treatment. The energy charge (EC) is a measure on the energy status of the cell, and this was calculated (as described in Appendix B.3) using normalized valued of the technical replicas. The EC for hypoxic 48 and 72 hour DU-145 sample groups were found to be 0,95 and 0,94, respectively, whereas the ECs for corresponding normoxic sample groups were 0,93 and 0,92. Overall, the average EC is not found to be altered in hypoxic treated samples compared to normoxic treated samples.

### 3.4.3 Overall Hypoxic Effect on Metabolism

The metabolic profiling of the amino acid pool and organic acid pool after the 48 hour hypoxic treatment, indicate mainly moderate and statistically non-significant metabolic changes. However, some prominent and significant metabolic alternations are observed within the phosphometabolome pool. To get an overview of the hypoxic effect on metabolism, all experimentally investigated metabolites (amino acids, organic acids and phosphometabolites) and corresponding metabolic pathways are summarized in Figure 3.11. The results are presented as a heat map, applying the same principles as in previous plots. However, statistically significant and non-significant changes are not marked.
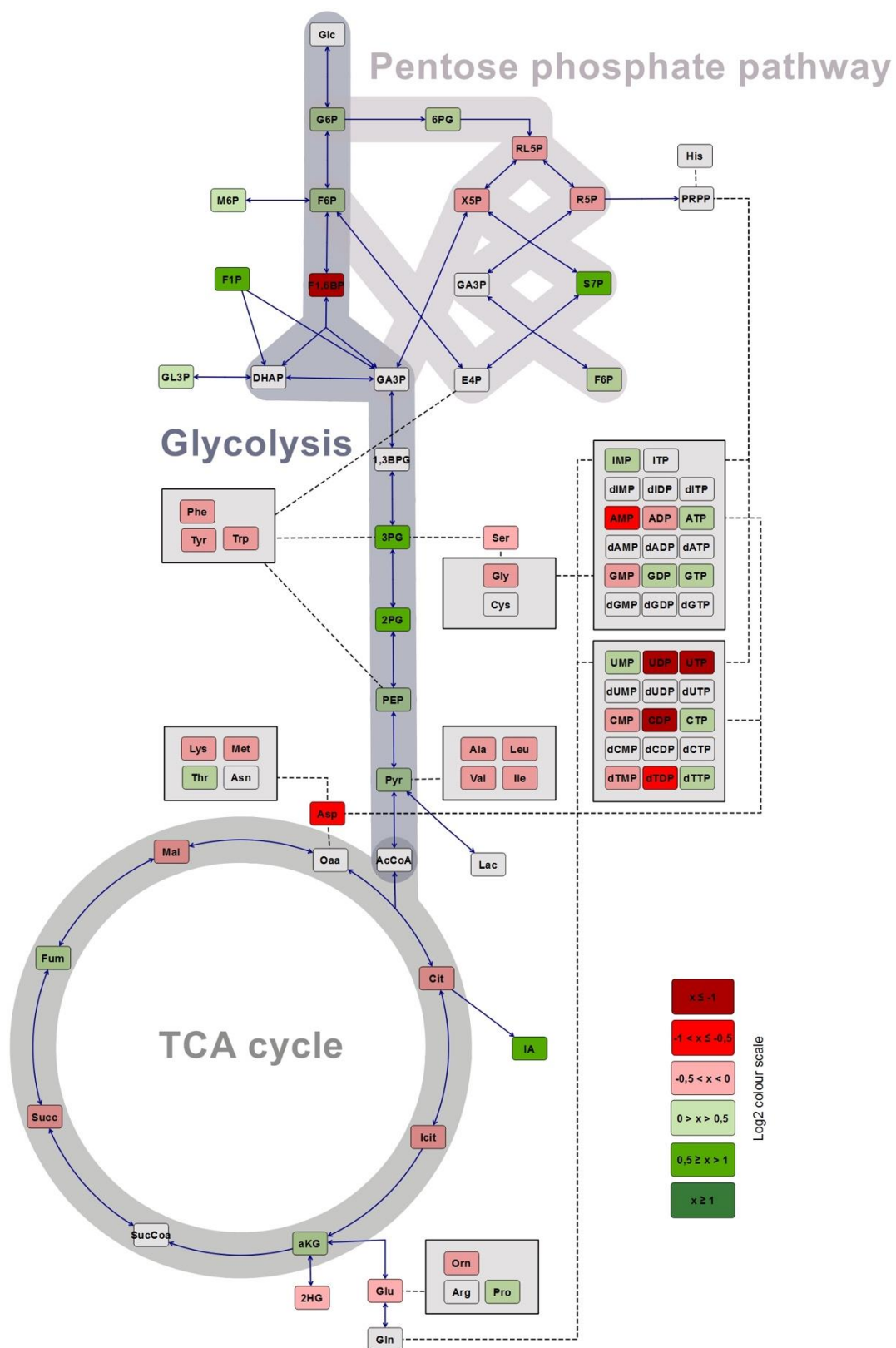
**Figure 3.11:** Overview of metabolic pathways affected by the 48 hour hypoxic treatment in DU-145 cells. Affected metabolites are colored by log2 fold change heat mapping. Log2 values are colored as shown in the bar. Plot was obtained from Omix.

Metabolic profiling of the amino acid pool and phosphometabolome indicate that the 72 hour hypoxic treatment induce several prominent metabolic changes. To put data in a metabolic perspective, all experimentally investigated metabolites and corresponding metabolic pathways is visualized in Figure 3.12. The results are presented as a heat map, applying the same principles as in previous plots. However, statistically significant and non-significant changes are not marked.
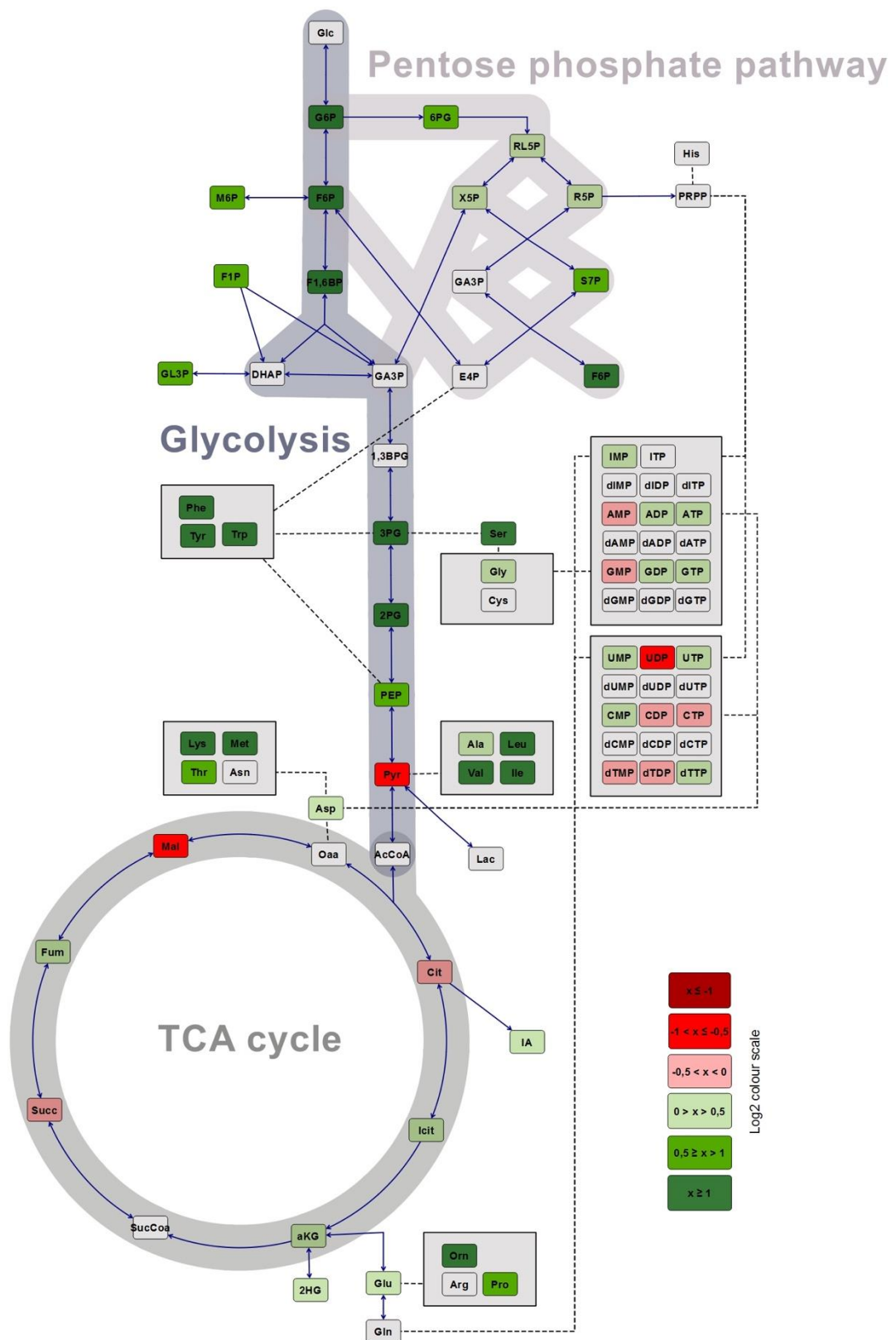
**Figure 3.12:** Overview of metabolic pathways affected by the 72 hour hypoxic treatment in DU-145 cells. Affected metabolites are colored by log2 fold change heat mapping. Log2 values are colored as shown in the bar. Plot was obtained from Omix.

## 3.5  Overall Hypoxic Effects on U-87 MG Cell Growth

As for DU-145 cells, a U-87 MG cell count study was performed to evaluate a hypoxic treatment effect on cell growth, and to use as a method for normalizing metabolome data. The counted numbers of U-87 MG cells in the differently treated sample groups are presented in Table 3.5. Growth curves used for normalization of metabolome data is given in Figure G.2 in Appendix G.

**Table 3.5:** The number of counted U-87 MG cells in culture plates after hypoxic and normoxic treatment for 48, 72 and 96 hours. Each sample group include two technical replicas (numbered 1-2). Average number of cell counts and standard deviation (std) are given. Reduced cell growth for each hypoxic treatment relative to normoxic treatment is calculated as percentage.

| Sample group | | Number of cells/mL [$x10^5$] | | | | |
|---|---|---|---|---|---|---|
| Treatment | Treatment length [h] | 1 | 2 | Average | Std | % reduction |
| Normoxia | 48 | 1,75 | 1,65 | 1,70 | 0,07 | - |
| | 72 | 2,52 | 2,58 | 2,55 | 0,042 | - |
| | 96 | 4,29 | 3,82 | 4,06 | 0,33 | - |
| Hypoxia | 48 | 1,77 | 1,59 | 1,68 | 0,13 | 1,2 |
| | 72 | 2,26 | 2,24 | 2,25 | 0,012 | 11,8 |
| | 96 | 2,87 | 3,11 | 2,99 | 0,017 | 26,3 |

A modest cell growth reduction under hypoxic conditions compared to normoxic conditions is observed between 48 and 72 hours of incubation However, a prominent reduction (~26%) in cell growth is observed after 96 hours of hypoxic incubation, indicating growth arrest. Normoxic treated cells have experienced a close to exponential growth until 72 hours of incubation (as seen in Figure G.2). Nevertheless, the growth is clearly less than exponential after 72 hours of incubating, indicating growth arrest at this time point. Still, the cell growth after 72 hours is reduced under hypoxic conditions compared to under normoxic conditions.

## 3.6 Quantification of Extracellular Metabolites in U-87 MG

U-87 MG exometabolome samples where analysed by NMR to study whether the hypoxic treatment have a pronounced effect on the consumption glucose and glutamine, and on production of lactate. Unnormalized glucose, glutamine and lactate concentrations are found in Table 3.2 in Appendix E.2. Glucose and glutamine consumption and lactate production were calculated and normalized to the average cell count in the mid treatment. As glucose could not be detected in 96 hour treated samples, downstream metabolic analysis of 96 hour of sample groups were not performed. Glucose could not be quantified in the 72 hour treated hypoxic replica 1 and 2, indicating more or less glucose exhaustion in all sample groups at this time point. Further on, metabolome data for the 72 hour sample group should therefore be interpreted cautiously.

### 3.6.1 Glucose/Glutamine Consumption and Lactate Production

Average normalized glucose/glutamine consumption and lactate production in the time intervals 0-48 hour and 48-72 hour is presented in Figures 3.13 and 3.14, respectively.
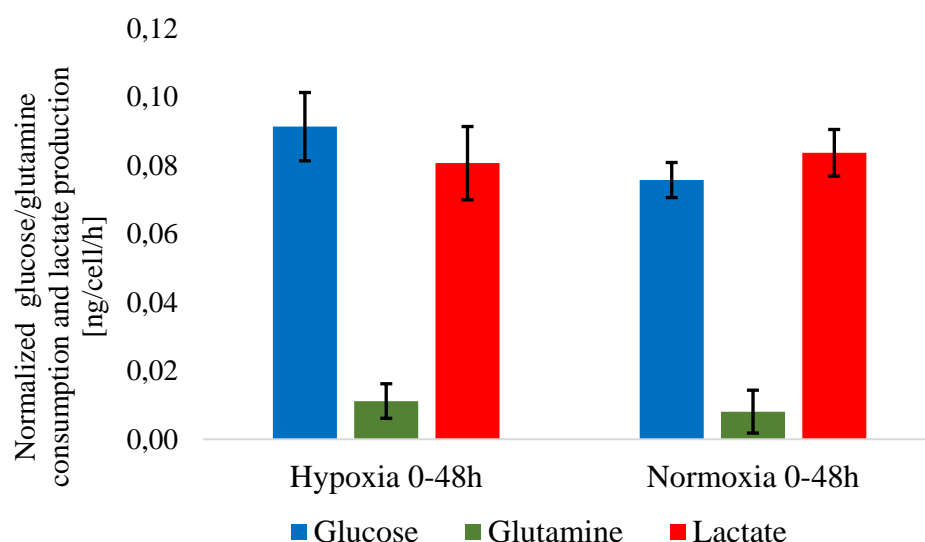
**Figure 3.13:** Average normalized glucose/glutamine consumption and lactate production in the time interval 0-48 hours in hypoxic and normoxic treated U-87 MG cells. Consumption/production are based on the average of technical replicas within each sample group. Averages are given with error bars, which represent standard deviations. Glucose consumption in given in blue, glutamine consumption in green and lactate production in red.
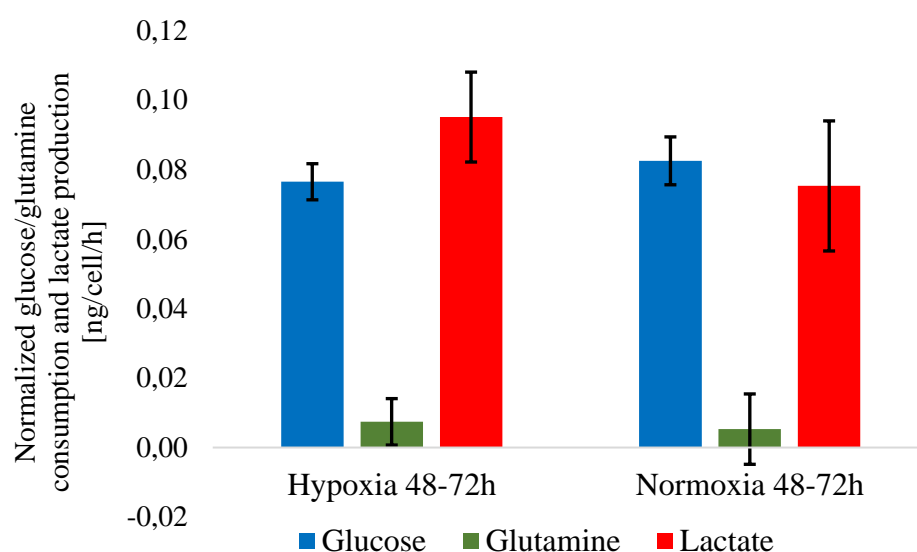


**Figure 3.14:** Average normalized glucose/glutamine consumption and lactate production in the time interval 48-72h in hypoxic and normoxic treated U-87 MG cells. Consumption/production are based on the average of technical replicas within each sample group. Averages are given with error bars, which represent standard deviations. Glucose consumption in given in blue, glutamine consumption in green and lactate production in red.

The normalized glucose consumption during the the first 48 hours of incubation, is slightly higher in the hypoxic treated sample group, but approximately the same for hypoxic and normoxic treated samples in the 48-72 hour period. ANOVA test results confirmed a significant difference between the glucose consumption of hypoxic and normoxic treated sample groups in the 0-48 hour time period. The normalized lactate production is higher in the hypoxic treated sample group in the 48-72 hour time period, but approximately the same in hypoxic and normoxic treated sample groups during the first 48 hours of incubation. Similar trends of glucose consumption and lactate production were also observed within DU-145 samples (Section 3.3). Nevertheless, the normoxic treated U-87 MG samples show less variation in production and consumption compared to the normoxic treated DU-145 samples. Interestingly, the glutamine consumption seems to be slightly higher in the hypoxic treated U-87 MG sample groups compared to the normoxic ones. However, large standard deviations are observed regarding glutamine, making it difficult to conclude with a trend in consumption. The ratios between lactate production and glucose consumption for the different sample groups were studied in Section 3.6.2.

### 3.6.2 Yield of Lactate from Glucose

The average consumption of glucose (ng/cell/h) and production of lactate (ng/cell/h) was used to calculate the yield of lactate (as described in Appendix B.2). Table 3.6 shows the average yields for each sample group, and the percentage reduced yield in hypoxic sample groups compared to the corresponding normoxic sample groups.

**Table 3.6:** The average yield of lactate from glucose in the time intervals 0-48 hours and 48-72 hours in hypoxic and normoxic treated DU-145 sample groups. Averages are based on the four technical replicas within each sample group. The percentage reduced lactate yield for each hypoxic treated sample group relative to corresponding normoxic treated sample group is calculated.

| | Sample group | Average yield $_{lactate/glucose}$ | % reduction |
|---|---|---|---|
| Treatment | Treatment interval [h] | | |
| Normoxia | 0-48 | 1,11 | - |
| | 48-72 | 0,91 | - |
| Hypoxia | 0-48 | 0,88 | 20 |
| | 48-72 | 1,24 | -36 |

A slightly reduced yield is observed during the first 48 hours of hypoxic treatment, and a moderate increased yield is observed after hypoxic treatment in the 48-72 hour time period. Similar elevations/reduction in yields after hypoxic treatment are also observed within DU-145 samples. As seen from Figure 3.16, the increased lactate yield observed in the 48-72 hour time period, is mainly the result of an greater amount of glucose contributing to lactate production during hypoxic treatment. From Table 3.6, it is evident that the variation in lactate yield is slightly larger between the hypoxic treated sample groups than between the normoxic sample groups. Overall, more or less 50% of the glucose consumed contributes to the production of lactate in both hypoxic and normoxic treated cells.

## 3.7 Quantification of Intracellular Metabolites in U-87 MG

A potential hypoxic effect at metabolite level was investigated by analysing endometabolome samples by RP LC-MS/MS covering the amino acid pool, and capIC-MS/MS covering phosphorylated metabolites and low molecular weight organic acids. All metabolome datas presented herein were normalized to the average cell count at the time of sampling, automatically scaled and analysed by PCA.

### 3.7.1 Metabolic Profiling of Amino Acids Pool

RP LC-MS/MS profiling methods were conducted on all four technical replicates within each sample group. The concentrations of metabolites included in the RP LC-MS/MS analysis are listed in Table H.3 in Appendix H. Replica 2 deviated from the other technical replicas within the 48 hour hypoxic treated sample group in means of concentration, and was hence excluded from the PCA and all further downstream analyses. Preliminarily PCA testing resulted showed that glutamate dominated the separation, and it was excluded from PCA to observe to study the impact of other metabolites on sample separation. Glutamate was found to be highly elevated in 72 hour hypoxic replica 1 and 2 (replicas in which glucose could not be quantified), compared to the other replicas. The PCA scores plot including 17 out of 18 quantified amino acids is presented in Figure 3.15.
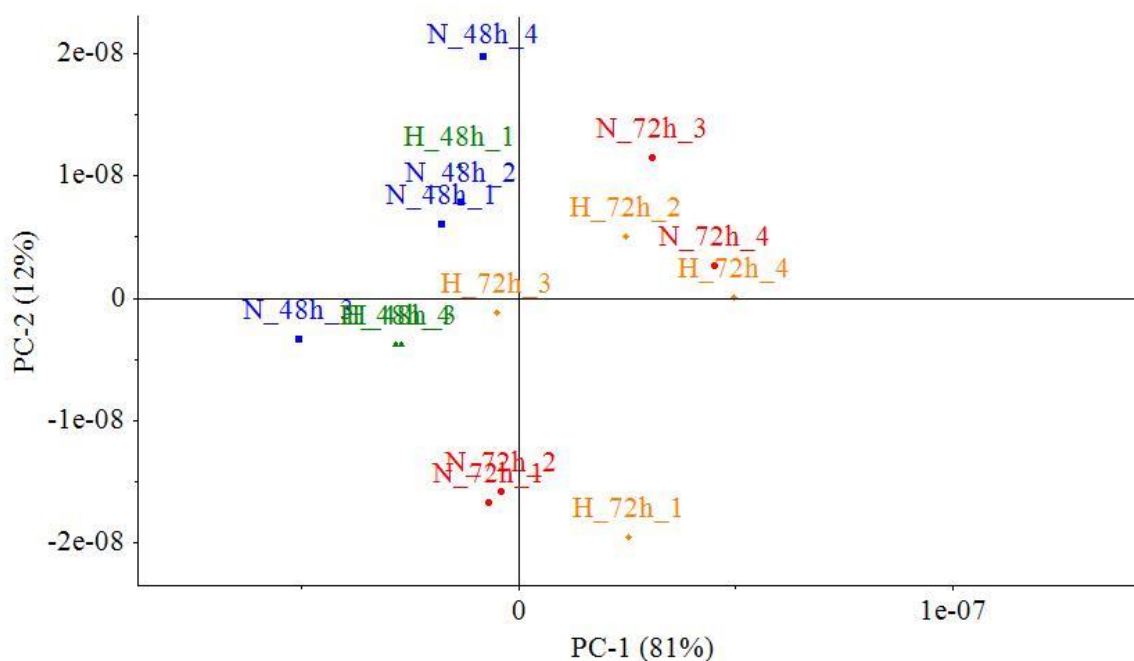
**Figure 3.15:** The PCA scores plot of data obtained from RP LC-MS/MS analysis of amino acids in U-87 MG sample groups. The metabolome data was averaged based on the techinal reaplicas, normalized to the average cell count at the time of sampling, and automatically scaled. Technical replicas (numbered 1-4) are colored with respect to sample groups: 48 hour normoxic replicas in blue, 48 hour hypoxic replicas in green, 72 hour normoxic replicas in red and 72 hour hypoxic replicas in yellow. Abbreviations: N represent normoxi, H represent hypoxi.

The 48 and 72 hour sample groups are clearly located away from each other, considering that the 48 hour sample groups cluster together in the upper left panel of the plot, and 72 hour sample groups are located lower and to the right (Figure 3.15). This clustering pattern suggests that sample groups sampled at the same time are close in amino acid content. As sample groups sampled at the same time clearly overlap, no discrimination according to treatment type can be made.

The 48 and 72 hour sample groups were further analysed by PCA in separate (Appendix K.1.2). The 48 hour treated replicas clearly overlapped within the scores plot, and no separation according to treatment type could be observed (Figure K.5). No clustering or separation of replicas exposed to the same treatment type was either observed within the scores plot of the 72 hour samples (Figure K.7).

ANOVA was performed on technical replicas to test whether time-matched hypoxic and normoxic treated sample groups were significantly different in specific amino acids, applying a confidence level of 95%. Log2-comparisons ($\frac{\text{hypoxia 48h}}{\text{normoxia 48h}}$ and $\frac{\text{hypoxia 72h}}{\text{normoxia 72h}}$) provided with heat mapping is presented in Table 3.7 applying the same rules as earlier, where green represent an increase and red represent a decrease in amino acid concentrations, and significant differences are marked bold and colored black (**X**), whereas non-significant differences are colored grey (X).

**Table 3.7:** Results of log2 comparisons and ANOVA test results of amino acids detected by RP LC-MS/MS analysis, including $\frac{\text{hypoxia 48h}}{\text{normoxia 48h}}$ and $\frac{\text{hypoxia 72h}}{\text{normoxia 72h}}$. Log2 comparisons are marked as a cross, and visualized as a heat-map. Log2 values of $X \geq 1$ or $X \leq -1$ are colored dark green and red (**X** and **X**), values of $0,5 \leq X < 1$ or $-1 < X \leq -0,5$ are colored green and red and values between $0 \leq X < 0,5$ and $-0,5 < X \leq 0$ are colored bright green and red. Significant differences are marked bold and colored black (**X**), whereas non-significant differences are colored grey (X). Log2 values greater than 1 correspond to a at least a doubling relative to control, whereas log2 values less than -1 correspond to at least a halving relative to control.

| Metabolite | Hypoxia 48h/ Normoxia 48h | Hypoxia 72h/ Normoxia 72h |
|---|---|---|
| Gly | X | X |
| Ala | X | X |
| Ser | X | X |
| Pro | X | X |
| Val | X | X |
| Thr | X | X |
| OHpro | X | X |
| Leu | X | X |
| Ile | X | X |
| Met | X | X |
| Phe | X | X |
| Asp | X | X |
| Tyr | X | X |
| Glu | X | X |
| Trp | X | X |
| Orn | X | X |
| Lys | X | X |

Mainly moderate metabolic alternations are present in samples exposed to hypoxic treatment (Table 3.7). Whereas the majority of the amino acids are slightly reduced in samples exposed to 48 hour hypoxic treatment, the majority of the amino acids are slightly elevated in samples exposed to 72 hour hypoxic treatment. The most prominent metabolic changes are observed within the hydoxyproline (OHpro) and serine (Ser) pools.

### 3.7.2 Metabolic Profiling of Phosphometabolome Pool and Organic Acid Pool

CapIC MS/MS was conducted on two technical replicates (parallel 1 and 2) within each sample group. It should be kept in mind that glucose could not be quantified in 72 hour hypoxic paralleles 1 and 2. The concentrations of metabolites included in the capIC-MS/MS analysis are listed in Table I.5-I.7 in Appendix I.I.3. The resulting PCA scores plot including all measured metabolites is presented in Figure 3.16.
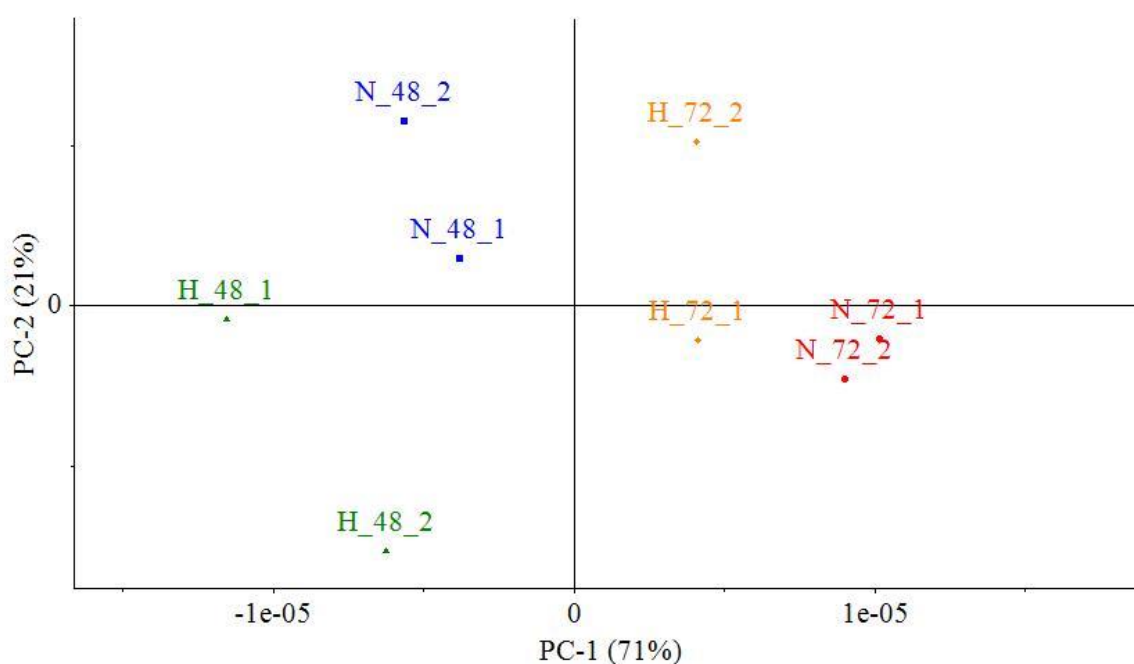


**Figure 3.16:** The scores plot of data obtained from capIC-MS/MS analysis of phosphometabolites and organic acids in U-87 MG sample groups. The metabolome data was normalized to the average cell count, and automatically scaled. Technical replicas (numbered 1-2) are colored with respect to sample groups: normoxic 48 hour samples in blue, hypoxic 48 hour samples in green, normoxic 72 hour samples in red and hypoxic 72 hour samples in yellow. Abbreviations: N represent normoxi, H represent hypoxi.

The most prominent trend observed in Figure 3.16, is a separation of 48 hour and 72 hour replicas along PC-1. This trend suggests that the main effect on metabolite contents is the time of sampling. Still, a separation between hypoxic and normoxic replicas sampled at the same time is evident. The 72 hour hypoxic replicas are clearly located to the left for the time-matched normoxic replicas, whereas the 48 hour hypoxic replicas are clearly located below the time-matched normoxic replicas. As performed earlier, the 48 and 72 hour sample groups were analysed by PCA in separate. The scores and loadings plots obtained can be found in Appendix K.2.1.

Some separation of 48 hour treated hypoxic and normoxic treated replicas on PC-1 was observed within the scores plot of 48 hour sample groups (Figure K.13). The separation of replicas is mostly caused by ATP, malate and citrate (Figure K.14). Interestingly, malate and citrate levels seems to be reduced in the 48 hour treated hypoxic replicas compared to the time-matched normoxic replicas. Within the scores plot of 72 hour treated sample groups, a clear separation between hypoxic and normoxic treated replicas along PC-1 was observed (Figure K.15). Several metabolites contributed to the observed separation of replicates, but ATP and malate were mostly responsible for the separation (Figure K.16). As for hypoxic treated 48 hour replicas, the malate level seems to be reduced in the 72 hour hypoxic treated replicas compared to the time-matched normoxic treated replicas. In addition, the ATP concentration seems to be elevated in the 72 hour hypoxic treated replicas compared to time-mathced normoxic treated replicas. Interestingly, an elevated ATP concentration was also observed in 48 and 72 hour hypoxic treated DU-145 sample groups (Section 3.4).

To study metabolic changes in details, log2-comparisons and ANOVA tests were conducted. ANOVA was performed on technical replicas to test whether time-matched hypoxic and normoxic treated sample groups were significantly different in specific organic acids and phosphometabolites, applying a confidence level of 95%. Log2 comparisons provided with heat mapping is presented in table 3.8, applying the same rules as earlier.

**Table 3.8:** Results of log2 comparisons and ANOVA test results of amino acids detected by capIC-MS/MS analysis, including $\frac{hypoxia\ 48h}{normoxia\ 48h}$ and $\frac{hypoxia\ 72h}{normoxia\ 72h}$. Log2 comparisons are marked as a cross, and visualized as a heat-map. Log2 values of $X \geq 1$ or $X \leq -1$ are colored dark green and red (X and X), values of $0,5 \leq X< 1$ or $-1< X \leq -0,5$ are colored green and red and values between $0 \leq X< 0,5$ and $-0,5 < X \leq 0$ are colored bright green and red. Significant differences are marked bold and colored black (**X**), whereas non-significant differences are colored grey (X). Log2 values greater than 1 correspond to a at least a doubling relative to control, whereas log2 values less than -1 correspond to at least a halving relative to control.

| Metabolite | Hypoxia 48h/ normoxia 48h | Hypoxia 72h/ normoxia 72h |
|---|---|---|
| AMP | X | X |
| ADP | X | X |
| ATP | X | X |
| GMP | X | X |
| GDP | X | X |
| GTP | X | X |
| dTMP | X | X |
| dTDP | X | X |
| dTTP | X | X |
| CMP | X | X |
| CDP | X | X |
| **CTP** | **X** | X |
| UMP | X | X |
| UDP | X | X |
| UTP | X | X |
| IMP | X | X |
| Pyruvate | X | X |
| Fumarate | X | X |
| Succinate | X | X |
| IA | X | X |
| **Malate** | **X** | X |
| α-ketoglutarate | X | X |
| 2HG | X | X |
| **Citrate** | **X** | X |
| **Isocitrate** | **X** | X |
| PEP | X | X |
| **GL3P** | **X** | X |
| 3PG/2PG | X | X |
| 6PG | X | X |
| GlcN-1P | X | X |
| Gal-1P | X | X |
| G1P | X | X |

| | | |
|---|---|---|
| M1P | X | X |
| **F1P** | **X** | X |
| G6P | X | X |
| F6P | X | X |
| M6P | X | X |
| S7P | X | X |
| **R5P/X5P/RL5P** | **X** | X |
| F16BP | X | X |

Mainly moderate metabolic alternations are present in samples exposed to 48 hour hypoxic treatment. Nevertheless, the PPP intermediates: R5P/X5P/RL5P and glycerol 3-phosphate (GL3P) were found to be slightly significantly elevated in the 48 hour hypoxic treated sample compared to the 48 hour normoxic treated sample. The TCA intermediates experience small reduction in pools after 48 hour of hypoxic treatment, some of these significant.
The hypoxic 72 hour treated sample experience a high reduction in glycolytic intermediate pools. Except for these clearly altered glycolytic intermediate pools, mainly moderate alternations are observed within the 72 hour hypoxic treated sample.

Interestingly, the majority of the nucleoside mono-di- and triphosphates experience slightly elevated pools after 72 hour hypoxic treatment, but slightly reduced pools after 48 hour hypoxic treatment. Among others, AMP and ATP are slightly elevated in the 72 hour hypoxic treated sample, and slightly reduced in the 48 hour hypoxic treated sample.
The average EC for the different sample groups were calculated using normalized valued of the technical replicas (Appendix B.2). The EC for U-87 MG hypoxic 48h and 72h sample groups was 0,92 for both, whereas the EC for corresponding normoxic sample groups was 0,93 and 0,92. Thus, the overall EC is unaffected by the hypoxic treatment.

### 3.7.3 Overall Hypoxic Effects on Metabolome
The overall metabolic profiling indicates that the 48 hour hypoxic treatment induce mainly modest and non-significant metabolic alternations. Nevertheless, a few significantly changed metabolites, including TCA cycle intermediates was detected after 48 hour hypoxic treatment. All investigated metabolites and corresponding metabolic pathways are visualized in Figure 3.17. The results are presented as a heat map, applying the same principles as in previous plots. However, significant and non-significant changes are not marked.
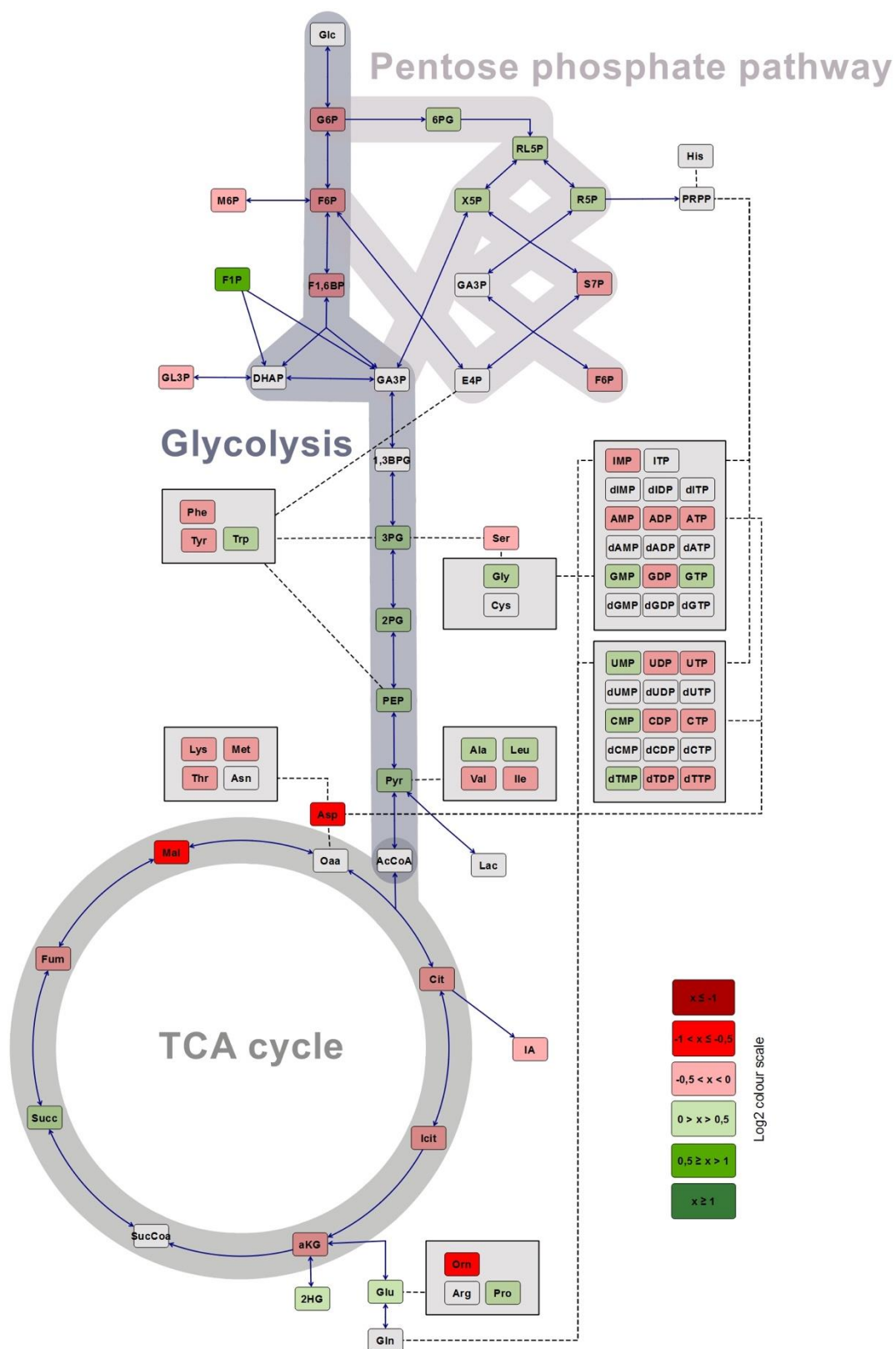
**Figure 3.17:** Overview of metabolic pathways affected by the 48 hour hypoxic treatment in U-87 MG cells. Affected metabolites are colored by log2 fold change heat mapping. Log2 values are colored as shown in the bar. Plot was obtained from Omix.

Some clearly changed glycolytic intermediates were observed after 72 hours of hypoxic treatment. To get an overview of the hypoxic effect on the overall metabolism in U-87 MG cells, investigated metabolites and corresponding metabolic pathways is summarized in Figure 3.18. The results are presented as a heat map, applying the same principles as in previous plots.
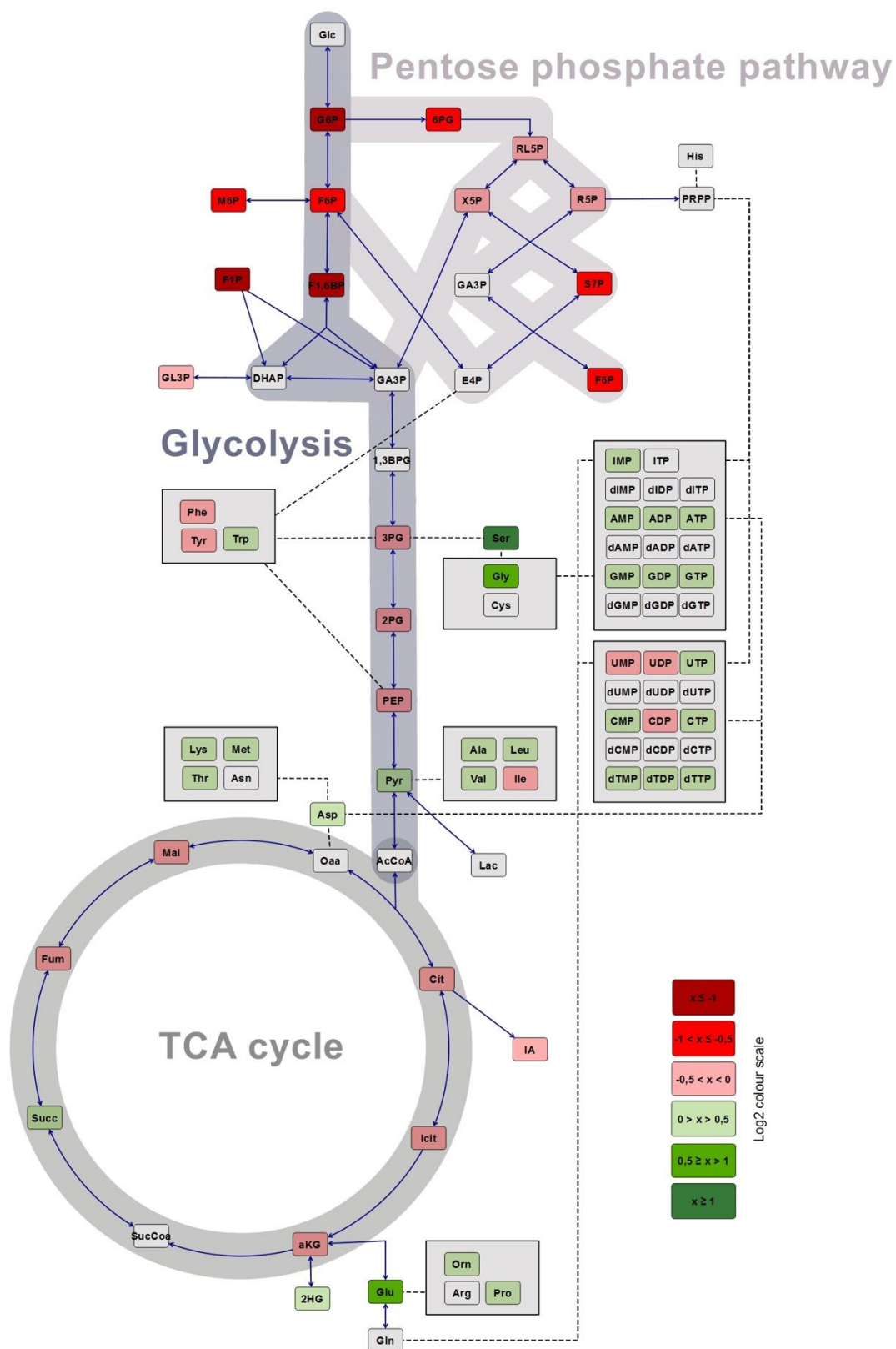
**Figure 3.18:** Overview of metabolic pathways affected by the 72 hour hypoxic treatment in U-87 MG cells. Affected metabolites are colored by log2 fold change heat mapping. Log2 values are colored as shown in the bar. Plot was obtained from Omix.

## 3.8 HIF-1α Detection

It was of great interest to detect the amount of HIF-1α in hypoxic and normoxic treated DU-145 and U-87 MG sample groups. Detection of HIF-1α was performed applying a HIF-1α ELISA assay on cell extracts. Linear calibration curves were generated from the standard series with known HIF-1α concentrations. However, several of the standard concentrations were excluded from the obtained standard curve as they were clearly outlier data points. Additionally, the amount of HIF-1α in several samples was below the quantification limits of the ELISA assay. The reliability of results obtained from the ELISA assay is questionable, and was therefore chosen not to be presented.

# 4. Discussion

In this master thesis, hypoxic effects on the DU-145 and U-87 MG metabolome were studied. In addition, the efficacy of ATX-101 on DU-145 and F98 cells under hypoxic incubating conditions was detected.

## 4.1 Part 1

- **Evaluation of the F98 Cell line**

Inspection of F98 growth data revealed low reproducible growth patterns between experiments. The use of different cell passage numbers could explain the variations in growth between experiments. Additionally, the degree of confluence in the culture flask at the time of seeding could have affected the growth. Nevertheless, as the F98 cells change between periods of slow and rapid growth, the F98 datas are not considered reliable to evaluate ATX-101 efficacy.

- **Growth under Hypoxic Conditions**

Within 72 hours of incubation, the hypoxic incubation did not cause F98 or DU-145 cell growth reduction. This indicate that the hypoxic treated cells experience sufficient levels of ATP, reducing power and macromolecules to support rapid cell growth and division. The reduced oxygen availability may induced metabolic shift from oxidative phosphorylation (OXPHOS) to aerobic glycolysis [5]. Stabilization of HIF-1 may be involved in maintaining the rapid cellular proliferation observed in hypoxic treated cells. The cessation of growth observed after 72 hour of hypoxic exposure may be related to a limited glucose supply, as this is used in excessive amounts to drive up regulated aerobic glycolysis [5]. Limited supplies of major carbon and energy sources likely induce cell cycle arrest to reduce bioenergetics and biosynthetic needs [9].

- **Efficacy of ATX-101 in Hypoxic Conditions**

Result indicate that ATX-101 increase the sensitivity of DU-145 cells towards cisplatin under both hypoxic and normoxic incubating conditions [41]. Although result indicate a modest growth arrest in ATX-101 and ATX-101+cisplatin treated DU-145 cells between 24 and 48 hours of hypoxic incubation, the growth restores after 48 hours (Figure 3.3). Overall, the efficacy of ATX-101, as a single agent and in combination with cisplatin, was not found to be altered in hypoxic treated compared to normoxic treated DU-145 cells. Result suggest that

DU-145 cells are robust and maintain a high cellular proliferation despite genotoxic and hypoxic-induced stress. From a clinical perspective, it is positive that the efficacy of ATX-101 is not altered under hypoxia, a closely mimicked in vivo tumor condition [4]. Whereas many hypoxic cancer cells respond poorly to cancer therapies such as radiotherapy and chemotherapy, our study strengthen the role of ATX-101 in cancer treatment [54].

## 4.2. Hypoxic Effects on Extracellular Metabolites

Lactate production and glucose consumption did not vary notably between hypoxic treated DU-145 cells in the 0-48 hour and 48-72 hour time periods (Section 3.3). Interestingly, large variations in lactate production and glucose consumption was observed between the 0-48 hour and 48-72 hour time periods in normoxic treated DU-145 cells. On the other hand, U-87 MG cells maintained a more or less constant glucose consumption and lactate production under both hypoxic and normoxic incubation conditions (Section 3.6). It appears that DU-145 cells consume more glutamine than U-87 MG cells, but that hypoxic treated U-87 MG cells consume slightly more glutamine than corresponding normoxic U-87 MG cells.
The overall trend indicate that DU-145 and U-87 MG cells maintain a high consumption of the major carbon and energy sources under both normoxic and hypoxic conditions. Additionally, U-87 MG and DU-145 cells have high rates of aerobic glycolysis (Warburg effect), and this does not appear to be affected by the hypoxic treatment.

## 4.3 Hypoxic Effects on Carbon Metabolism

As seen in Figures 3.10, 3.12, 3.17 and 3.18, some intracellular metabolites were found prominently and/or significantly changed by the hypoxic treatment. However, single metabolite changes may still not result in a biological effect, such as influencing metabolic fluxes or energy charge. Whether this occurs depends on the concentration of substrate and the kinetic behaviour of the enzyme [22]. At the current state it can not be drawn conclusions on whether an altered metabolite pool cause a physiological effect, and the following interpretations of metabolome alternations in Figures 3.10, 3.12, 3.17 and 3.18 remain speculations.

**4.3.1 Hypoxic 48 hour Treatment Effect on DU-145**

The 48 hour hypoxic treatment resulted in increased level of 6-phosphogluconate (6PG) and decreased level of ribose-5P (R5P), suggesting inhibition of 6-phosphogluconate dehydrogenase (G6PDH), the enzyme which regulates the entry step into the pentose phosphate pathway (PPP) [26]. The R5P is involved in *de novo* nucleotide (NTP, dNTP) synthesis. Interestingly, aspartate and glycine, also involved in *de novo* nucleotide synthesis, experienced reduction in pools by the hypoxic treatment. All together, these observations and the significantly reduced uridine diphosphate (UDP), cytidine monophosphate (CMP) and deoxythymidine diphosphate (dTDP) pools suggest a decreased *de novo* nucleotide synthesis. However, as the cellular proliferation under hypoxia is not altered at this time point, the reduction of free cellular nucleotides does not likely affect the overall nucleic acid synthesis.

The hypoxic treatment resulted in slightly reduced amino acid pools, indicating decreased uptake from the medium (all are provided by the medium), decreases synthesis or increased consumption. Several triacylcarboxylic acid (TCA) cycle intermediates were are also slightly decreased after hypoxic treatment. This may be due to an increased shunting of intermediates towards biosynthetic pathways and/or reduced influx of carbon intermediates to the TCA cycle. Together, the reduced levels of TCA cycle-derived amino acids and TCA cycle intermediates may be due to a reduced entry of either glucose derived-carbons or glutamine-derived carbons into the TCA cycle, causing decreased flux through the TCA cycle. HIF-1 is known to activate PDK1, which inhibit decarboxylation of pyruvate to acetyl-CoA [23]. A hypothesized reduced flux of glucose-derived carbon into the TCA cycle may be a strategy to prevent NADH and $FADH_2$ production, as the downstream catabolism of these electron carriers generates mitochondrial ROS when oxygen in unavailable to bind electrons [22]. Nevertheless, as the glutamine consumption is not affected by the hypoxic treatment and the α-ketoglutarate (α-KG) level is slightly elevated, glutamine probably fuels the TCA cycle [9].

The effect of the hypoxic treatment is generally summed up in the EC. The high EC in both hypoxic and normoxic treated cells indicate energy sufficient metabolic states. If the OXPHOS is not effectively working in the oxygen deprived environment, the glycolytic rate must be greatly enhanced to maintain a high EC. Glycolytic intermediates, except for fructose 1,6-bisphosphate (F1,6BP), are elevated in hypoxic treated cells, suggesting either accumulation or increased glycolytic flux. As hypoxic treated cells appear to have reduced nucleotide levels, an accumulation of glycolytic intermediates could serve to divert carbons

into the serine synthesis pathway and PPP for nucleotide synthesis [14]. This scenario could involve up-regulation of PKM2, which block glycolytic flux towards pyruvate production [15]. On the other hand, elevated glycolytic intermediates may indicate an enhanced glycolytic flux. If this is the case, the pyruvate should be reduced to lactate for regeneration of NAD+ to favour a high glycolytic rate [5]. Nevertheless, an increased lactate yield (aerobic glycolysis) is not observed after hypoxic treatment.

As it is questionable how a favourable high glycolytic rate is maintained without driving pyruvate towards lactate production, an alternative hypothesis was developed. The alterations in TCA cycle intermediate pools may not be sufficiently large to affect the flux through the TCA cycle. This hypothesis is supported by the TCA intermediate pools ability to sustain a carbon flux over a wide range of concentrations [55]. If this is the case, $NADH/FADH_2$ production by the TCA cycle is coupled to OXPHOS in the mitochondria, assuming that the oxygen transfer/concentration is high enough to saturate COX [56]. A sustained OXPHOS under low cellular oxygen concentrations may involve HIF-1 induced replacement of subunit COX4-1 with subunit COX4-2, resulting in increased efficacy of COX under aerobic conditions [5]. A sustained flux through the TCA cycle and hence OXPHOS is thought to be the most likely explanation to the unaltered EC observed after hypoxic treatment. Further on, it would be interesting to perform a metabolic flux experiment with carbon-13 ($^{13}C$) to reveal which pathways glucose is directed towards, and to prove or disapprove some of these alternative hypothesis.

**4.3.2 Hypoxic 48 hour Treatment Effect on U-87 MG**

The 48 hour hypoxic treatment resulted in slightly reduced nucleotide pools, and slightly altered levels of glycolytic intermediates in U-87 MG cells. The observed decreased level of several glycolytic intermediates in the preparatory phase could be due to a glycolytic shift, where glucose-derived carbons are diverted towards the serine pathway and PPP[14]. The R5P pool was significantly elevated in hypoxic treated U-87 MG cells, indicating a hypoxic induction of the PPP [25], perhaps through PKM2 [15]. Diversion of glucose-derived carbons into the PPP and serine pathway could be a strategy to replenish the nucleotide pool. By increasing the concentration of free nucleotides, the nucleic acid synthesis and cellular proliferation may be further supported. It would have been beneficial to have deoxyribonucleotide data (other than thymidine mono-di-triphosphates) to prove or disapprove a decreased production of deoxyribonucleotides from ribonucleotides.

Nevertheless, the observed sustained growth rate in the next 24 hours of hypoxic incubation indicate that nucleic acids are not scarce. The PPP also allows for generation of NADPH, which may be of importance to counteract toxic effects of hypoxia-induced ROS [22].

If glucose-derived carbons are diverted towards the serine pathway and PPP, glutamine could be used as an alternative carbon source to support bioenergetics and biosynthesis [9]. Nevertheless, the glutamine uptake is not increased after hypoxic treatment. Significantly reduced levels of several TCA intermediates were observed in hypoxic treated U-87 MG cells. Amino acids, including those derived from the TCA cycle, are generally decreased during hypoxic treatment. The reduction of TCA cycle intermediate pools and TCA-cycle intermediate derived amino acids is probably due to reduced input of glucose-derived carbon atoms in the TCA cycle which is not balanced out by an increased input of glutamine-derived carbons. The observed elevated levels of 3-phosphoglycerate (3PG), 2-phosphoglycerate (2PG), phosphoenolpyruvate (PEP) and pyruvate may be due to accumulations, if they are prevented from entering the TCA cycle. This could be due to activation of PKM2 and/or HIF-1 induction of PDK1 [15, 23]. Nevertheless, the overall EC is not altered by the hypoxic treatment. As the lactate production and glucose production is not increased after hypoxic treatment, this indicate a sustained flux of glucose into the TCA cycle and OXPHOS.


### 4.3.3 Hypoxic 72 hour Treatment Effect on DU-145

The 72 hour hypoxic treatment caused a doubling or more than doubling of amino acids and slightly elevated nucleotide pools in DU-145 cells. Important in this context, is the cessation of cell growth observed between 72 and 96 hours of hypoxic exposure which indicate growth arrest. The growth arrest is probably induced as the media is nearly deprived of glutamine, a carbon and nitrogen source. As the requirement of macromolecules is lower under growth arrest compared to that under rapid cellular proliferation, induction of growth arrest is probably a strategy to reduce biosynthetic and bioenergetics needs [9]. Thus, the elevated amino acid pools and nucleotide pools at 72 hours indicate preparation for growth arrest through decreased protein and nucleotide synthesis. Additionally, an elevated glycerol 3-phosphate (GL3P) level is observed after hypoxic treatment. This is likely caused by reduced fatty acid synthesis under growth arrest, and accumulation due to feedback inhibition. All together, down-regulating of anabolic pathways, such as protein, nucleic acid and fatty acid synthesis, reduces the rewquirement for energy and likely serves to sustain the high EC observed in hypoxic treated cells.

### 4.3.4 Hypoxic 72 hour Treatment Effect on U-87 MG

Glucose could not be quantified in the 72 hour treated hypoxic replica 1 and 2 which were used for capIC analysis. The highly reduced levels of glycolytic intermediates observed in U-87 MG cells after 72 hours of hypoxic incubation, is probably due to a reduced glucose uptake as the culture media is deprived of glucose. The cessation of growth between 72 and 96 hours of hypoxic exposure, indicate growth arrest. It is therefore likely that the 72 hour hypoxic treated cells are either in a state of little growth, or prepares for growth arrest. The nucleotide pool and amino acid pools are slightly elevated after hypoxic treatment, indicating a decreased consumption. This is probably related to decreased requirements of nucleotides/dexoribonucleotides and proteins under growth arrest [9]. The R5P and 6PG pools are also altered. Accumulation of NADHP generated in the PPP likely inhibit the G6PDH, resulting in less diversion of glucose-derived carbons towards the PPP. Additionally, the hypoxic treatment resulted in reduced GL3P and citrate pools. This is probably due to reduced requirement for fatty acid synthesis during growth arrest. The overall EC is not altered in these glucose-deprived cells. As suggested for 72 hour hypoxic treated DU-145 cells, down-regulation of energy-consuming anabolic pathways likely serve to sustain a high EC. As the carbon metabolism is clearly affected by limitations in glucose and glutamine supply, this emphasizes the importance of measuring their consumption when performing central carbon metabolic profiling.

## 4.4 Further Outlook

Based on the experiences made during the study, it is recommended to perform the following matters applying the same experimental setup:

- Establish an earlier time frame for evaluation of metabolic profile, for instance after 6, 24 and 48 hours of hypoxic incubation, in order to reveal whether the effects observed in this study are also present earlier during incubation.
- Assess the abundance and ratios of NADP+/NADPH and NAD+/NADH, to evaluate to evaluate cellular redox state. Methods for detecting NADP+/NADPH and NAD+/NADH ratios are, at the time of writing, being developed.

# 5. Conclusion

The hypoxic treatment did not result in altered cell growth nor energy charge. The consumption of the major carbon and energy sources was either affected. Overall, most metabolites were only modest altered by the hypoxic treatment. Some intracellular metabolites were found prominently and/or significantly changed by the hypoxic treatment, and these may be further investigated for identification of metabolic adaptions under hypoxic conditions. The efficacy of ATX-101, as a single agent and in combination with cisplatin, was not altered under hypoxic conditions, strengthening its role in cancer treatment.

# References

1.  Hanahan, D. and Robert A. Weinberg, *Hallmarks of Cancer: The Next Generation.* Cell. **144**(5): p. 646-674.
2.  kreftforskning, K.I.f.p., *Cancer incidence, mortality, survival and prevalence in Norway.* 2015.
3.  Weinberg, R.A., *How cancer arises.* Sci Am, 1996. **275**(3): p. 62-70.
4.  Luoto, K.R., R. Kumareswaran, and R.G. Bristow, *Tumor hypoxia as a driving force in genetic instability.* Genome Integr, 2013. **4**(1): p. 5.
5.  Eales, K.L., K.E.R. Hollinshead, and D.A. Tennant, *Hypoxia and metabolic adaptation of cancer cells.* Oncogenesis, 2016. **5**: p. e190.
6.  Brown, J.M., *Tumor hypoxia in cancer therapy.* Methods Enzymol, 2007. **435**: p. 297-321.
7.  Yang, L., et al., *Hypoxia and hypoxia-inducible factors in glioblastoma multiforme progression and therapeutic implications.* Experimental Cell Research, 2012. **318**(19): p. 2417-2426.
8.  Cairns, R.A., I.S. Harris, and T.W. Mak, *Regulation of cancer cell metabolism.* Nat Rev Cancer, 2011. **11**(2): p. 85-95.
9.  DeBerardinis, R.J., et al., *The biology of cancer: metabolic reprogramming fuels cell growth and proliferation.* Cell Metab, 2008. **7**(1): p. 11-20.
10. Kim, J.-w. and C.V. Dang, *Cancer's Molecular Sweet Tooth and the Warburg Effect.* Cancer Research, 2006. **66**(18): p. 8927-8930.
11. Weinberg, R., *The Biology of Cancer*. 2014, New York: Carland Science, Taylor % Francis Group.
12. Vander Heiden, M.G., L.C. Cantley, and C.B. Thompson, *Understanding the Warburg Effect: The Metabolic Requirements of Cell Proliferation.* Science (New York, N.Y.), 2009. **324**(5930): p. 1029-1033.
13. Yin, C., S. Qie, and N. Sang, *Carbon Source Metabolism and Its Regulation in Cancer Cells.* Critical reviews in eukaryotic gene expression, 2012. **22**(1): p. 17-35.
14. Ward, Patrick S. and Craig B. Thompson, *Metabolic Reprogramming: A Cancer Hallmark Even Warburg Did Not Anticipate.* Cancer Cell, 2012. **21**(3): p. 297-308.
15. Dong, G., et al., *PKM2 and cancer: The function of PKM2 beyond glycolysis.* Oncology Letters, 2016. **11**(3): p. 1980-1986.
16. DeBerardinis, R.J. and T. Cheng, *Q's next: The diverse functions of glutamine in metabolism, cell biology and cancer.* Oncogene, 2010. **29**(3): p. 313-324.
17. Newsholme, P., et al., *Glutamine and glutamate as vital metabolites.* Brazilian Journal of Medical and Biological Research, 2003. **36**: p. 153-163.
18. Wang, G.L., et al., *Hypoxia-inducible factor 1 is a basic-helix-loop-helix-PAS heterodimer regulated by cellular O2 tension.* Proceedings of the National Academy of Sciences of the United States of America, 1995. **92**(12): p. 5510-5514.
19. Huang, L.E., et al., *Regulation of hypoxia-inducible factor 1alpha is mediated by an O2-dependent degradation domain via the ubiquitin-proteasome pathway.* Proc Natl Acad Sci U S A, 1998. **95**(14): p. 7987-92.
20. Semenza, G.L., *Hypoxia-inducible factor 1: master regulator of O2 homeostasis.* Curr Opin Genet Dev, 1998. **8**(5): p. 588-94.

21. Kuschel, A., P. Simon, and S. Tug, *Functional regulation of HIF-1alpha under normoxia--is there more than post-translational regulation?* J Cell Physiol, 2012. **227**(2): p. 514-24.

22. Nelson, D.L.a.C., M.M, *Lehninger Principles of Biochemistry*. 2008: W.H-Freeman and company.

23. Kim, J.-w., et al., *HIF-1-mediated expression of pyruvate dehydrogenase kinase: A metabolic switch required for cellular adaptation to hypoxia.* Cell Metabolism. **3**(3): p. 177-185.

24. Amelio, I., et al., *Serine and glycine metabolism in cancer().* Trends in Biochemical Sciences, 2014. **39**(4): p. 191-198.

25. Masson, N. and P.J. Ratcliffe, *Hypoxia signaling pathways in cancer metabolism: the importance of co-selecting interconnected physiological pathways.* Cancer & Metabolism, 2014. **2**: p. 3-3.

26. Sosa, V., et al., *Oxidative stress and cancer: An overview.* Ageing Research Reviews, 2013. **12**(1): p. 376-390.

27. Fendt, S.-M., et al., *Reductive glutamine metabolism is a function of the α-ketoglutarate to citrate ratio in cells.* Nature communications, 2013. **4**: p. 2236-2236.

28. Kucharzewska, P., H.C. Christianson, and M. Belting, *Global Profiling of Metabolic Adaptation to Hypoxic Stress in Human Glioblastoma Cells.* PLoS ONE, 2015. **10**(1): p. e0116740.

29. Monneret, C., *Platinum anticancer drugs. From serendipity to rational design.* Ann Pharm Fr, 2011. **69**(6): p. 286-95.

30. Wang, D. and S.J. Lippard, *Cellular processing of platinum anticancer drugs.* Nat Rev Drug Discov, 2005. **4**(4): p. 307-20.

31. Kartalou, M. and J.M. Essigmann, *Mechanisms of resistance to cisplatin.* Mutat Res, 2001. **478**(1-2): p. 23-43.

32. Galluzzi, L., et al., *Molecular mechanisms of cisplatin resistance.* Oncogene, 2012. **31**(15): p. 1869-1883.

33. Siddik, Z.H., *Cisplatin: mode of cytotoxic action and molecular basis of resistance.* Oncogene, 2003. **22**(47): p. 7265-79.

34. Cheung-Ong, K., G. Giaever, and C. Nislow, *DNA-Damaging Agents in Cancer Chemotherapy: Serendipity and Chemical Biology.* Chemistry & Biology, 2013. **20**(5): p. 648-659.

35. Shen, D.-W., et al., *Cisplatin Resistance: A Cellular Self-Defense Mechanism Resulting from Multiple Epigenetic and Genetic Changes.* Pharmacological Reviews, 2012. **64**(3): p. 706-721.

36. Moldovan, G.L., B. Pfander, and S. Jentsch, *PCNA, the maestro of the replication fork.* Cell, 2007. **129**(4): p. 665-79.

37. Tsurimoto, T., *PCNA binding proteins.* Front Biosci, 1999. **4**: p. D849-58.

38. Naryzhny, S.N. and H. Lee, *Proliferating cell nuclear antigen in the cytoplasm interacts with components of glycolysis and cancer.* FEBS Lett, 2010. **584**(20): p. 4292-8.

39. Rosental, B., et al., *Proliferating cell nuclear antigen is a novel inhibitory ligand for the natural cytotoxicity receptor NKp44.* J Immunol, 2011. **187**(11): p. 5693-702.

40. Gilljam, K.M., et al., *Identification of a novel, widespread, and functionally important PCNA-binding motif.* J Cell Biol, 2009. **186**(5): p. 645-54.

41.     Muller, R., et al., *Targeting proliferating cell nuclear antigen and its protein interactions induces apoptosis in multiple myeloma cells.* PLoS One, 2013. **8**(7): p. e70430.

42.     Gederaas, O.A., et al., *Increased Anticancer Efficacy of Intravesical Mitomycin C Therapy when Combined with a PCNA Targeting Peptide.* Transl Oncol, 2014. **7**(6): p. 812-23.

43.     Zhang, A., et al., *Modern analytical techniques in metabolomics analysis.* Analyst, 2012. **137**(2): p. 293-300.

44.     Patti, G.J., O. Yanes, and G. Siuzdak, *Innovation: Metabolomics: the apogee of the omics trilogy.* Nat Rev Mol Cell Biol, 2012. **13**(4): p. 263-269.

45.     Roberts, L.D., et al., *Targeted Metabolomics.* Current Protocols in Molecular Biology, 2012. **CHAPTER**: p. Unit30.2-Unit30.2.

46.     Dr. Silas G. Villas-Bôas, D.U.R., Dr. Michael A. E. Hansen, Dr. Jørn Smedsgaard, Dr. Jens Nielsen, *Metabolome Analysis: An Introduction*. 2007: A John Wiley & Sons, Inc., Publication.

47.     Alonso, A., S. Marsal, and A. Julià, *Analytical Methods in Untargeted Metabolomics: State of the Art in 2015.* Frontiers in Bioengineering and Biotechnology, 2015. **3**: p. 23.

48.     Tuzimski, T.S., P, *High Performance Liquid Chromatography in Pesticide Residue Analysis*. 2015: CRC press.

49.     Buszewski, B. and S. Noga, *Hydrophilic interaction liquid chromatography (HILIC)—a powerful separation technique.* Analytical and Bioanalytical Chemistry, 2012. **402**(1): p. 231-247.

50.     Dunn, W.B. and D.I. Ellis, *Metabolomics: Current analytical platforms and methodologies.* TrAC Trends in Analytical Chemistry, 2005. **24**(4): p. 285-294.

51.     Kvitvang, H.F.N., K.A. Kristiansen, and P. Bruheim, *Assessment of capillary anion exchange ion chromatography tandem mass spectrometry for the quantitative profiling of the phosphometabolome and organic acids in biological extracts.* Journal of Chromatography A, 2014. **1370**: p. 70-79.

52.     Čuperlović-Culf, M., et al., *Cell culture metabolomics: applications and future directions.* Drug Discovery Today, 2010. **15**(15–16): p. 610-621.

53.     Græ, M.A., *Mass Spectrometry Based Metabolite Profiling of Cytostatic Induced Stress Response in the Prostate Cancer Cell Line DU 145*

. 2014.

54.     Kizaka-Kondoh, S., et al., *Tumor hypoxia: a target for selective cancer therapy.* Cancer Sci, 2003. **94**(12): p. 1021-8.

55.     Owen, O.E., S.C. Kalhan, and R.W. Hanson, *The Key Role of Anaplerosis and Cataplerosis for Citric Acid Cycle Function.* Journal of Biological Chemistry, 2002. **277**(34): p. 30409-30412.

56.     Fontanesi, F., I.C. Soto, and A. Barrientos, *Cytochrome c Oxidase Biogenesis: New levels of Regulation.* IUBMB life, 2008. **60**(9): p. 557-568.

# A   Additional Reading

## A.1 Hypoxic Condition Strategy

In this experimental setting, cellular hypoxia was induced by incubating cultured cancer cells in complete growth medium in a sealed SubChamber System. This chamber was placed in a controlled incubator and connected to a $O_2/CO_2$ controller (ProOx C21, Biospherix). From outside the chamber, this instrument sensed $O_2$ and $CO_2$ inside the SubChamber, and infused gas to control both levels. To lower $O_2$ level inside the SubChamber, $N_2$ was infused to displace it. To obtain hypoxic conditions, the SubChamber was set to 1% $O_2$ and 5% $CO_2$. Any disturbances in the desired set point were immediately detected and corrected.

## A.2 MTT Assay

Cell viability assays are methods used to estimate the number of viable cells in multi-well plates. The 3-(4,5-dimethylthiazol-2-yl)-2,5-diphenyltetrazolium bromide (MTT) reduction assay is a cell viability assay broadly applied to measure in vitro cytotoxic effects of drugs on cell lines. The assay is based on the conversion of yellow water-soluble MTT into a purple colored formazan product by living cells with active metabolism. MTT can be reduced by cleavage of the tetrazolium ring by various enzymes, including the mitochondrial succinate dehydrogenase enzyme. Dead cells have lost the ability to convert MTT into formazan, and color formation is thus a convenient marker of only viable cells. The formazan product is an insoluble precipitate which is deposited inside cells, near the cell surface and in the culture medium. The amount of formazan-product which is detected depends on the concentration of MTT, the length of the incubation period, the number of viable cells and their metabolic activity. Prior to quantification of the formazan product, it must be solubilized. Various methods can be applied to solubilize the formazan product, including applying acidified isopropanol. Acidification of the solution changes the color of phenol red to yellow color, which interefere less with the absorbance reading. The formazan product has maximum absorbance near 565 nm, and formazan can be quantified by recording absorbance at 565 nm.

## A.3 HIF-1A ELISA Kit

The HIF-1A ELISA kit by Thermo Scientific measure HIF-1A protein serum, plasma and cell culture lysates. The kit utilizes a quantitative sandwich ELISA method, where the HIF-1A standard and samples are captured by a polyclonal HIF-1A antibody placed on a precoted plate, and detected using a monoclonal HIF-1A antibody that binds to the polyclonal antibody. The latter antibody is bound to streptavidin-horseradish peroxidase (HRP). HRP is

an enzyme which catalyse the conversion of 3,3′,5,5′-Tetramethylbenzidine (TBM) substrate to a colored product. The amount of product formed is directly proportional to the amount of HIF1A present in the sample. The amount of product can be measured at 450 nm.

# B    Calculations
## B.1 Statistical Calculations

**Relative Standard Deviation**

The relative standard deviation (RSD) inform whether the standard deviation is small or large in quantity when compared to the average of the dataset. The RSD is calculated as:

$$RSD = \frac{\sigma_x}{\bar{x}} \times 100 \tag{B.1}$$

where $\sigma_x$ is the standard deviation, and $\bar{x}$ is the average.

## B.2 Yield
The yield of lactate from glucose calculated as:

$$Yield_{lactate/glucose} = \frac{C_{lactate}}{C_{glucose}} \tag{B.2}$$

where C is the number of grams of compound (lactate or glucose) per cell per hour.

## B.3 Energy Charge
The energy charge (E.C) is used to measure the energy status in the cell and is related to ATP, ADP and AMP concentrations. The E.C is defined as:

$$E.C = \frac{[ATP] + \frac{1}{2}[ADP]}{[ATP] + [ADP] + [AMP]} \tag{B.3}$$

The energy charge can have a value between 0 (no ATP) to 1 (all ATP).

## B.4 Medium formulation

Glutamine concentration in RMPI medium:

$$C_{\text{L-glutamine}} = \frac{(0,3 \text{ g/L x } 0,5 \text{ L}) + (0,2 \text{ mol/L x } 146,15 \text{ g/mol x } 0,005 \text{ L})}{0,565 \text{ L}} = 0,524 \text{ g/L}$$

where 0,3 g/L is the amount of L-glutamine in the medium obtained from Sigma Aldrich, and 0,5 L is the total amount of this culture medium. Culture medium is supplemented with glutamine (0.2 mol/L, 5 mL, 146,15 g/mol), FBS (50 mL), Amphoterecin B (5 mL) and Gentamicin (5 mL) to a total volume of 0,565 L.

Glucose concentration in RPMI medium:

$$C_{\text{D-glucose}} = \frac{(2 \text{ g/L x } 0,5 \text{ L})}{0,565 \text{ L}} = 1,77 \text{ g/L}$$

where 2 g/L is the amount of D-glucose in the medium (0,5 L), and 0,565 L is the total volume of the culture media after addition of supplementary solutions.

Glutamine concentration in minimum essential medium:

$$C_{\text{L-glutamine}} = \frac{(0,292 \text{ g/L x } 0,5 \text{ L}) + (0,2 \text{ mol/L x } 146,15 \text{ g/mol x } 0,005 \text{ L})}{0,565 \text{ L}} = 0,517 \text{ g/L}$$

where 0,292 g/L is the amount of L-glutamine in the medium obtained from Sigma Aldrich (0,5 L). Culture medium is supplemented with glutamine (0.2 mol/L, 5 mL, 146,15 g/mol), FBS (50 mL), Amphoterecin B (5 mL) and Gentamicin (5 mL) to a total volume of 0,565 L.

Glucose concentration in miminum essential medium:

$$C_{\text{glucose}} = \frac{(1 \text{ g/L x } 0,5 \text{ L})}{0,565 \text{ L}} = 0,885 \text{ g/L}$$

where 1 g/L is the amount of D-glucose in the medium (0,5 L), and 0,565 L is the total volume of the culture media after addition of supplementary solutions.

Neither RMPI medium nor Minimum Essential Medium is supplemented with Lactate.

# C    Statistical Analysis
## ANOVA
One way analysis of variance (ANOVA) was performed on metabolome data from NMR and MS analyses (RP LC-MS/MS and capIC-MS/MS). The ANOVA test was performed using StatPlus, a statistical analysis program. The significance level was chosen to be 0,05, i.e 95% confidence interval.

The one way ANOVA test examines equality or non-equality of sample group means. The term one way indicates that there is only a single explanatory variable. The ANOVA tests the null hypothesis, $H_o$ (means of all sample groups are equal) against the alternative hypothesis $H_1$ (means of sample groups are not equal). Specifically, the Anova tests the null hypothesis:

$$H_0 = \mu_1 = \mu_2 = \mu_3 = \ldots = \mu_k,$$

where $\mu$ is the sample group mean and k is the number of sample groups.

A p-value smaller than the chosen significant level, indicates that at least one sample group differs from the others, and the $H_0$ is rejected. A p-value larger than the significant level indicate a non-significant difference between sample groups, and the $H_1$ is accepted.

# D    Normalization of Endometabolome and HIF-1A data
Endometabolome and HIF-1A data was normalize to the average cell count at the time of sampling in respective samples.

Endometabolome and HIF-1A data was normalized applying equation D.1,

$$X_{normalized\ concentration} = \frac{X}{Y} \tag{D.1}$$

where

X = metabolite/HIF-1A concentration

Y = average cell number (at time of sampling) for each treatment sample.

# E    Glucose, Glutamine and Lactate Concentrations

## E.1 DU-145

The unnormalized glucose, glutamine and lactate concentrations for the different DU-145 sample groups are given in table E.1. LOQ (limit of quantification) means that the concentration is below limit of quantification, and hence no values could be obtained. LOD (limit of detection) means that the concentration of the metabolite could be detected, but not quantified. The 96 hour hypoxic replica 3 was excluded due to technical aspects.

**Table E.1.** Glucose, lactate and glutamine concentrations for the different sample groups included in the DU-145 experimental setup. The concentration of glucose, glutamine and lactate in fresh medium sample is also given.

| Sample group | Technical replica | Concentration [g/L] | | |
| --- | --- | --- | --- | --- |
| | | Glucose | Glutamine | Lactate |
| Fresh medium | | 1,64 | 0,42 | 0,14 |
| Normoxia 48h | 1 | 1,44 | 0,28 | 0,55 |
| | 2 | 1,23 | 0,27 | 0,52 |
| | 3 | 1,37 | 0,28 | 0,56 |
| | 4 | 1,36 | 0,32 | 0,54 |
| Normoxia 72h | 1 | 0,77 | 0,14 | 0,80 |
| | 2 | 0,85 | 0,19 | 0,87 |
| | 3 | 0,83 | 0,18 | 0,77 |
| | 4 | 0,95 | 0,20 | 0,87 |
| Normoxia 96h | 1 | 0,38 | LOQ | 1,45 |
| | 2 | 0,46 | LOQ | 1,64 |
| | 3 | 0,44 | LOQ | 1,47 |
| Hypoxia 48h | 1 | 1,24 | 0,31 | 0,58 |
| | 2 | 1,02 | 0,29 | 0,49 |
| | 3 | 1,43 | 0,29 | 0,62 |
| | 4 | 1,17 | 0,30 | 0,56 |
| Hypoxia 72h | 1 | 0,71 | 0,30 | 1,19 |
| | 2 | 0,84 | 0,26 | 0,89 |
| | 3 | 0,75 | 0,25 | 1,15 |
| | 4 | 0,78 | 0,19 | 1,09 |
| Hypoxia 96h | 1 | 0,27 | LOQ | 1,18 |
| | 2 | 0,33 | LOQ | 1,59 |
| | 3 | 0,35 | LOQ | 1,61 |
| | 4 | 0,29 | LOQ | 1,59 |

## E.2 U-87 MG

The unnormalized glucose, glutamine and lactate concentrations for the different U-87 MG sample groups are given in table E.2.

**Table E.2.** Glucose, lactate and glutamine concentrations for the different sample groups included in the U-87 MG experimental setup. The concentration of glucose, glutamine and lactate in fresh medium sample is also given.

| Sample group | Technical replica | Concentration [g/L] | | |
| --- | --- | --- | --- | --- |
| | | Glucose | Glutamine | Lactate |
| Fresh medium | | 0,94 | 0,43 | 0,13 |
| Normoxia 48h | 1 | 0,51 | 0,35 | 0,35 |
| | 2 | 0,50 | 0,39 | 0,39 |
| | 3 | 0,52 | 0,37 | 0,37 |
| | 4 | 0,49 | 0,43 | 0,43 |
| Normoxia 72h | 1 | 0,08 | 0,35 | 0,35 |
| | 2 | 0,08 | 0,31 | 0,31 |
| | 3 | 0,13 | 0,38 | 0,38 |
| | 4 | 0,06 | 0,39 | 0,39 |
| Normoxia 96h | 1 | LOD | 0,27 | 0,27 |
| | 2 | LOD | 0,29 | 0,29 |
| | 3 | LOD | 0,27 | 0,27 |
| | 4 | LOD | 0,32 | 0,32 |
| Hypoxia 48h | 1 | 0,42 | 0,35 | 0,55 |
| | 2 | 0,43 | 0,34 | 0,63 |
| | 3 | 0,42 | 0,41 | 0,60 |
| | 4 | 0,42 | 0,37 | 0,58 |
| Hypoxia 72h | 1 | LOQ | LOQ | LOQ |
| | 2 | LOQ | 0,35 | LOQ |
| | 3 | 0,06 | 0,33 | 1,07 |
| | 4 | 0,07 | 0,32 | 1,01 |
| Hypoxia 96h | 1 | LOD | 0,27 | 1,07 |
| | 2 | LOD | 0,34 | 1,05 |
| | 3 | LOD | 0,34 | 1,07 |
| | 4 | LOD | 0,31 | 1,01 |

# F  Calculation of Metabolite Production and Consumption

Metabolite production and consumption after 48 hour of treatment exposure was calculated using the difference in metabolite concentration between fresh medium samples collected at the time of treatment addition and endpoint sample. Average glucose and glutamine consumption, and lactate production were calculated from all technical replicas within each sample groups. However, metabolites that could not be detected or quantified, were excluded.

Average glucose and glutamine production after 72 and 96 hours of hypoxic/normoxic incubation was calculated using the following equation:

$$\text{Metabolite production}_{(i)} = X_{(i-24)} - X_{(i)}, \tag{F.1}$$

where

$X$ = average metabolite concentration based on technical replicas within the sample group,

$I$ = time (72 or 96 hours) after treatment.

Average lactate consumption after 72 and 96 hours of hypoxic/normoxic was calculated using the following equation:

$$\text{Metabolite consumption}_{(i)} = X_{(i)} - X_{(i-24)}, \tag{F.2}$$

where

$X$ = average metabolite concentration based on technical replicas within the sample group,

$I$ = time (72 or 96 hours) after treatment.

# G   Normalization of Exometabolome Data

Exometabolome data was normalized with respect to average cell counts in respective treatment samples. This normalization was performed to correct for cell reduction observed by treatment effects.

Cell counts were preformed after 48, 72 and 96 hours of treatment addition. Estimated cell counts in the middle of each time interval (0-48h, 48-72h and 72-96h) were calculated. The cell number$_{0h}$ could be calculated as the seeding cell number$_{-24h}$ and cell number$_{48h}$ were known. First, the population doubling time was calculated utilizing the following equation:

$$\text{Doubling time} = \frac{x *\log(2)}{\log (\text{cell number}_{48h}) - \log (\text{cell number}_{-24h})} \tag{G.1}$$

where

X = treatment duration.

Hereafter, the cell number$_{0h}$, was calculated utilizing the following equation:

$$\text{Cell number}_{0h} = \text{Cell number}_{-24h} \times 2^g, \tag{G.2}$$

where

G = number of generations that have passed during the time interval.

The following assumptions are made; cell growth is constant, the glucose/glutamine consumption and lactate production is constant, and that the cell number$_{0h}$ is equal for all treatment samples. Cell number$_{0h}$ was found to be 33769 cells/mL for DU-145 cells, and 65766 cells/mL for U-87 MG cells.

The DU-145 and U-87 MG cell growth curves are presented in Figures G.1 and G.2, respectively.
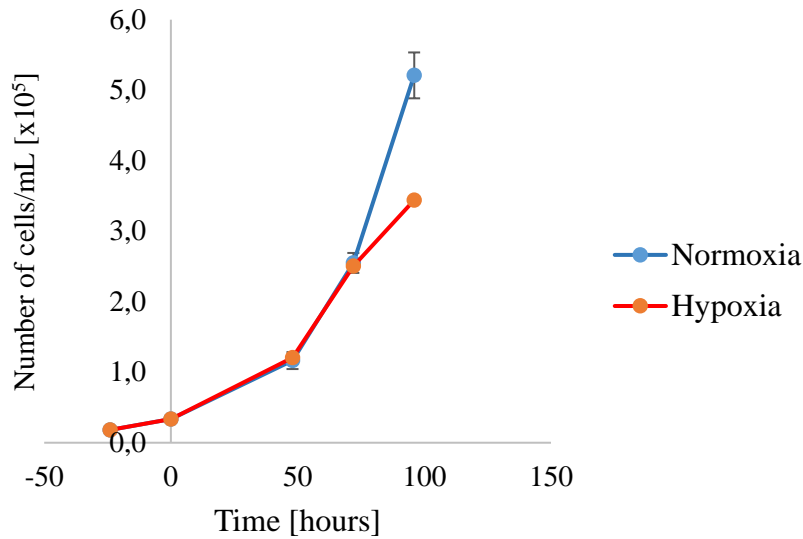
**Figure G.1:** The number of DU-145 cells in normoxic and hypoxic treated sample groups. The standard deviation between technical replicas is shown.
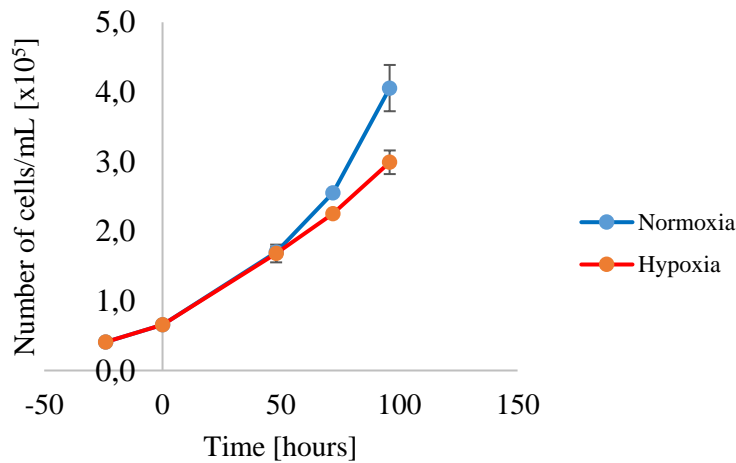


**Figure G.2:** The number of U-87 MG cells in normoxic and hypoxic treated sample groups. The standard deviation between technical replicas is shown.

Exometabolome data was normalized applying equation G.3,

$$X_{\text{normalized metabolite concentration}} = \frac{X}{Y} \tag{G.3}$$

where

X = extracellular metabolite concentration

Y = average cell number (in mid treatment) for each treatment sample.

# H RP LC-MS/MS Analysis

## H.1 Quantification of Amino Acidds

Targeted RP LC-MS/MS of amino acids was peformed using a Waters Acuity I-Class UPLC system coupled to a Waters TQ-S triple quadrupole mass spectrometer. The RP LC-MS/MS ptorocol is given in section H.1.1, whereas the standard mixture used for quantification from RP LC-MS/MS data is presented in section H.1.2. Details about the MS settings, including MRM-transitions can be obtained from supervisor P. Bruheim.

### H.1.1 RP LC-MS/MS Protocol for Amino Acids

Phenomenex EZ faast AAA-MS column 250x0,2 mm, 4 μm particle size.

| | |
|---|---|
| Column temperature: | 25 gc |
| Flow rate: | 250 μL/min |
| Injection volume: | 1 μL |
| Mobile phase A: | $H_2O$ with 10 mM ammonium formate |
| Mobile phase B: | Methanol with 10 mM ammonium formate |

*Mobile phase gradient:*

| | |
|---|---|
| 0-1 min: | 68% B |
| 1-11 min: | 68-85% B |
| 11-11,1 min: | 85-68% B |
| 15 min: | End |

### H.1.2 RP LC-MS/MS Standard Mixture

Metabolites included in the standard mixture used for target analysis of amino acids by RP LC-MS/MS are given in Table H.1.

**Table H.1** Compounds in the standard mixture used for targeted analysis of amino acids by RP LC-MS/MS.

| Amino acid standard mixture (1 mM) |
| --- |
| Alanine |
| Asparagine |
| Glutamine |
| Glycine |
| Histidine |
| Hydroxyproline |
| Isoleucine |
| Leucine |
| Lysine |
| Methionne |
| Ornithine |
| Phenylalanine |
| Proline |
| Serine |
| Tryptophan |
| Tyrosine |
| Valine |

### H.1.3 Amino Acid Raw Data

### DU-145 cells

Concentrations [µM] of amino acids obtained from the RP LC-MS/MS processed by TargetLynx (MassLynx 4.1, Waters) are presented in Table H.2 for DU-145. Technical replicas and metabolites excluded in the downstream analysis are marked in grey, and gaps indicate no detected measurement.

**Table H.2** Concentrations [μM] of all amino acids included in the RP LC-MS/MS analysis for DU-145 sample groups.

| | Paralelle | Gly | Ala | Ser | Pro | Val | Thr | OHpro | Leu | Ile | Met | Phe | Asp | Tyr | Glu | Trp | Orn | Lys |
|---|---|---|---|---|---|---|---|---|---|---|---|---|---|---|---|---|---|---|
| Hypoxia 48 | 1,0 | 3,3 | 7,0 | 3,0 | 3,5 | 2,3 | 3,3 | 2,3 | 4,8 | 5,0 | 0,3 | 0,8 | 9,5 | 1,0 | 42,0 | 0,3 | 1,5 | 2,3 |
| | 2,0 | 5,5 | 15,3 | 7,3 | 7,3 | 3,5 | 4,3 | 4,0 | 9,0 | 9,0 | 3,8 | 1,5 | 13,5 | 1,8 | 61,0 | 0,5 | 2,8 | 4,0 |
| | 3,0 | 6,3 | 15,3 | 6,8 | 6,8 | 3,5 | 4,3 | 3,8 | 8,0 | 8,0 | 3,5 | 1,3 | 13,3 | 1,5 | 57,0 | 0,5 | 2,3 | 3,3 |
| | 4,0 | 2,5 | 8,5 | 2,3 | 3,3 | 1,5 | 1,0 | 1,3 | 3,0 | 2,8 | 1,3 | 0,5 | 9,0 | 0,5 | 43,0 | 0,3 | 1,0 | 1,0 |
| Hypoxia 72 | 1,0 | 2,0 | 10,8 | 1,0 | 3,0 | 1,0 | 2,3 | 0,8 | 1,5 | 1,5 | 0,8 | 0,3 | 4,8 | 0,3 | 39,5 | 0,0 | 0,8 | 0,5 |
| | 2,0 | 0,3 | 49,3 | 15,5 | 18,5 | 9,5 | 5,3 | 0,3 | 21,0 | 21,8 | 8,5 | 3,5 | 25,3 | 4,8 | 115,3 | 1,3 | 7,3 | 9,5 |
| | 3,0 | 14,0 | 42,0 | 17,3 | 18,3 | 10,3 | 7,3 | 11,0 | 19,5 | 23,0 | 7,8 | 3,5 | 33,5 | 4,0 | 140,5 | 1,0 | 7,3 | 9,3 |
| | 4,0 | 3,3 | 18,8 | 2,8 | 5,8 | 1,3 | 1,0 | 1,5 | 3,3 | 3,5 | 1,5 | 0,5 | 8,0 | 0,5 | 60,5 | 0,3 | 1,3 | 1,0 |
| Hypoxia 96 | 1,0 | 3,8 | 23,8 | 1,3 | 7,3 | 1,0 | 1,5 | 1,0 | 2,0 | 2,3 | 0,5 | 0,3 | 5,0 | 0,3 | 42,5 | 0,3 | 0,8 | 0,5 |
| | 2,0 | 11,5 | 63,3 | 5,8 | 19,0 | 3,5 | 3,8 | 3,8 | 7,8 | 7,5 | 3,0 | 1,3 | 13,8 | 1,5 | 100,3 | 0,5 | 3,0 | 3,0 |
| | 3,0 | 7,0 | 36,0 | 3,8 | 11,8 | 2,3 | 3,0 | 2,8 | 4,3 | 5,3 | 1,5 | 0,8 | 12,5 | 0,8 | 85,8 | 0,3 | 1,8 | 1,5 |
| | 4,0 | 6,5 | 34,0 | 2,8 | 10,5 | 1,8 | 2,5 | 2,0 | 3,8 | 4,0 | 1,5 | 0,8 | 11,0 | 0,5 | 97,0 | 0,3 | 1,5 | 1,3 |
| Normoxia 48 | 1,0 | 4,5 | 8,3 | 5,5 | 4,0 | 3,8 | 3,3 | 3,3 | 6,8 | 7,0 | 2,5 | 1,3 | 18,5 | 1,8 | 69,8 | 0,5 | 2,8 | 3,8 |
| | 2,0 | 4,0 | 9,8 | 3,5 | 4,0 | 2,5 | 1,8 | 2,3 | 5,3 | 5,5 | 2,0 | 0,8 | 13,8 | 1,0 | 36,8 | 0,3 | 1,3 | 1,8 |
| | 4,0 | 6,5 | 16,8 | 6,5 | 6,5 | 4,3 | 3,5 | 3,8 | 8,8 | 8,8 | 3,5 | 1,5 | 26,8 | 1,8 | 74,0 | 0,5 | 2,3 | 3,3 |
| Normoxia 72 | 1,0 | 4,0 | 27,5 | 3,5 | 7,0 | 1,8 | 3,0 | 2,5 | 4,0 | 4,5 | 1,5 | 0,8 | 18,0 | 0,8 | 76,3 | 0,3 | 1,0 | 0,8 |
| | 3,0 | 3,0 | 18,0 | 2,3 | 4,5 | 1,5 | 2,0 | 1,8 | 3,3 | 3,3 | 1,0 | 0,5 | 10,8 | 0,3 | 52,0 | 0,3 | 1,0 | 1,0 |
| | 4,0 | 6,0 | 32,0 | 3,3 | 7,0 | 2,5 | 2,8 | 2,5 | 5,3 | 5,8 | 1,8 | 0,8 | 20,5 | 0,8 | 94,5 | 0,3 | 1,0 | 1,3 |
| Normoxia 96 | 1,0 | 5,5 | 54,5 | 3,0 | 12,0 | 2,0 | 1,8 | 3,3 | 5,3 | 6,3 | 1,8 | 0,8 | 13,8 | 1,0 | 77,5 | 0,3 | 2,0 | 1,5 |
| | 2,0 | 5,5 | 42,8 | 2,0 | 9,5 | 1,8 | 1,3 | 2,0 | 4,0 | 4,3 | 1,3 | 0,5 | 8,8 | 0,5 | 54,0 | 0,3 | 1,3 | 1,0 |
| | 3,0 | 10,3 | 93,8 | 4,8 | 20,5 | 2,5 | 3,8 | 4,3 | 5,8 | 5,8 | 2,3 | 1,0 | 26,3 | 1,0 | 211,8 | 0,3 | 2,0 | 1,5 |

Metabolite [uM]

**U-87 MG cells**

Concentrations [μM] of amino acids obtained from the RP LC-MS/MS processed by TargetLynx (MassLynx 4.1, Waters) are presented in Table H.3 for U-87 MG. Technical replicas and metabolites excluded in the downstream analysis are marked in grey, and gaps indicate no detected measurement.

**Table H.3** Concentrations [µM] of all amino acids included in the RP LC-MS/MS analysis for U-87 MG sample groups.

| | Paralelle | Gly | Ala | Ser | Pro | Val | Thr | OHpro | Leu | Ile | Met | Phe | Asp | Tyr | Glu | Trp | Orn | Lys |
|---|---|---|---|---|---|---|---|---|---|---|---|---|---|---|---|---|---|---|
| Hypoxia 48 | 1 | 1,3 | 6,5 | 0,5 | 1,8 | 3,0 | 4,0 | 0,3 | 4,3 | 4,5 | 1,8 | 2,0 | 1,3 | 2,5 | 47,5 | 0,8 | 0,5 | 2,3 |
| | 3 | 1,0 | 6,0 | 0,3 | 2,0 | 2,5 | 3,5 | 0,0 | 2,5 | 2,5 | 0,8 | 1,0 | 1,3 | 0,8 | 52,3 | 0,3 | 0,3 | 1,0 |
| | 4 | 0,5 | 5,8 | 0,5 | 1,8 | 2,3 | 2,5 | 0,0 | 2,8 | 2,8 | 1,0 | 1,3 | 0,8 | 1,5 | 40,3 | 0,5 | 0,3 | 1,3 |
| Hypoxia 72 | 1 | 2,3 | 19,5 | 0,8 | 4,0 | 4,5 | 5,0 | 0,3 | 4,5 | 4,8 | 2,0 | 2,3 | 4,5 | 3,0 | 162,5 | 0,8 | 0,8 | 2,8 |
| | 2 | 2,3 | 16,8 | 2,0 | 4,3 | 5,0 | 10,0 | 0,5 | 5,0 | 5,8 | 2,5 | 2,8 | 4,8 | 3,5 | 129,0 | 1,0 | 1,0 | 4,5 |
| | 3 | 0,5 | 11,8 | 0,5 | 3,0 | 4,3 | 5,5 | 0,3 | 4,5 | 5,8 | 1,5 | 2,3 | 3,0 | 2,0 | 89,3 | 0,8 | 0,5 | 2,5 |
| | 4 | 2,0 | 22,0 | 0,8 | 4,0 | 6,8 | 8,5 | 0,3 | 7,3 | 7,3 | 3,8 | 3,5 | 3,3 | 4,5 | 87,3 | 1,3 | 1,3 | 5,5 |
| Hypoxia 96 | 1 | 5,5 | 33,3 | 1,3 | 5,5 | 5,0 | 6,0 | 0,3 | 5,3 | 5,8 | 2,5 | 3,0 | 7,3 | 3,8 | 108,5 | 0,8 | 0,8 | 2,5 |
| | 2 | 3,8 | 23,3 | 1,0 | 3,8 | 3,5 | 4,3 | 0,3 | 4,0 | 4,3 | 1,5 | 2,0 | 5,3 | 2,3 | 65,0 | 0,5 | 0,5 | 1,5 |
| | 3 | 3,8 | 21,3 | 0,8 | 3,3 | 3,3 | 3,8 | 0,3 | 3,8 | 4,0 | 1,0 | 2,3 | 3,3 | 2,5 | 53,5 | 0,8 | 0,5 | 1,5 |
| | 4 | 6,0 | 40,8 | 1,0 | 5,3 | 6,0 | 7,8 | 0,3 | 6,0 | 6,3 | 3,3 | 3,5 | 9,5 | 4,8 | 152,8 | 1,0 | 1,3 | 4,5 |
| Normoxia 48 | 1 | 0,8 | 6,5 | 0,5 | 2,0 | 3,0 | 5,0 | 0,3 | 3,0 | 3,5 | 1,3 | 1,5 | 1,8 | 2,0 | 47,5 | 0,5 | 0,5 | 1,5 |
| | 2 | 1,5 | 7,0 | 0,8 | 2,3 | 3,3 | 6,0 | 0,3 | 3,0 | 3,3 | 1,3 | 1,5 | 2,5 | 1,8 | 71,5 | 0,5 | 0,5 | 1,8 |
| | 3 | 0,3 | 2,8 | 0,5 | 1,0 | 1,5 | 3,0 | 0,0 | 1,3 | 1,5 | 0,5 | 0,8 | 1,0 | 0,5 | 25,0 | 0,3 | 0,3 | 0,3 |
| | 4 | 0,8 | 6,5 | 0,3 | 2,0 | 4,0 | 4,5 | 0,3 | 5,0 | 5,8 | 2,3 | 2,5 | 1,3 | 3,0 | 32,5 | 0,8 | 0,8 | 3,0 |
| Normoxia 72 | 1 | 0,5 | 15,0 | 0,5 | 3,5 | 3,5 | 4,8 | 0,3 | 3,5 | 3,5 | 1,0 | 2,3 | 3,0 | 2,8 | 68,3 | 0,8 | 0,3 | 1,8 |
| | 2 | 1,0 | 15,5 | 0,5 | 3,3 | 3,8 | 4,8 | 0,3 | 4,0 | 4,5 | 0,5 | 2,0 | 3,5 | 2,5 | 70,8 | 0,5 | 0,5 | 2,0 |
| | 3 | 2,5 | 19,3 | 0,8 | 3,8 | 6,8 | 9,5 | 0,3 | 8,0 | 9,3 | 3,3 | 4,3 | 3,8 | 5,5 | 83,3 | 1,3 | 1,3 | 6,3 |
| | 4 | 1,3 | 23,5 | 0,5 | 4,5 | 7,8 | 8,8 | 0,3 | 8,3 | 9,5 | 3,8 | 4,5 | 3,5 | 5,8 | 98,3 | 1,3 | 1,3 | 6,0 |
| Normoxia 96 | 1 | 3,5 | 42,5 | 1,3 | 6,3 | 5,5 | 10,0 | 0,5 | 5,5 | 6,3 | 1,3 | 3,5 | 32,5 | 4,8 | 133,0 | 1,0 | 0,5 | 2,3 |
| | 2 | 4,3 | 43,8 | 1,5 | 6,0 | 5,3 | 8,8 | 0,5 | 5,3 | 6,5 | 2,3 | 3,5 | 23,8 | 4,8 | 117,0 | 1,0 | 0,8 | 2,5 |
| | 3 | 3,3 | 35,5 | 0,8 | 4,3 | 4,0 | 7,3 | 0,3 | 4,3 | 4,8 | 2,3 | 2,8 | 17,3 | 3,5 | 98,0 | 0,8 | 0,5 | 1,8 |
| | 4 | 4,3 | 50,0 | 1,0 | 6,0 | 5,8 | 9,0 | 0,3 | 6,0 | 6,5 | 3,3 | 3,8 | 21,0 | 4,8 | 116,8 | 1,0 | 0,8 | 2,3 |

# I    CapIC- MS/MS Analysis
## I.1 Quantification of Phosphorylated Metabolites and Organic Acids

Targeted capIC-MS/MS of phosphorylated metabolites and organic acids was peformed using a Thermo Dionex ICS-4000 Capillary High Pressure Ion Chromatograph system coupled to a Waters TQ-S triple quadrupole mass spectrometer. The CapIC-protocol is given in section I.1.1, whereas the standard mixture used for quantification from CapIC-MS/MS data is presented in section I.1.2. Details about the MS settings, and the interphasing details of capIC to MS can be obtained from supervisor P. Bruheim.


### I.1.1 CapIC-protocol for Phosphorylated Metabolites
AG-11-HC column, 4 um particle size

| | |
|---|---|
| Column temperature: | 15 gc |
| Flow rate: | 18 uL/min |
| Injecion volume: | 5 uL |
| Mobile phase: | Potassium hydroxide (KOH) |

| *Mobile phase gradient:* | |
|---|---|
| 0-1 min: | 4 mM KOH |
| 1-5 min: | 4-12 mM KOH |
| 5-13 min: | 12-20 mM KOH |
| 13-22 min: | 20-70 mM KOH |
| 22-29,5 min: | 70 mM KOH |
| 29,5-31 min: | 70-100 mM KOH |
| 31-36 min: | 100 mM KOH |
| 36-40 min: | 100-4 mM KOH |
| 50 min: | End |

| | |
|---|---|
| Aces suppressor: | 18 mA |
| Interphasing to MS: | Make-up flow 0,03 mL/min 50% ACN/MQ-water with 0,01% ammonium hydroxide |


### I.1.2 CapIC MS/MS Standard Mixture
Metabolites included in the standard mixture used for target analysis of phosphorylated metabolites and low molecular weight organic acids by capIC-MS/MS are given in Table 1.1.

**Table I.1** Compounds in the standard mixture used for targeted analysis of amino acids by capIC-MS/MS.

| capIC standard mixture |
| --- |
| ADP |
| AMP |
| ATP |
| Citrate |
| dAMP |
| dATP |
| Dimethylallyl pyrophosphate |
| Gernayl pyrophasphate |
| Glucosamin 6-phosphate |
| Glucose 1-phosphate |
| Glucose 1-phosphate |
| GDP |
| GMP |
| GTP |
| Glyceraldehydre 3-phosphate |
| Mannose 6-phosphate |
| Sedoheptulose 7-phosphate |
| Succinate |
| UDP N-acetylglucosamine |

### I.1.3 Phosphometabolite and Organic Acid Raw Data

**DU-145**

The concentrations [nM] of phosphometabolites and organic acids obtained from capIC-MS/MS analysis of technical replicas 1-4 within each DU-145 sample group are presented in Tables I.2, I.3 and I.4. Technical replicas and metabolites excluded in the downstream analysis are marked in grey, and gaps indicate no detected measurement.

**Table I.2** Concentrations [nM] of all nucleotides included in the capIC-MS/MS analysis for techinal replica 1-4 within each DU-145 sample group.

| | Paralelle | AMP | ADP | ATP | GMP | GDP | GTP | TMP | TDP | dTTP | CMP | CDP | CTP | UMP | UDP | UTP | IMP |
|---|---|---|---|---|---|---|---|---|---|---|---|---|---|---|---|---|---|
| Hypoxia 48 | 1 | 47,4 | 694,7 | 6191,2 | 21,1 | 214,2 | 1817,3 | 9,1 | 4,1 | 63,4 | 35,3 | 12 | 1387,2 | 1619,2 | 138,7 | 1902,1 | 5,6 |
| | 2 | 34,8 | 684,5 | 7098,1 | 19,6 | 198,4 | 1907,1 | 11,8 | 4 | 71,6 | 37,8 | 10,9 | 1548,2 | 1766,9 | 112,5 | 2427,9 | 4,5 |
| Hypoxia 72 | 1 | 50,5 | 826,2 | 9583,5 | 32,6 | 323,5 | 2937,7 | 6,5 | 4,3 | 65,6 | 72,9 | 25,5 | 1647,7 | 2224,4 | 219,3 | 3492,9 | 7,8 |
| | 2 | 122 | 2099,4 | 13378,9 | 35,5 | 682,6 | 4294 | 16,9 | 11 | 111,6 | 61,9 | 112,9 | 2206,4 | 3169,1 | 206,5 | 5087,6 | 13,7 |
| Hypoxia 96 | 1 | 87,6 | 884,7 | 9168 | 24,8 | 252,4 | 2976 | 5,8 | 2,3 | 39,8 | 55,3 | 3,1 | 1354,7 | 1842,2 | 134,3 | 2580,5 | 6 |
| | 2 | 89 | 981,2 | 3608,2 | 22,2 | 276,9 | 2524,8 | 4,9 | 2,1 | 30,2 | 46,1 | 2,6 | 1042,4 | 1512,5 | 149,2 | 2217,8 | 6,7 |
| Normoxia 48 | 1 | 70 | 883,3 | 5385,4 | 17,6 | 244,2 | 1642,9 | 14,7 | 6,5 | 65,8 | 49,2 | 44,1 | 1388,5 | 1554 | 268,2 | 2446,6 | 4,8 |
| | 2 | 71,5 | 756,2 | 5747,2 | 24,1 | 186,1 | 1601,6 | 9,8 | 5,6 | 63,4 | 47,4 | 30,8 | 1260 | 1434,4 | 228 | 2273,7 | 4,6 |
| Normoxia 72 | 1 | 148 | 1053,3 | 8567,2 | 39,5 | 339,3 | 2922,7 | 15,4 | 6,9 | 84 | 43,7 | 67,4 | 2302 | 2291,6 | 356,5 | 4337,6 | 7,8 |
| | 2 | 82,2 | 1474,7 | 8566,5 | 29,6 | 402,3 | 2536,3 | 16,7 | 8,8 | 80,9 | 60,1 | 102,7 | 2061,2 | 2134,2 | 467,2 | 3798,9 | 8,7 |
| Normoxia 96 | 1 | 476,4 | 2801,3 | 18626,5 | 52 | 928,3 | 5281,7 | 13,6 | 13,7 | 142,1 | 101,9 | 188,2 | 3331,7 | 3809,1 | 929,7 | 8156 | 6,7 |
| | 2 | 92,7 | 1028,7 | 6713,9 | 25,5 | 287,6 | 1897,5 | 7,8 | 4,5 | 39,3 | 47,6 | 33,7 | 1400 | 1611 | 299,7 | 2550,9 | 3,9 |

**Table I.3** Concentrations [nM] of all organic acids included in the capIC-MS/MS analysis for techinical replica 1-4 within each DU-145 sample group.

| | Paralelle | Pyruvate | Fumarate | Succinate | Itatonic acid | Malate | a-ketogluratate | 2HG | Citrate | Isocitrate |
|---|---|---|---|---|---|---|---|---|---|---|
| | | | | | | Metabolite [nM] | | | | |
| Hypoxia 48 | 1 | 65 | 50 | 1902 | 192 | 3306 | 202 | 132 | 780 | 127 |
| | 2 | 43 | 49 | 1866 | 187 | 3711 | 272 | 130 | 752 | 98 |
| Hypoxia 72 | 1 | 80 | 73 | 2417 | 242 | 5590 | 528 | 146 | 1165 | 190 |
| | 2 | 28 | 135 | 611 | 169 | 1607 | 543 | 161 | 2406 | 300 |
| Hypoxia 96 | 1 | 69 | 49 | 1311 | 103 | 3751 | 346 | 129 | 1133 | 157 |
| | 2 | 53 | 38 | 1455 | 207 | 3036 | 295 | 136 | 1021 | 125 |
| Normoxia 48 | 1 | 32 | 41 | 1883 | 18 | 3898 | 141 | 127 | 1157 | 161 |
| | 2 | 52 | 47 | 2501 | 205 | 3282 | 203 | 161 | 872 | 139 |
| Normoxia 72 | 1 | 86 | 87 | 1779 | 138 | 6071 | 492 | 117 | 1625 | 195 |
| | 2 | 80 | 85 | 2351 | 182 | 6419 | 411 | 138 | 2000 | 262 |
| Normoxia 96 | 1 | 367 | 192 | 2552 | 120 | 11796 | 769 | 162 | 4209 | 514 |
| | 2 | 73 | 47 | 1193 | 132 | 3786 | 353 | 102 | 1155 | 176 |

**Table I.4** Concentrations [nM] of all sugarphosphates included in the capIC-MS/MS analysis for technical replica 1-4 within each DU-145 sample group.

| | Paralelle | PEP | GA3P | GL3P | 3PG/2PG | 6PG | GlcN-1P | Gal-1P | G1P/M1P | F1P | G6P | F6P | M6P | S7P | R5P/RL5P/X5P | F1,6BP |
|---|---|---|---|---|---|---|---|---|---|---|---|---|---|---|---|---|
| Hypoxia 48 | 1 | 11 | 3225 | 301 | 120 | 128 | 2 | 11 | 16 | 66 | 118 | 126 | 162 | 31 | 23 | 3 |
| | 2 | 11 | 3194 | 359 | 135 | 140 | 2 | 10 | 14 | 70 | 201 | 85 | 121 | 27 | 31 | 4 |
| Hypoxia 72 | 1 | 14 | 4009 | 545 | 116 | 256 | 3 | 18 | 20 | 74 | 321 | 133 | 170 | 58 | 33 | 55 |
| | 2 | 20 | 8385 | 853 | 296 | 372 | 5 | 25 | 43 | 126 | 442 | 214 | 334 | 114 | 67 | 3 |
| Hypoxia 96 | 1 | 11 | 3976 | 803 | 105 | 171 | 3 | 23 | 26 | 9 | 423 | 88 | 216 | 151 | 27 | 40 |
| | 2 | 9 | 3072 | 643 | 80 | 176 | 2 | 17 | 23 | 17 | 365 | 83 | 206 | 161 | 26 | 9 |
| Normoxia 48 | 1 | 7 | 2419 | 257 | 86 | 97 | 2 | 8 | 19 | 31 | 147 | 95 | 151 | 24 | 26 | 2 |
| | 2 | 9 | 1780 | 279 | 78 | 87 | 1 | 6 | 10 | 39 | 138 | 51 | 80 | 14 | 27 | 39 |
| Normoxia 72 | 1 | 12 | 3645 | 448 | 90 | 164 | 3 | 14 | 14 | 56 | 117 | 48 | 114 | 47 | 43 | 13 |
| | 2 | 11 | 3600 | 436 | 97 | 174 | 3 | 11 | 17 | 57 | 221 | 98 | 156 | 59 | 51 | 1 |
| Normoxia 96 | 1 | 23 | 10760 | 1148 | 155 | 385 | 7 | 36 | 42 | 93 | 742 | 182 | 437 | 381 | 180 | 2 |
| | 2 | 8 | 2466 | 426 | 45 | 121 | 2 | 12 | 20 | 30 | 355 | 80 | 186 | 144 | 31 | 13 |

**U-87 MG**

The concentrations [nM] of phosphometabolites and organic acids obtained from capIC-MS/MS analysis of technical replicas 1-4 within each U-87 MG sample group are presented in Table I.2 for DU-145. Technical replicas and metabolites excluded in the downstream analysis are marked in grey, and gaps indicate no detected measurement.

**Table I.5** Concentrations [nM] of all nucleotides included in the capIC-MS/MS analysis for technical replica 1-4 within each U-87 MG sample groups.

| | Parallele | AMP | ADP | ATP | GMP | GDP | GTP | TMP | TDP | dTTP | CMP | CDP | CTP | UMP | UDP | UTP | IMP |
|---|---|---|---|---|---|---|---|---|---|---|---|---|---|---|---|---|---|
| Hypoxia 48 | 1 | 53 | 1016 | 7703 | 31 | 369 | 3430 | 8 | 6 | 89 | 67 | 48 | 1404 | 1211 | 105 | 1622 | 2 |
| | 2 | 131 | 1065 | 6190 | 24 | 340 | 3358 | 8 | 5 | 84 | 72 | 49 | 1416 | 1045 | 99 | 1519 | 5 |
| Hypoxia 72 | 1 | 208 | 1533 | 8827 | 40 | 479 | 3579 | 8 | 8 | 93 | 88 | 73 | 1744 | 1270 | 196 | 2455 | 8 |
| | 2 | 271 | 1005 | 9954 | 27 | 490 | 4030 | 8 | 7 | 106 | 87 | 66 | 2036 | 1693 | 145 | 2886 | 10 |
| Hypoxia 96 | 1 | 357 | 1964 | 8399 | 56 | 913 | 4098 | 9 | 10 | 69 | 114 | 132 | 1672 | 1068 | 310 | 2173 | 10 |
| | 2 | 187 | 2417 | 9925 | 67 | 826 | 3743 | 11 | 10 | 63 | 0 | 117 | 1504 | 978 | 289 | 1839 | 5 |
| Normoxia 48 | 1 | 131 | 899 | 7519 | 23 | 345 | 3047 | 8 | 5 | 82 | 57 | 52 | 1534 | 1149 | 111 | 1594 | 3 |
| | 2 | 90 | 1277 | 8249 | 32 | 473 | 3326 | 8 | 8 | 92 | 70 | 69 | 1520 | 1117 | 166 | 1844 | 8 |
| Normoxia 72 | 1 | 231 | 1126 | 9213 | 36 | 514 | 4052 | 8 | 7 | 98 | 102 | 98 | 2119 | 1921 | 235 | 2938 | 8 |
| | 2 | 181 | 1365 | 9107 | 36 | 479 | 3731 | 8 | 8 | 93 | 91 | 85 | 1979 | 1817 | 275 | 3083 | 11 |
| Normoxia 96 | 1 | 205 | 2094 | 9741 | 52 | 792 | 3811 | 10 | 15 | 114 | 98 | 150 | 2085 | 1378 | 500 | 3591 | 10 |
| | 2 | 329 | 2312 | 8744 | 54 | 806 | 3860 | 10 | 13 | 106 | 99 | 0 | 2090 | 1401 | 520 | 3348 | 7 |

**Table I.6** Concentrations [nM] of all organic acids included in the capIC-MS/MS analysis for technical replica 1-4 within each U-87 MG sample groups.

| | Paralelle | Pyruvate | Fumarate | Succinate | Itatonic acid | Malate | α-KG | 2HG | Citrate | Isocitrate |
|---|---|---|---|---|---|---|---|---|---|---|
| | | | | | | **Metabolite [nM]** | | | | |
| Hypoxia 48 | 1 | 35 | 22 | 1758 | 163 | 2168 | 566 | 453 | 1578 | 250 |
| | 2 | 33 | 27 | 1821 | 121 | 2488 | 551 | 509 | 1709 | 229 |
| Hypoxia 72 | 1 | 49 | 56 | 1563 | 140 | 5612 | 831 | 810 | 2496 | 302 |
| | 2 | 39 | 58 | 1866 | 115 | 6207 | 1000 | 871 | 2650 | 379 |
| Hypoxia 96 | 1 | 62 | 79 | 1938 | 164 | 6260 | 762 | 555 | 3076 | 371 |
| | 2 | 60 | 47 | 1375 | 109 | 4978 | 623 | 586 | 2619 | 247 |
| Normoxia 48 | 1 | 24 | 32 | 1675 | 133 | 3456 | 566 | 375 | 2130 | 321 |
| | 2 | 33 | 34 | 1682 | 157 | 3494 | 604 | 376 | 2235 | 319 |
| Normoxia 72 | 1 | 45 | 58 | 1915 | 149 | 7803 | 1140 | 821 | 3430 | 405 |
| | 2 | 34 | 79 | 1608 | 153 | 7352 | 1153 | 712 | 3205 | 477 |
| Normoxia 96 | 1 | 65 | 140 | 2425 | 241 | 9814 | 280 | 600 | 2846 | 348 |
| | 2 | 78 | 68 | 2387 | 170 | 9566 | 676 | 372 | 370 | 318 |

**Table I.7** Concentrations [nM] of all sugarphosphates included in the capIC-MS/MS analysis for technical replica 1-4 within each U-87 MG sample groups.

| | Parallele | PEP | DHAP | GA3P | GL3P | 3PG/2PG | 6PG | GlcN-1P | Gal-1P | G1P/M1P | F1P | G6P | F6P | M6P | S7P | R5P/X5P/RL5P | F1,6BP |
|---|---|---|---|---|---|---|---|---|---|---|---|---|---|---|---|---|---|
| Hypoxia 48 | 1 | 8 | 276 | 6736 | 773 | 275 | 374 | 3 | 67 | 39 | 267 | 923 | 133 | 468 | 87 | 60 | 62 |
| | 2 | 12 | 195 | 6780 | 757 | 263 | 360 | 2 | 73 | 38 | 229 | 848 | 152 | 379 | 79 | 58 | 36 |
| Hypoxia 72 | 1 | 7 | 10 | 6443 | 1089 | 177 | 118 | 3 | 108 | 18 | 10 | 251 | 64 | 223 | 124 | 31 | 1 |
| | 2 | 15 | 30 | 8249 | 1467 | 267 | 225 | 2 | 134 | 25 | 19 | 264 | 55 | 354 | 163 | 55 | 6 |
| Hypoxia 96 | 1 | 13 | 1 | 8252 | 556 | 109 | 26 | 3 | 60 | 11 | 6 | 253 | 51 | 108 | 66 | 10 | 1 |
| | 2 | 14 | 1 | 6645 | 558 | 119 | 26 | 3 | 57 | 14 | 7 | 241 | 25 | 89 | 61 | 10 | 1 |
| Normoxia 48 | 1 | 9 | 333 | 2374 | 891 | 226 | 363 | 2 | 73 | 43 | 136 | 944 | 181 | 550 | 90 | 50 | 55 |
| | 2 | 11 | 232 | 6608 | 870 | 254 | 378 | 2 | 2 | 49 | 135 | 931 | 125 | 481 | 111 | 49 | 49 |
| Normoxia 72 | 1 | 14 | 57 | 7135 | 1520 | 311 | 331 | 3 | 113 | 32 | 29 | 535 | 84 | 511 | 196 | 58 | 15 |
| | 2 | 12 | 43 | 6849 | 1529 | 325 | 397 | 3 | 137 | 51 | 38 | 989 | 157 | 639 | 275 | 65 | 10 |
| Normoxia 96 | 1 | 14 | 2 | 8587 | 265 | 108 | 28 | 4 | 83 | 17 | 9 | 267 | 52 | 139 | 98 | 39 | 1 |
| | 2 | 14 | 1 | 8623 | 334 | 111 | 41 | 3 | 79 | 19 | 10 | 311 | 43 | 143 | 108 | 43 | 0 |

# J    HIF-1α Data

## J.1 Calibration Curves

Linear calibration curves were generated from the standard series with known HIF-1α concentrations, and curves were used for quantification of HIF-1α in samples. Several of the measured HIF-1α concentrations were excluded from the standard curve as they were clearly outlier data points. Standard curves obtained by plotting average absorbance against known HIF-1α concentrations, are presented in Figures J.1 (for DU-145) and J.2 (for U-87 MG). Datas are given with a linear regression line, and corresponding equation and $R^2$ values in Table J.1.
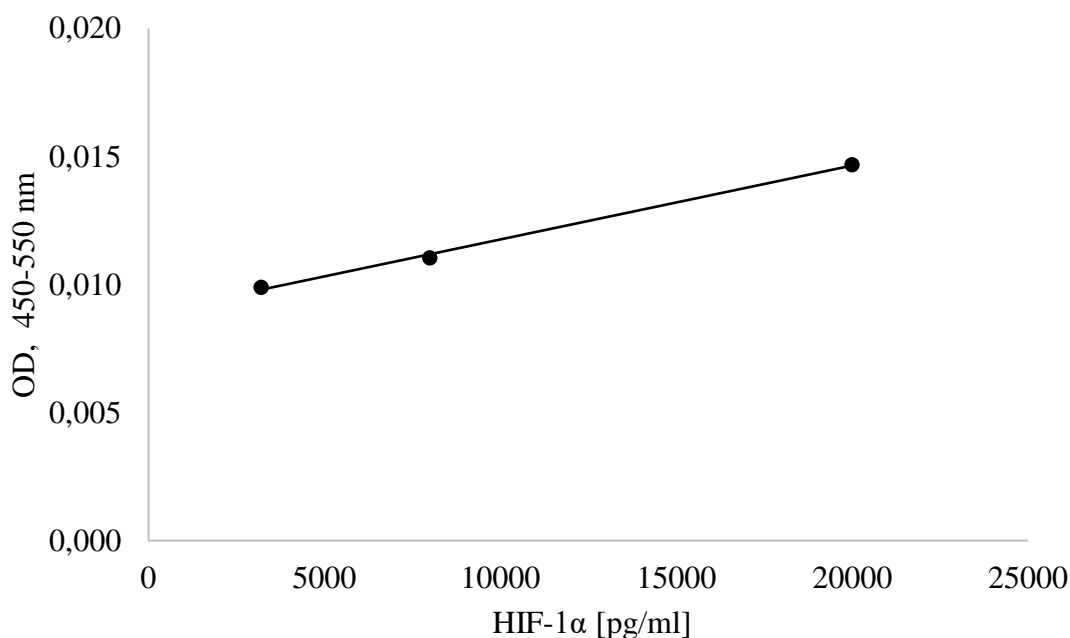


**Figure J.1**: HIF-1α calibration curve made from optical density (450 nm-550 nm) and known HIF-1α concentrations in a standard series for DU-145. The standard curve points are given with a linear regression line, with corresponding equation and $R^2$ value in table J.1. Each standard point is based on
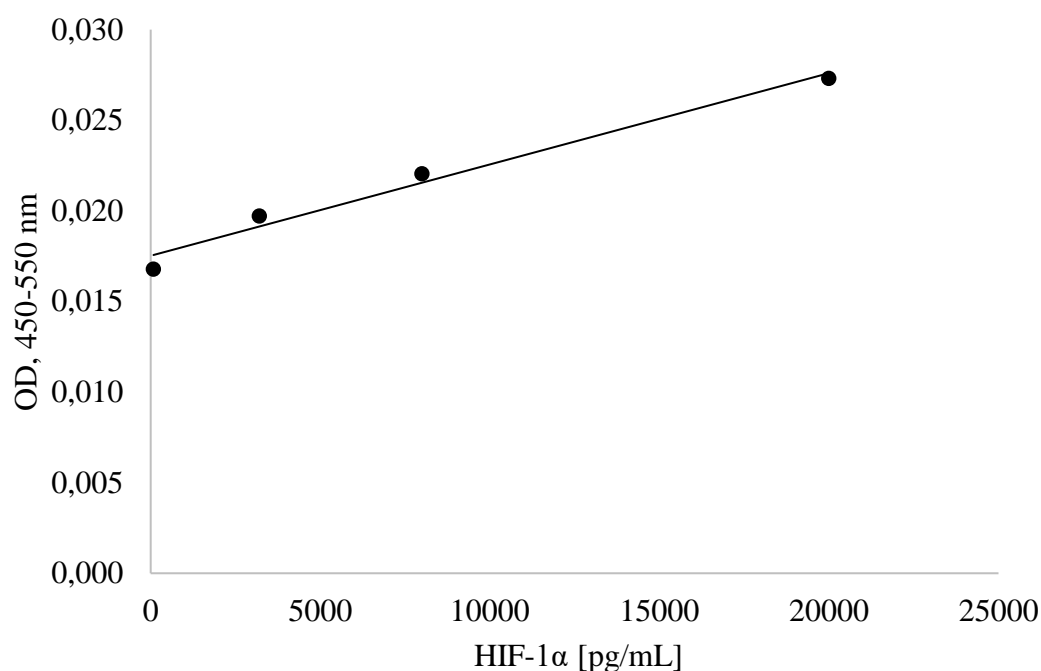
**Figure J.2**: HIF-1α calibration curve made from optical density (450 nm-550 nm) and known HIF-1α concentrations in a standard series for DU-145. The standard curve points are given with a linear regression line, with corresponding equation and $R^2$ value in table J.2.

**Table J.1.** The equation of the linear regression lines is given with $R^2$ value.

| Cell line | Slope | Intercept | $R^2$ |
|-----------|---------|-----------|--------|
| DU-145 | $5*10^7$ | 0,0175 | 0,9784 |
| U-87 MG | $3*10^7$ | 0,0089 | 0,9975 |

## J.2 Concentration of HIF-1α

By using the linear equations given in table J.1, and measured absorbance values of HIF-1α, the HIF-1α concentration in sample groups was calculated. Samples with HIF-1α concentrations higher of lower compared to the concentration of the standard series (i.e concentrations outside the standard curve) were excluded from the analysis. The average zero OD was not subtracted from standards and samples as this would result in close to zero or negative values.

Further on, HIF-1α concentrations were normalized with respect to average cell counts in respective treatment samples. Normalized HIF-1α concentrations in DU-145 and U-87 MG sample groups are presented in Table J.2. Averages are based on two technical replicas within each sample group.

**Table J.2:** The average normalized HIF-1α concentration in DU-145 and U-87 MG sample groups. The averages are based on two technical replicas within each sample group. HIF-1A was not quantified in samples marked with asterisk (*).

| Cell line | Treatment | Sample group Treatment length [h] | Concentration of HIF-1α [pg/cell] |
|-----------|-----------|-----------------------------------|-----------------------------------|
| DU-145 | Normoxia | 48 | * |
| | | 72 | * |
| | Hypoxia | 48 | * |
| | | 72 | 0,008 |
| U-87 MG | Normoxia | 48 | * |
| | | 72 | 0,039 |
| | Hypoxia | 48 | * |
| | | 72 | 0,054 |

# K    PCA Scores and Loadings Plots
## K.1  RP LC-MS/MS Data
Data obtained from RP LC-MS/MS analysis of amino acids in 48 hour and 72 hour treated

sample groups were analysed in separate by PCA.


### K.1.1 DU-145
Data obtained from RP LC-MS/MS analysis of amino acids in 48 hour and 72 hour treated

DU-145 sample groups were analysed in separate by PCA. The resulting scores and loadings

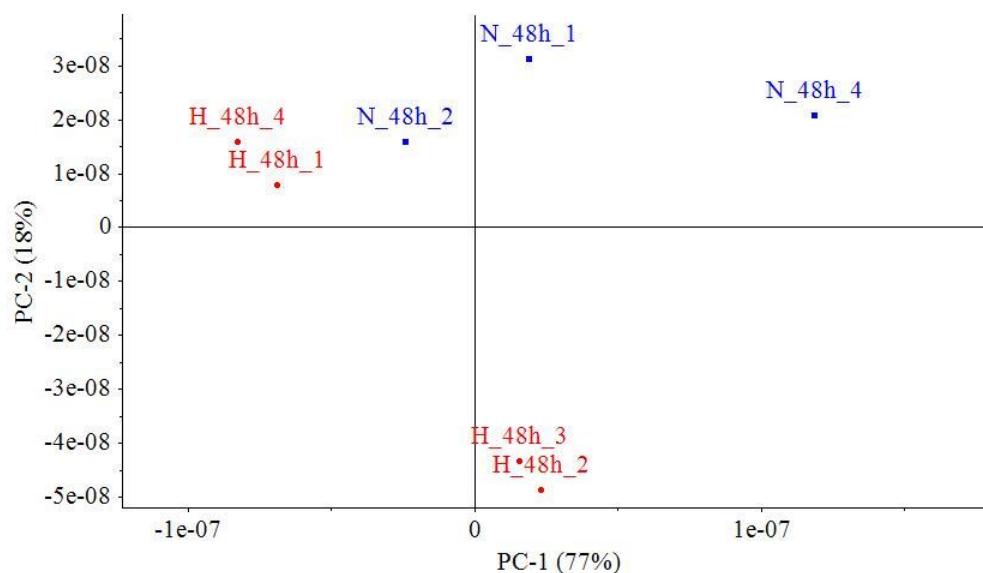plots of 48 hour treated sample groups are presented in Figures K.1 and K.2.



**Figure K.1:** The scores plot of data obtained from RP LC-MS/MS analysis of amino acids in 48 hour DU-145

sample groups. The metabolome data was normalized to the average cell count, and automatically scaled.
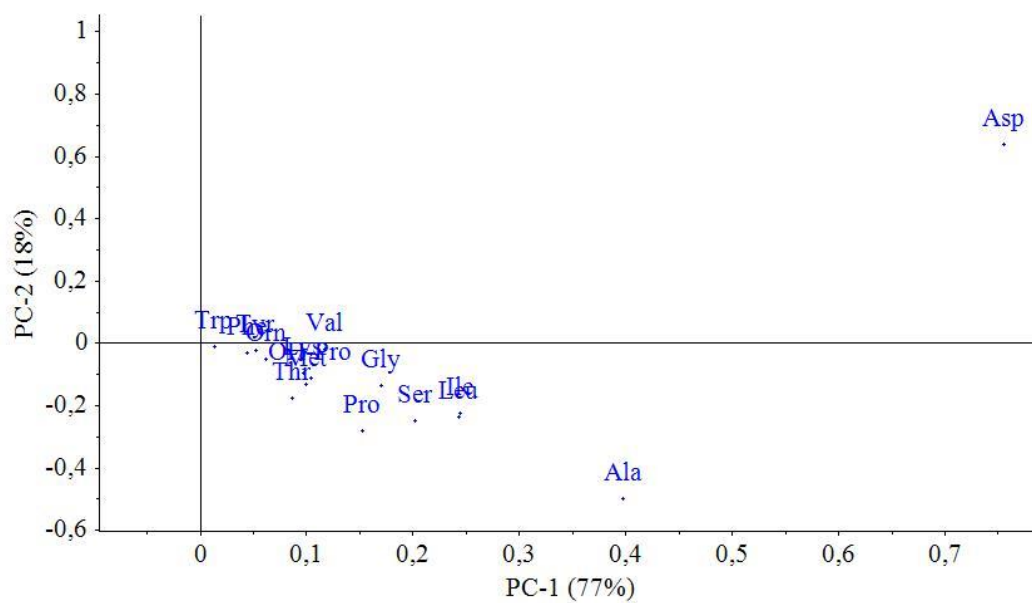
Hypoxic replicas in red and normoxic replicas in blue.

**Figure K.2:** The loadings plot of data obtained from RP LC-MS/MS analysis of amino acids in 48 hour DU-145 sample groups. The metabolome data was normalized to the average cell count, and automatically scaled.

The resulting scores and loadings plots of 72 hour treated sample groups are presented in Figures K.3 and K.4
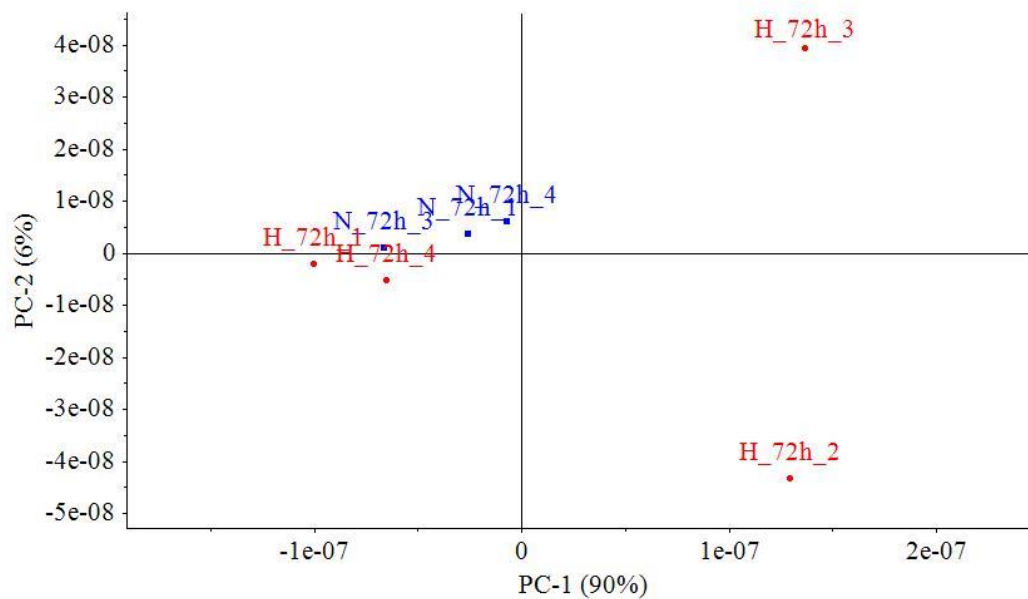
**Figure K.3:** The scores plot of data obtained from RP LC-MS/MS analysis of amino acids in 48 hour DU-145 sample groups. The metabolome data was normalized to the average cell count, and automatically scaled. Hypoxic replicas in red and normoxic replicas in blue.
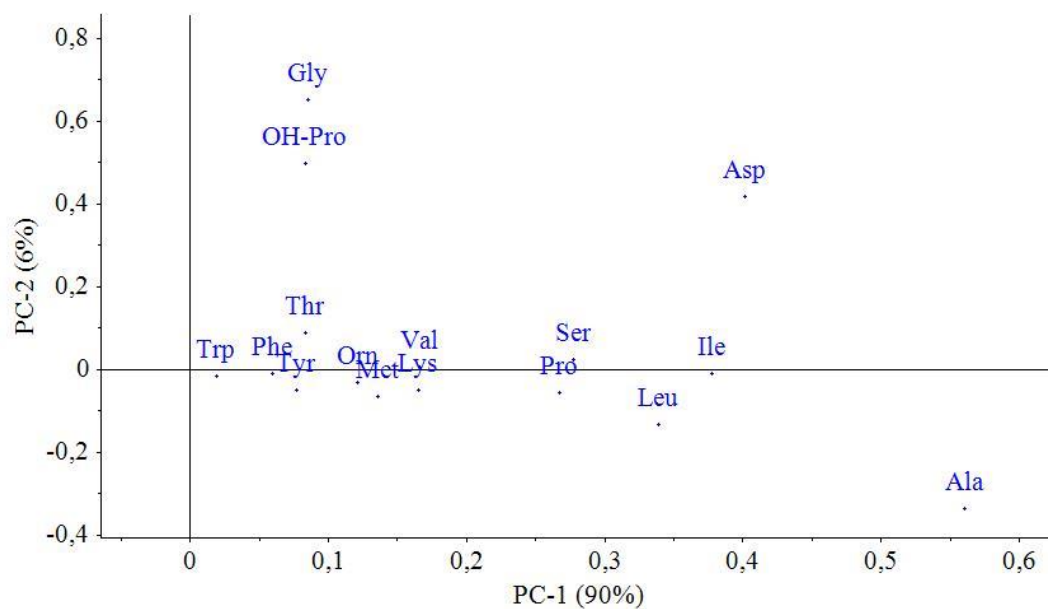


**Figure K.4:** The loadings plot of data obtained from RP LC-MS/MS analysis of amino acids in 72 hour DU-145 sample groups. The metabolome data was normalized to the average cell count, and automatically scaled.

## K.1.2 U-87 MG

Data obtained from RP LC-MS/MS analysis of amino acids in 48 hour and 72 hour treated U-87 MG sample groups were analysed in separate by PCA. The resulting scores and loadings plots of 48 hour treated sample groups are presented in Figures K.5 and K.6
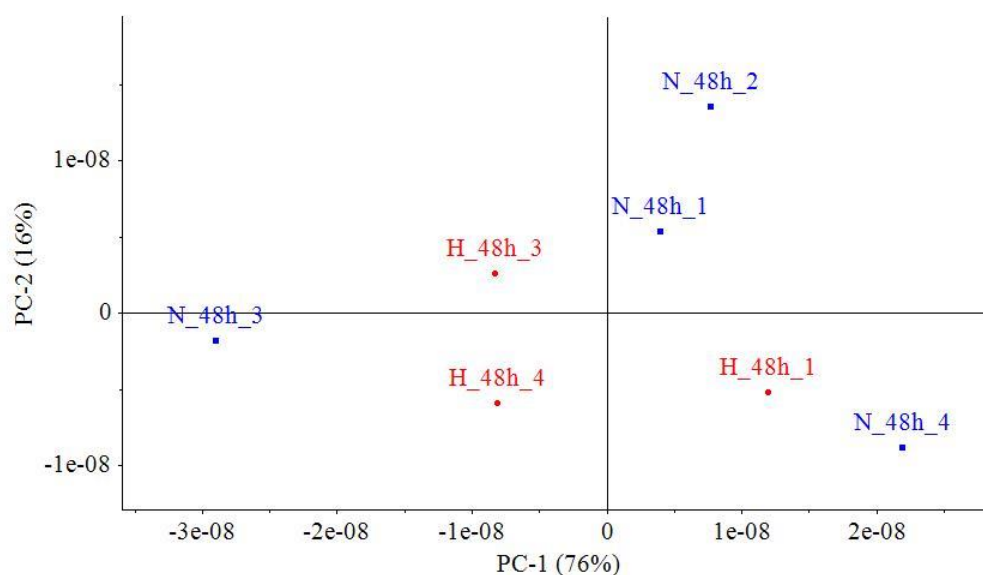


**Figure K.5:** The scores plot of data obtained from RP LC-MS/MS analysis of amino acids in 48 hour U-87 MG sample groups. The metabolome data was normalized to the average cell count, and automatically scaled. Hypoxic replicas in red and normoxic replicas in blue.
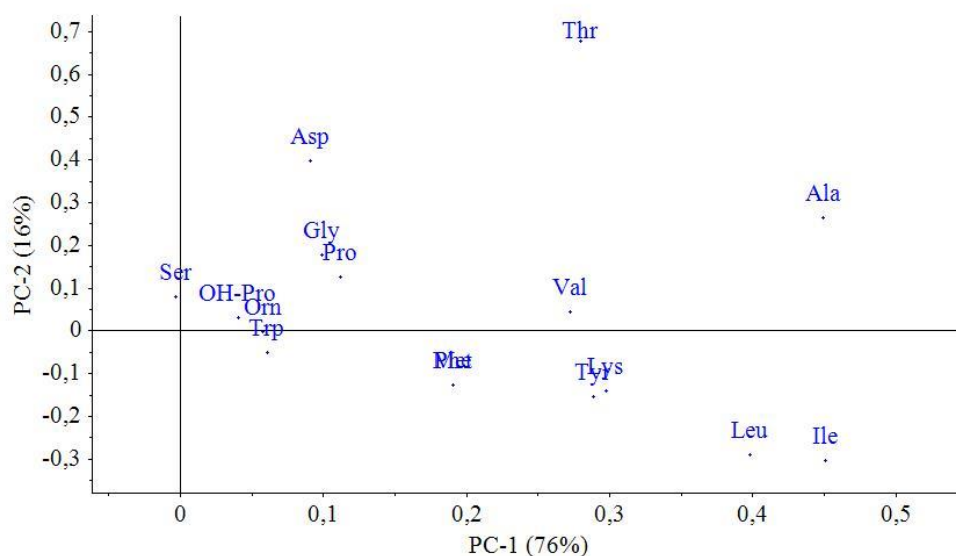


**Figure K.6:** The loadings plot of data obtained from RP LC-MS/MS analysis of amino acids in 48 hour U-87 MG sample groups. The metabolome data was normalized to the average cell count, and automatically scaled.

Scores and loadings plots of 72 hour treated sample groups are presented in Figures K.7 and K.8.
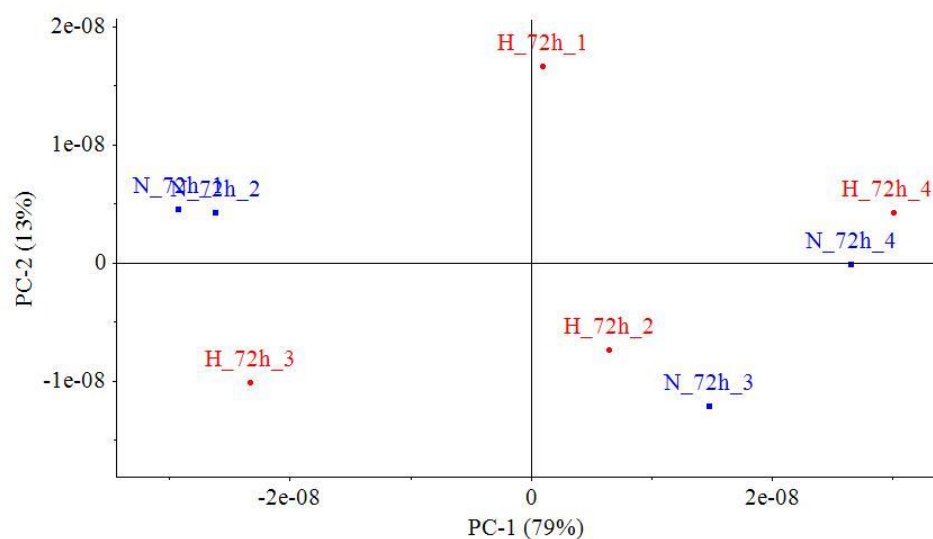


**Figure K.7:** The scores plot of data obtained from RP LC-MS/MS analysis of amino acids in 72 hour U-87 MG sample groups. The metabolome data was normalized to the average cell count, and automatically scaled. Hypoxic replicas in red and normoxic replicas in blue.



**Figure K.8:** The loadings plot of data obtained from RP LC-MS/MS analysis of amino acids in 72 hour U-87 MG sample groups. The metabolome data was normalized to the average cell count, and automatically scaled.

## K.2 CapIC-MS/MS Data
### K.2.1 DU-145
Data obtained from RP LC-MS/MS analysis of organic acids and phosphometabolites in 48 hour and 72 hour treated DU-145 sample groups were analysed in separate by PCA. The resulting scores and loadings plots of 48 hour treated sample groups are presented in Figures K.9 and K-10.



**Figure K.9:** The scores plot of data obtained from capIC-MS/MS analysis of phosphometabolites and organic acids in 48h DU-145 sample groups. The metabolome data was normalized to the average cell count, and automatically scaled. Hypoxic replicas in red and normoxic replicas in blue.
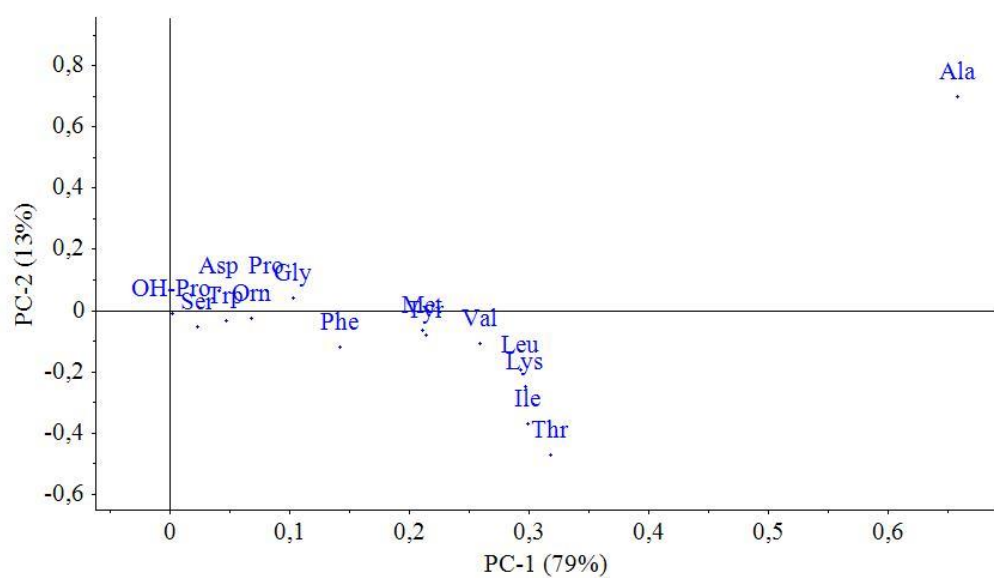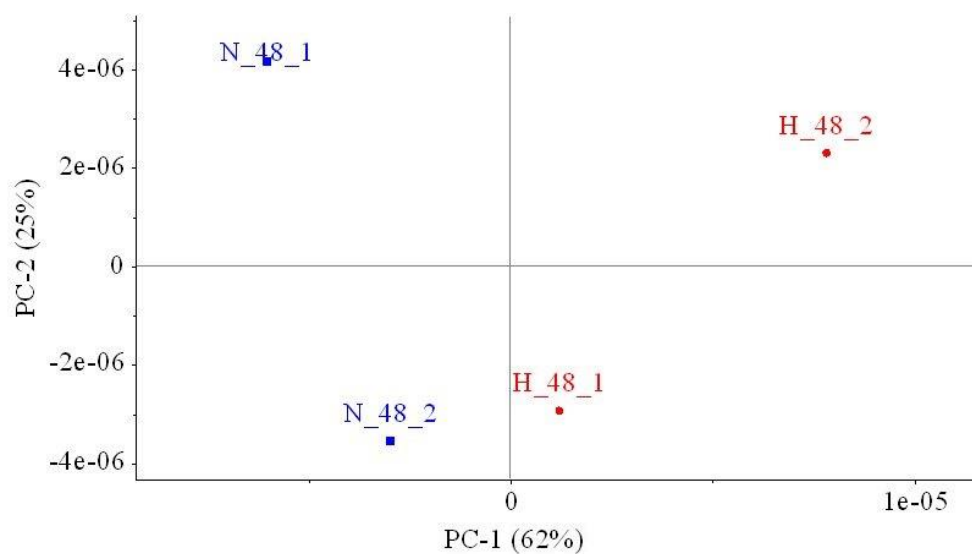
**Figure K.10:** The loadings plot of data obtained from CapIC-MS/MS analysis of phosphometabolites and organic acids in 48 hour DU-145 sample groups. The metabolome data was normalized to the average cell count, and automatically scaled.

Scores and loadings plots of 74 hour treated sample groups are presented in Figures K.11 and K.12.



**Figure K11:** The scores plot of data obtained from capIC-MS/MS analysis of phosphometabolites and organic acids in 72 hour DU-145 sample groups. The metabolome data was normalized to the average cell count, and automatically scaled. Hypoxic replicas in red and normoxic replicas in blue.
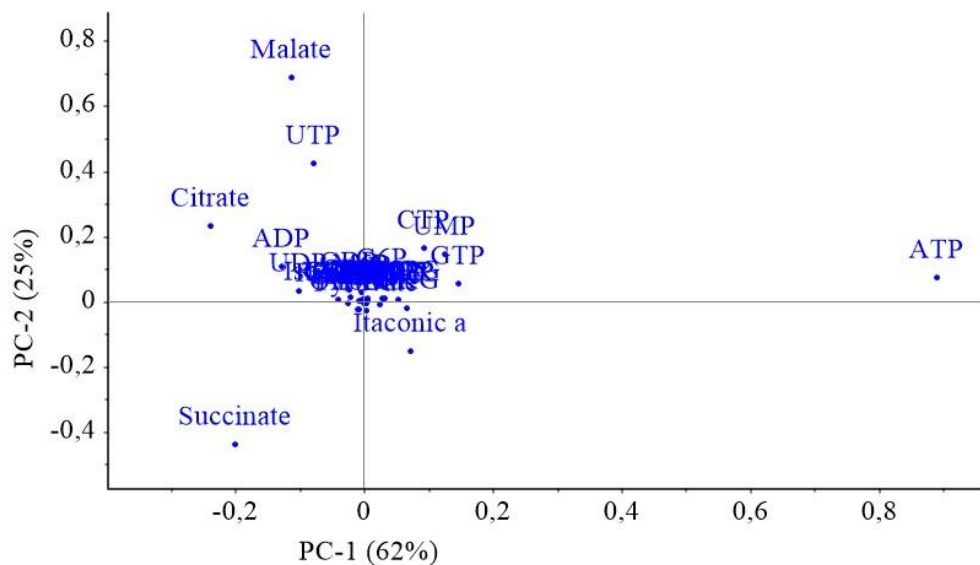
**Figure K.12:** The loadings plot of data obtained from CapIC-MS/MS analysis of phosphometabolites and organic acids in 72 hour DU-145 sample groups. The metabolome data was normalized to the average cell count, and automatically scaled.


### K.2.1 U-87 MG

Data obtained from RP LC-MS/MS analysis of organic acids and phosphometabolites in 48 hour and 72 hour treated U-87 MGsample groups were analysed in separate by PCA. The resulting scores and loadings plots of 48 hour treated sample groups are presented in Figures K.13 and K.14.

**Figure K.13:** The scores plot of data obtained from CapIC-MS/MS analysis of phosphometabolites and organic acids in 48 hour U-87 MG sample groups. The metabolome data was normalized to the average cell count, and automatically scaled. Hypoxic replicas in red and normoxic replicas in blue.



**Figure K.14:** The loadings plot of data obtained from CapIC-MS/MS analysis of phosphometabolites and organic acids in 48 hour U-87 MG sample groups. The metabolome data was normalized to the average cell count, and automatically scaled.

Scores and loadings plots of 74 hour treated sample groups are presented in Figures K.15 and K.16.
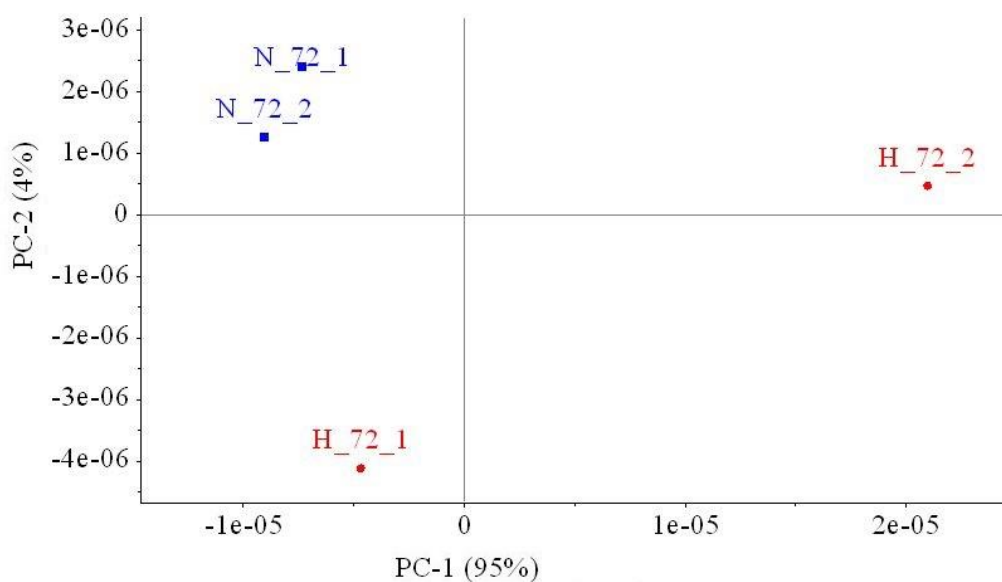
**Figure K.15:** The scores plot of data obtained from CapIC-MS/MS analysis of phosphometabolites and organic acids in 72 hour U-87 MG sample groups. The metabolome data was normalized to the average cell count, and automatically scaled. Hypoxic replicas in red and normoxic replicas in blue.
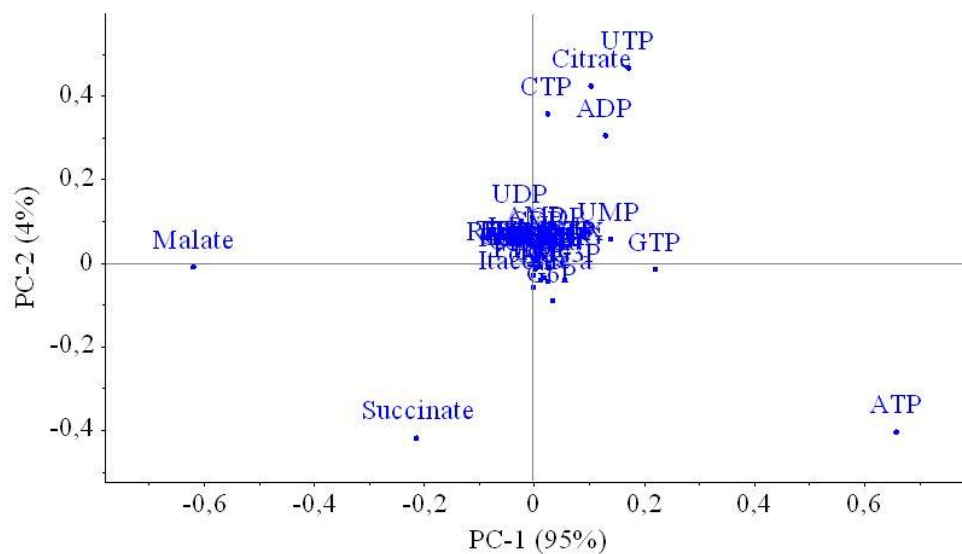


**Figure**

**K.16:** The loadings plot of data obtained from CapIC-MS/MS analysis of phosphometabolites and organic acids in 72 hour U-87 MG sample groups. The metabolome data was normalized to the average cell count, and automatically scaled.